Parameter Estimation and Mathematical Modeling of Visceral Leishmaniasis Transmission

by

Kamal Barley

A Dissertation Presented in Partial Fulfillment
of the Requirements for the Degree
Doctor of Philosophy

Approved March 2016 by the
Graduate Supervisory Committee:

Carlos Castillo-Chavez, Co-Chair
Anuj Mubayi, Co-Chair
Muntaser Safan

ARIZONA STATE UNIVERSITY

May 2016

ABSTRACT

The Visceral Leishmaniasis (VL) is primarily endemic in five countries, with India and Sudan having the highest burden. The risk factors associated with VL are either unknown in some regions or vary drastically among empirical studies. Here, a dynamical model, motivated and informed by field data from the literature, is analyzed and employed to identify and quantify the impact of region dependent risks on the VL transmission dynamics. Parameter estimation procedures were developed using model-derived quantities and empirical data from multiple resources. The dynamics of VL depend on the estimates of the control reproductive number, $\mathcal{R}_C$, interpreted as the average number of secondary infections generated by a single infectious individual during the infectious period. The distribution of $\mathcal{R}_C$ was estimated for both India (with mean 2.1 ± 1.1) and Sudan (with mean 1.45 ± 0.57). This suggests that VL can be established in naive regions of India more easily than in naive regions of Sudan. The parameter sensitivity analysis on $\mathcal{R}_C$ suggests that the average biting rate and transmission probabilities between host and vector are among the most sensitive parameters for both countries. The comparative assessment of VL transmission dynamics in both India and Sudan was carried out by parameter sensitivity analysis on VL-related prevalences (such as prevalences of asymptomatic hosts, symptomatic hosts, and infected vectors). The results identify that the treatment and symptoms' developmental rates are parameters that are highly sensitive to VL symptomatic and asymptomatic host prevalence, respectively, for both countries. It is found that the estimates of transmission probability are significantly different between India (from human to sandflies with mean of 0.39 ± 0.12; from sandflies to human with mean 0.0005 ± 0.0002) and Sudan (from human to sandflies with mean 0.26 ± 0.07; from sandflies to human with mean 0.0002 ± 0.0001). The results have significant implications for elimination. An increasing focus on elimination requires a review of priorities

within the VL control agenda. The development of systematic implementation of control programs based on identified risk factors (such as monitoring of asymptomatically infected individuals) has a high transmission-blocking potential.

DEDICATION

To my late grandmother Beryl Johnny who was my whole world. She was and continue to be a great inspiration in my life.

ACKNOWLEDGMENTS

First and foremost I would like to thank the Lord my God. Without Him nothing is possible.

My sincere thanks and appreciation to the administrative staff at Mathematical, Computational and Modeling Science Center (MCMSC) who work to maintain the program throughout the years. I wish to express my appreciation to Dr. Carlos Castillo-Chavez, Dr. Anuj Mubayi, and Dr. Muntaser Safan for their continued mentorship and support through my doctoral journey. Thanks to the support of all my friends and colleagues during my journey, Terrence Blackman, Alhaji Cherif, Bichara Derdei, Arlene M. Evangelista Elenor Holder, Robert Mamada, Romie Morales, Emmanuel Morales, Fereshteh Nazari , OyitaUdiani, Daniel Romero, Andre Robinson, Kehinde Salau, and Alicia Urdapilleta. I always enjoyed the good conversation we had in exchange of knowledge.

This dissertation has been partially funded by the Alfred P. Sloan Foundation (through the ASU-Sloan National Pipeline Program in Mathematical Science), the Mathematical, Computational and Modeling Science Center (MCMSC) and ASU's Western Alliance to Expand Student Opportunities (WAESO) and Graduate Education at Mountain States Alliance (MGE@MSA) Credit: Arizona State University.

TABLE OF CONTENTS

CHAPTER Page

LIST OF TABLES

Table Page

APPENDIX Page

LIST OF FIGURES

Figure Page

Chapter 1

GENERAL INTRODUCTION AND OVERVIEW

1.1 About This Thesis

This dissertation is driven by my desire to ameliorate the impact of neglected infectious diseases at the population level. I have chosen to focus on VL not only because of the lack of political interest in reducing its prevalence but also, because I had an opportunity to gather, assess, and analyze data from two of the most affected countries of the world: India and Sudan. This dissertation is organized into four chapters. In the remainder of this chapter, I review the epidemiology of Leishmaniasis, with emphasis on the spread of Visceral Leishmaniasis in India and Sudan. Chapter 2 presents two VL-related data sets obtained from the literature and a novel procedure to estimate parameters of a mathematical model that captures transmission dynamics of VL and the risk associated with its spread. In Chapter 3, estimates from Chapter 2 are used to carry out a comparative study of VL dynamics between India and Sudan. Notably, the comparative analysis identifies and assesses country-dependent risks related to the spread and maintenance of VL. Some mathematical details of VL transmission dynamics model are collected in Chapter 4. The dissertation ends with the collection of implications from this study on VL transmission dynamics in Chapter 5.

1.2 Epidemiology of Leishmaniasis

Leishmaniasis refers to a range of complex vector-borne diseases caused by parasitic protozoa parasites (Kinetoplastida: Trypanosomatidae) from the genus *Leishma-*

nia (Subgenus *Leishmania* and *Viannia*), which naturally multiply within a vertebrate host and are transmitted between hosts by the bites of infected female *phlebotomine* sandflies (*Diptera*, Psychodidae: Phlebotominae). Occasionally, non-vector transmission occurs congenitally or via by blood transfusion or needle sharing (118). The leishmaniases are endemic to 98 countries throughout the tropics and sub-tropics and currently affect more than 12 million people worldwide, with an additional 350 million people thought to be at risk of infection (152). The incidence of clinical cases is at an all-time high (between 1.5 and 2.5 cases) with more than 1.3 million new cases diagnosed annually (including 500,000 new cases of VL) (97; 152). Moreover, the world's leishmaniasis prevalence is between 10 and 12 million, a number that may not represent the actual burden of the infection because cases are often misdiagnosed or unreported.

The majority of those at risk are from developing countries and are among the poorest people in society, where leishmaniasis is associated with poor socio-economic status, malnutrition, illiteracy, population displacement, gender discrimination, poor immune status (6), and, increasingly, urbanization (39). The World Health Organization (WHO) has designated leishmaniasis as one of the "Neglected Tropical Diseases (NTD)" (154). The World Health Assembly approved a resolution in 2007 that aimed at improving awareness of leishmaniasis, standardizing diagnosis, and evaluating current medicines, [increasing access to affordable healthcare through cost reduction policies directed at drug-producing laboratories] (151).

The epidemiology of leishmaniasis is highly complex, diverse, and distributed worldwide with marked regional differences in vector and parasite species, transmission routes, environments, reservoirs, and clinical profiles. It can be anthroponotic (human reservoir) or zoonotic (animal reservoir), depending on different vertebrate hosts. Four major eco-epidemiological profiles have been recognized: zoonotic and an-

throponotic visceral leishmaniasis (ZVL and AVL) and zoonotic and anthroponotic cutaneous leishmaniasis (ZCL and ACL).

Depending on the etiological agent, the course of the disease is variable, ranging from ulcerative lesions of the skin or facial mucosa, known as Cutaneous Leishmaniasis (CL) and Mucocutaneous Leishmaniasis (MCL), to a lethal systemic disease, Visceral Leishmaniasis (VL), which primarily affects the internal organs and is usually fatal in the absence of treatment (52; 72; 107). Fewer common clinical disease manifestations include diffuse cutaneous leishmaniasis (DCL) and post kala-azar dermal leishmaniasis (PKDL), whereby nodular skin lesions appear all over the body (41; 76; 120). Though these two may seem similar, DCL is a clinical manifestation associated with CL-causing parasite species whereas PKDL is a cutaneous episode that follows the resolution of VL infection and it is mainly six months in Sudan and two to three years in India (110; 157).

Geographically, the distribution of leishmaniasis is complex with a taxonomy of 20 different species of Leishmania. The geographic occurrence is classified into Old World and New World leishmaniasis with infections occurring in humans and many domestic animal species. Old World leishmaniasis takes place in Africa, Asia, Middle East, Mediterranean Basin and clinically appears as cutaneous or visceral disease (85). New World leishmaniasis occurs in Central and South America and is caused by Leishmania species and occurs clinically appears as cutaneous, mucocutaneous, or visceral disease (85).

Infection by the leishmania protozoa is acquired primarily when an infected female sandfly bites a susceptible individual. There are many strains of Leishmania protozoa transmitted by two genera of sandflies. In the Old World, the sandfly vector is of the genus *Phlebotomus*, whereas in the New World, it is of the genus *Lutzomyia* (83; 148). Of these two genera, more that 30 species of sandfly can support the development of

leishmania in their guts and pass the pathogen to humans (29).

Leishmaniasis disease manifests in three forms: cutaneous (diffuse cutaneous, recidivans, or post-kala-azar dermal leishmaniasis), mucocutaneous, visceral, and viscerotropic forms.

1. **Cutaneous leishmaniasis (CL)**: CL is also known as "Baghdad Boil," "Oriental Sore," or "Uta," and it is the most common form of leishmaniasis. It causes skin lesions, mainly ulcers, on exposed parts of the body, leaving life-long scars and serious disability. Once infected with leishmania protozoa, a person enters an incubation period lasting between a week and several months during which no physical symptoms are presented (8; 34). When the incubation period is complete, multiple lesions form on the skin, often in exposed areas that have been targeted by sandflies. Parasites also persist at the original site of infection for many years, leading to concomitant immunity but also relapse.

   About 95% of CL cases occur in the Americas, the Mediterranean basin, the Middle East and Central Asia. More that two-thirds of new CL cases occur in 6 countries: Afghanistan, Algeria, Brazil, Colombia, the Islamic Republic of Iran, and (34). An estimated 0.7 million to 1.3 million new cases occur worldwide annually.

   Cutaneous leishmaniasis may be either anthroponotic (having humans as the sole host) or zoonotic (having another species as the primary reservoir). In areas of the Middle East and North Africa, cutaneous leishmaniasis is caused by leishmania and is mainly zoonotic. Its main reservoir is rodents, such as the great gerbil *Rhombomys opimus* and the fat sand rat *Psammomys obesus* (8). Leishmaniasis caused by *Leishmania Brazilians* in Brazil is also zoonotic and principally infects either rodents or dogs bitten by the sandfly *Lutzomyia*

whitmani. Human case numbers are especially high in drier areas in the north-east Brazil, where the absence of dense vegetation seems to increase sandfly prevalence. Anthroponotic cutaneous leishmaniasis is found in the drier western parts of India and in Afghanistan, where disease is commonly caused by *Leishmania tropica* spread by the sandfly *Phlebotomus sergenti* (152).

2. **Mucocutaneous Leishmaniasis (MCL)**: MCL leads to the partial or destruction of mucous membranes of the nose, mouth, and throat, sometimes occurring years after the first bout of cutaneous leishmaniasis. MCL is caused by Leishmania protozoa colonizing macrophages in the nasopharyngeal mucosa (29). Similar to other forms of leishmaniasis, clinical progression is dependent on the immune response of the host and on the strain of leishmania with which they are infected. Almost 90% of mucocutaneous leishmaniasis cases occur in the Plurinational State of Bolivia, Brazil, and Peru.

3. **Visceral Leishmaniasis**: VL occurs in Central and South America, the Mediterranean basin, Central Asia, the Indian subcontinent, the Middle East, and Africa. In Asia and Africa, VL is caused mainly by *Leishmania (Leishmania) donovani* and is transmitted by *Phlebotomus (Euphlebotomus) argentipes* in Asia and *P. (Larroussius) orientalis* and *P. (Synphlebotomus) martini* in Africa (83; 117).

   Humans act as reservoirs (Anthroponotic Visceral leishmaniasis). In the Mediterranean basin, *Leishmania (L.) infantum* is responsible for VL and it is transmitted mostly by *P. (La.) Perniciosus* and *P. (La.) ariasi*. Dogs are the main reservoirs (Zoonotic Visceral Leishmaniasis). In the New World, *L. (L.) infantum*(*syn L. chagasi*) is the causative parasite and *Lutzomyia* (Lutzomyia) longipalpis is the primary vector with dogs, foxes (117; 83) and jackals as reser-

voirs.

Cells of the reticuloendothelial system are the target of the parasite, causing fever, weight loss, hepatosplenomegaly, and pancytopenia with anemia, thrombopenia, and immunosuppression. *Lymphadenopathy* is common in Sudan, and *hyperpigmentation* is observed in Indian patients with prolonged disease (*kala-azar*, "black fever" in Hindi). Occasionally, a cutaneous form of the disease appears, usually post-treatment, with multiple nodular lesions, in particular on the face, called post-kala-azar dermal leishmaniasis (PKDL). PKDL is unpredictable and variable, occurring in 50% of treated patients in East Africa and 5-15% of treated patients in India (153).

Diagnosis and Treatment: Both parasitological and immunological techniques are used for leishmaniasis diagnosis. Clinical differential diagnosis includes tuberculosis, carcinoma, and dermatomycoses in CL and malaria, syphilis, tuberculosis, typhoid fever, brucellosis, histoplasmosis, and schistosomiasis in VL. Parasitological techniques for Leishmania detection include a direct microscopic examination of Giemsa-stained skin biopsies, scrapings, and impression smears for both CL and MCL, and aspirates from lymph nodes, bone marrow, liver, and spleen for VL (137).

To detect and identify leishmania, amplification of leishmania DNA by polymerase chain reaction (PCR, PCR-RT, PCR-RFLP) is a useful diagnostic method (37); however, it is expensive for developing countries and technically demanding. Molecular techniques are also used to quantify parasite load, treatment monitoring, determination of virulence or drug resistance and parasite tracking in epidemiology.

Immunological techniques include Montenegro (leishmanin) skin test (Delayed Type Hypersensitivity), antigen detection in urine (by latex agglutination), serodiagnosis by indirect immunofluorescence and enzyme-linked immunosorbent assay

(ELISA). Rapid methods such as *rK-39 ICT* (Immunochromatography) and DAT (Direct Agglutination Test) are also used (125; 2). At present on the Indian subcontinent, rK-39 ICT (Immunochromatographic nitrocellulose strips test) based on serum or finger-prick has been introduced with the aim to diagnose VL earlier (131). However, it is invasive and requires phlebotomists and sterilized needles. Because of the high proportion of refusals from children and healthy persons, great difficulty arises in sampling blood; as an alternative, rK39-based immunochromatographic test (ICT) has been suggested.

First-line treatment for visceral leishmaniasis is pentavalent antimonials (Sodium Stibogluconate-Pentostam and Meglumine antimoniate-Glucantim), Amphotericin B, (Fungizone and its liposomal formulation AmBisome) and Pentamidine (28; 142).

Despite their toxicity, antimonials are widely used, but treatment failure has been reported especially in Bihar ($> 60\%$) and Sudan. For CL, pentavalent antimonials are the first choice and miltefosine, topical paromomycin, imiquimod, or antifungal azoles, are also used (33).

Control and Prevention: Due to the lack of available and efficient treatment means different control techniques have been introduced which target disease prevention. Leishmaniasis control is complicated due to the geographic diversity of vectors, parasites, and reservoirs as well as the limitation to identify breeding and resting sites.

Some general control methods for leishmaniasis include the application of insecticides and insect repellents, covering exposed skin, and avoiding contact with known disease reservoirs. For example, in India, the National Kala-Azar Elimination Program is based on Integrated Vector Management including Indoor Residual Spraying (IRS) of houses and cattle sheds (130), personal protection using insecticide treated nets (ITN) (99), and micro-environmental management (106). DDT

(dichlorodiphenyl-trichloroethane), is the primary insecticide used in Bihar (one of the most VL epidemic zones) due to low cost; however, the sandfly in India, *Phlebotomus argentipes* (Diptera: Psychodidae), is becoming resistant (19). Culling dogs have been trialed as a control in Brazil but were only effective when incorporated with other control techniques. In some regions, new dogs replaced those culled so quickly that the effect of culling alone was small, and the reservoir soon replenished (38).

One of the current focal points for leishmaniasis research is the engineering of suitable vaccines for both cutaneous and visceral strains. The antigenic variety of the different strains coupled with the complex life cycle of the leishmania protozoa make the development of a vaccine complicated, and results obtained so far have not yet proven sufficcently successful (66). Sandfly control is key for leishmaniasis control, helping also with the reduction of biting nuisance, control of Carrion's disease (*Borrelia bacilliformis*), and arboviruses transmitted by sandflies in endemic areas (117).

Epidemiology of Visceral Leishmaniasis(VL) and global burden: VL is a fatal vector-borne parasitic disease thought to infect an estimated 500,000 new cases annually and to cause about 57,000 deaths worldwide each year (52; 72; 97). It constitutes a serious public health risk in countries throughout the tropics, subtropics, and the Mediterranean basin, especially those countries that are the least developing in the world. More than 90% of VL transmission occurs in five countries: Nepal, India, Bangladesh, Sudan, and Brazil (north-eastern region) (72; 97; 141; 143), where the burden of the disease falls most heavily on the poor and young (children less than ten years old).

India alone accounts for almost 50% of the global VL disease burden, with an estimated annual incidence of 100–200,000 (36). Within India, the northeastern state

of Bihar accounts for 90% of all reported cases of VL, contributing approximately half of the world's annual new cases (67; 147; 102), with 30 districts within the state classified as endemic and an estimated 67.5 million people at risk of acquiring VL (35). India, Nepal, and Bangladesh – three VL-endemic countries – were committed to eliminating VL as a public health problem from the region by 2015. Their fail to meet the target to reduce the annual VL incidence to less than one new case per 10,000 inhabitants in all endemic districts (112).

VL causes the loss of thousands of lives and prolonged morbidity, posing a tremendous challenge to both public health and the social and economic development of Bihar (133). The actual disease load in Bihar is considered to be significantly higher as a result of under-reporting to government health authorities (35; 134; 4), and unidentified reservoirs in endemic foci (4; 134), with some estimates suggesting incidence is 2-2.5 times higher than recorded incidence and five times higher than officially reported cases (147; 4). The shifting geography and epidemiology of VL in Bihar has seen increasing rates of VL in urban settings, despite historically being considered a predominantly rural disease. Notwithstanding the success of several historical control programs, increased and sustained transmission has raised questions about the level of asymptomatic infection in urban populations and its role in maintaining a reservoir that contributes to re-emerging infection and endemic disease burden in cities.

History of Visceral Leishmaniasis Epidemic: Focal and sporadic cases of VL have been observed in the majority of Bihar districts since 1977, when effective surveillance systems were first able to capture the VL disease burden in the state (145). The resurgence of endemic VL came from a point of near total eradication in the 1950s, with the large-scale "Malaria Eradication Programme" in the Gangetic Basin, reducing VL significantly. Susceptible to the same insecticides as the *Anopheles* mosquito, the malaria vector, the DDT (29) and its impact on the sandfly population high-

lighted the susceptibility of the VL transmission cycle to well-executed control measures. Similar eradication programmes were also undertaken in 1991-92 and again showed positive results, but funding was discontinued after three years with a significant number of asymptomatic individuals serving as a reservoir for the resurgence of infection (29).

Responding to concerns regarding the discontinuation of funding from the State Government of Bihar and the subsequent increased VL prevalence, the Indian Ministry of Health assumed central government control for the VL "Eradication Programmes" in 2005. Responding to the scale of VL infection throughout the Indian subcontinent, including significantly increased prevalence in urban areas of Bihar, India also co-signed a memorandum of understanding with Nepal and Bangladesh to undertake additional measures to eliminate the disease as a public health problem, in conjunction with the World Health Organization, by 2015 (102; 29).

VL transmission in the Indian subcontinent is anthroponotic, human-sandfly-human cycle of transmission via subsequent blood meals of a sandfly. The causal agent and vector is the parasite *Leishmania donovani*, transmitted by female *Phlebotomus argentipes* sandflies. The geographical distribution of leishmaniasis is linked to some factors relating to its vector: the abundance and presence of infected sandflies, sandfly life cycle, and parasite reservoirs (97). Climate, living conditions, and socioeconomic status are associated with increased sandfly density (97; 90; 74), as are conditions commonly found in urban Bihar, including thatched housing constructed with mud, insecure structures, damp floors, poor sanitation, and the presence of domestic animals and animal dung. The number and density of *Phlebotomus argentipes* sandflies are seasonal, correlated with outside temperature and rainfall (111). They are predominantly peridomestic (46; 111) and are disproportionately found in areas of high social and economic deprivation (90; 18; 7). In addition to anthroponotic trans-

mission, there have also been small but significant reports of transmission through unscreened blood transfusions and transplacental transmission (132; 133).

Asymptomatic *L. Donovani* Infection: *L. donovani* infection leading to clinical VL is suspected to be present in only a small percentage of the infected population, with a large majority of *L. donovani* infections not leading to overt clinical disease (133; 35; 113). Many cross-sectional surveys based on serological testing show significant numbers of positive individuals who have never reported clinical disease or progressed to VL in Bihar (105; 61). The actual number of the proportion of *L. donovani* infections that results in clinical VL are poorly documented due to an absence of the required large prospective epidemiological studies and the difficulty of assessing the actual level of asymptomatic infection in VL-endemic areas. As humans are the only reservoir for the parasite (35), any successful control program must provide appropriate management for both symptomatic and asymptomatic individuals. As such, further information regarding the role of asymptomatic infection in how infected individuals will develop VL, and its role in the transmission of VL in Bihar, is required. For a summary of the life cycle of the *Leishmania donovani* parasite, see (72); for a summary of the Leishmania Donovani Life Cycle in and human host, see (72)

Ross-Macdonald model: In 1902, Sir Ronald Ross was awarded the second Nobel Prize in Medicine and Physiology for his co-discovery of the life-history of malaria. His contribution not only increased our understanding of the dynamics of this deadly parasite(*Plasmodium falciparum*), but it also allowed the scientific community, particularly the public health community, to raise new questions. Perhaps the most important one was, "Can we ameliorate the impact of malaria at the population level now that we understand vector-host-vector and host-vector-host transmission?". Ross began to address this issue with the help of his model, the first nonlinear model for

the dynamics of vector-borne diseases. A critical conclusion of his model, later modified and applied by George Macdonald 1957, was that it was enough to bring the vector populations below some critical threshold to improve, and possibly eliminate, malaria.

The Ronald Ross- Mac Donald model, is summarized by the following system

$$\begin{aligned} \frac{dx}{dt} &= \left(ab\frac{M}{N}\right) y\,(1-x) - rx \\ \frac{dy}{dt} &= ax\,(1-y) - \mu y \end{aligned} \tag{1.1}$$

where x denotes the proportion of infected humans, y the proportion of infected mosquitoes, a the per-capita mosquito biting rate, b the per-bite of mosquito to human transmission probability, c the per bite human to mosquito transmission probability, r the per-capita individual recovery at rate, and μ the per-capita mosquito death rate.

Critical to this effort is the identification of the basic reproduction number,

$$\mathcal{R}_0 = \frac{a^2 bc\frac{M}{N}}{\mu r} \tag{1.2}$$

which gives the average number of secondary infections generated by a vector(host) on the vector(host) population.

This model started the field of mathematical and computational epidemiology (26). It allowed for the beginning of the mechanism responsible for the transmission dynamics of malaria. Years later as noted in the 1911 paper of Ross, this work would be expanded to the study of Sexually transmitted diseases in humans (Cooke and York 1973, (32); Hethcote and Yorke 1984, (156)).

The models used in this dissertation are the offspring of the Ross-MacDonald model. We make particular references to the models of Christopher Dye (50; 49; 51; 48) and Anuj Mubayi, et al., (97).

This dissertation concentrates on extensively reviewing, collecting, and establishing parameter estimates to study VL in varying geographic regions, which is instrumental (or vital) to the public health approach to control. The following chapter carefully drives and incorporates the epidemiological features of VL that are significant to study the disease dynamics at a population level on a daily time scale. All the events between humans and sandflies are evaluated to construct a model that reflects the disease transmission process. The main contribution of the chapter is to establish a model for VL that captures the epidemiological dynamics of interacting human and sandfly populations.

Chapter 2

RISK FACTORS FOR HYPERENDEMIC VISCERAL LEISHMANIASIS

2.1 Introduction

Visceral Leishmaniasis is the most severe form of the Leishmaniasis family of diseases because death is inevitable if untreated (123). Each year, there are an estimated 500,000 new cases and approximately 50,000 recorded deaths worldwide within the 1 to 2 million newly reported VL cases (40).

A mathematical model is used here to identify factors that may affect the dynamics of VL given that we have access to datasets that allow us to carry out these analyses. The control reproductive number ($\mathcal{R}_C$), rather than the basic reproduction number, is estimated and is used to measure the disease's ability to colonize in a VL naive population and to estimate the level of endemicity in the presence of treatment, a long-standing practice in hyperendemic areas. The model guarantees disease persistence when $\mathcal{R}_C > 1$. The case when $\mathcal{R}_C < 1$ corresponds to disease eradication (149).

There have been limited studies of the dynamics of VL using mathematical models. In 1988, Christopher Dye and Daniel M. Wolpert introduced what appears to be the first anthroponotic VL deterministic model for capturing the temporal dynamics. Their model was used to explain the observed VL inter-epidemic periods between 1875 and 1950 in Assam, India. Dye, C. et. al, (1992; 1996) later assessed the impact of control measures in endemic areas using appropriately modified models (49; 51; 48). The authors concluded that the observed dramatic upswing in VL cases might be attributed to "intrinsic"(host and vector dynamics birth, and death rates, immunity) factors (50). Recent studies have quantified the spatial distribution of

underreporting levels for VL in India (97).

The current study focuses exclusively on the transmission dynamics of VL in an area where control practices are common and long standing. The approach simplifies the epidemiology and considers two disease stages, asymptomatic and symptomatic. Since VL is hyperendemic in the regions considered, a model with traditional treatment is considered, as it captures the status quo. This is an essential assumption, since untreated individuals die relatively quickly. Parameters (transmission, death rates, etc.) are estimated for the VL model system under the per-capita treatment denoted by θ_h.

Here, we review the literature on VL data, estimate parameters for selected distributions for VL epidemiological parameters, and identify risk factors that may be crucial to the dynamics of VL.

2.2 Methods and Materials

2.2.1 Modeling Framework

The *Leishmania donovani* transmission cycle is anthroponotic and takes place from human to human via the bite of an infective female phlebotomine sandfly. A mathematical model of the transmission dynamics of VL infection is used here where the interacting populations of hosts and vectors are assumed to mix homogeneously. $N_h(t)$ denotes the density of humans and $N_v(t)$ the density of sandflies. The transmission dynamics of VL between populations is shown schematically in Figure 3.1. The dynamics within the human population are modeled using five compartments incorporating the number of susceptible individuals ($S_h(t)$), asymptomatic individuals ($A_h(t)$), individuals infectious with VL ($I_h(t)$), hospitalized individuals ($T_h(t)$), and recovered-immune to reinfection ($R_h(t)$); $N_h = S_h + A_h + I_h + T_h + R_h$. The sandfly

population is assumed to be divided into susceptible ($S_v(t)$) and infectious ($I_v(t)$), with $N_v = S_v + I_v$. The equations are:

$$\begin{aligned}
\frac{dS_h}{dt} &= \Lambda_h - \lambda_{vh} S_h - \mu_h S_h \\
\frac{dA_h}{dt} &= \lambda_{vh} S_h - (\phi_h + \mu_h) A_h \\
\frac{dI_h}{dt} &= \phi_h A_h - (\theta_h + \mu_h) I_h \\
\frac{dT_h}{dt} &= \theta_h I_h - (\gamma_h + \mu_h) T_h \\
\frac{dR_h}{dt} &= \gamma_h T_h - \mu_h R_h
\end{aligned} \tag{2.1}$$

$$\begin{aligned}
\frac{dS_v}{dt} &= \Lambda_v - \lambda_{hv} S_v - \mu_v S_v \\
\frac{dI_v}{dt} &= \lambda_{hv} S_v - \mu_v I_v
\end{aligned} \tag{2.2}$$

Some of The Risk Factors Captured in the Model	
Ecological	**Parameter**
Daily exposure to sandfly bites	b
Proportion of sandfies that successfully land on human host	ℓ
Natural mortality of sandfies	μ_v
Epidemiological	**Parameter**
Average time of treatment	ϕ
Average duration of asymptomatics	θ
Transmission probability of sandfly to human given a bite	β_{vh}
Transmission probability of human to sandfly given a bite	β_{hv}
Demographic	**Parameter**
Natural mortality in the human host	μ_h

Table 2.1: Risk Factors Associated With Demographic, Epidemiological, Ecological Factors.

Disease-induced mortality is not included because, due to institutionalized treatment, deaths from VL are negligible. For simplicity, the human population is assumed to be constant. Λ_h denotes the recruitment rate into the susceptible population, and μ_h

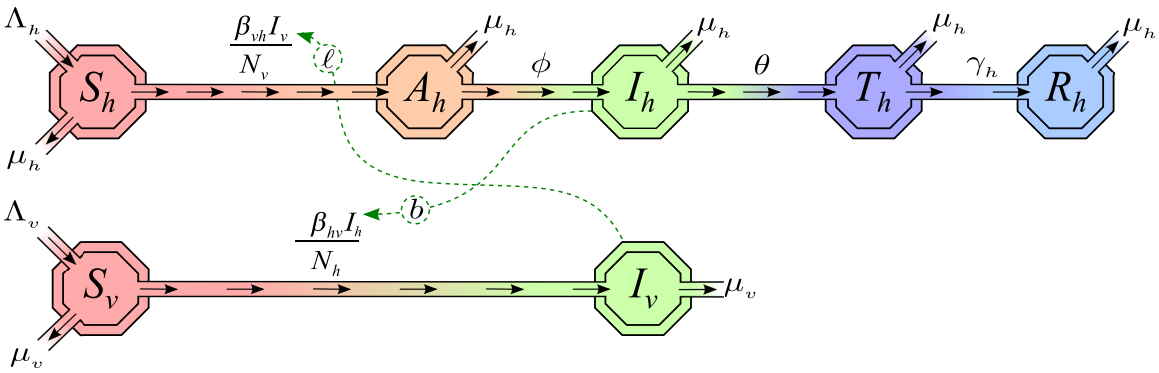

Figure 2.1: A Schematic Representation of The Mathematical Modeling Framework Consisting of Interacting Human(N_h) and sandfly(N_v) Population. Arrows Represent Transition Between Different Infection Stages in the Two Populations.

denotes the per-capita death rate. Because N_h approaches $\frac{\Lambda_h}{\mu_h}$ when t approaches ∞, we assume, without loss of generality, that $N_h = \frac{\Lambda_h}{\mu_h}$ (25). A susceptible individual acquires the *Leishmania Donovani* parasite following an effective contact with an infectious sandfly. The rate λ_{vh}, the force of infection on humans, is given by

$$\lambda_{vh} = b\beta_{vh}\frac{N_v}{N_h}\frac{I_v}{N_v} = b\, m_{v:h}\, \beta_{vh}\frac{I_v}{N_v}, \tag{2.3}$$

where the right-hand expression (Equation 2.3) is given by the product of the per-vector daily biting rate of sandflies (b), the VL infection transmission probability, given a bite from an infected sandfly to human (β_{hv}), the average number of sandflies per humans $m_{v:h}$, and the proportion of infectious sandflies in the vector population ($\mathrm{I_v}/\mathrm{N_v}$). It is assumed that all newly VL-infected humans go through a asymptomatic (symptomless) stage (A_h). After an asymptomatic period of several months, humans develop clinical symptoms at the per capita rate ϕ_h, moving to the infectious class I_h. During the infectious period, humans will seek VL treatment at the per capita rate θ_h, proper treatment leads to recovery at the per capita rate γ_h (recovered individuals gain lifelong immunity). Newly emerging adult female sandflies are recruited into the susceptible population at rate Λ_v and die at the per-capita rate μ_v. The sandfly population is assumed constant. A susceptible sandfly is infected following an effec-

tive contact with infectious humans at the per capita rate λ_{hv} (force of infection on sandflies). The rate λ_{hv} is given by

$$\lambda_{hv} = b\beta_{hv}\frac{I_h}{N_h}, \tag{2.4}$$

where the right-hand side is the product of: the per vector daily biting rate (b); the probability that susceptible sandflies acquire the *Leishmania* parasite while feeding on a VL-infected individuals (β_{hv}); the proportion of VL infectious humans in the human population ($\mathrm{I_h}/\mathrm{N_h}$). It is also assumed that the *Leishmania* parasite has no impact on an infected sandfly's lifespan; the sandflies' natural mortality per-capita rate is the same for infected and uninfected, namely, μ_v. See Appendix A for complete model derivation.

2.2.2 Incidence as a Function of the Landing Rates

We use landing rate data to estimate the transmission probabilities from sandfly to humans (β_{hv}) and humans to sandflies (β_{hv}). The section provides a careful derivation of incidence rates, as a function of landing and biting rates, using data on the landing rates.

The human incidence rate is a function of the average contact rate, which in turn is directly proportional to the proportions of infectious sandfly $\left(\frac{I_v^*}{N_v^*}\right)$. Letting b denote the average number of bites per sandfly per unit time and ρ the average number of bites received per human per unit time, and assuming that all sandfly bites are to humans only, we must have that the total number of bites made by all sandflies per unit of time (bN_v^*) equals the total number of bites received by all human hosts per unit of time (ρN_h^*). Thus, we have that

$$bN_v^* = \rho N_h^* \Rightarrow \rho = b\frac{N_v^*}{N_h^*}, \quad \text{(constant by assumption)} \tag{2.5}$$

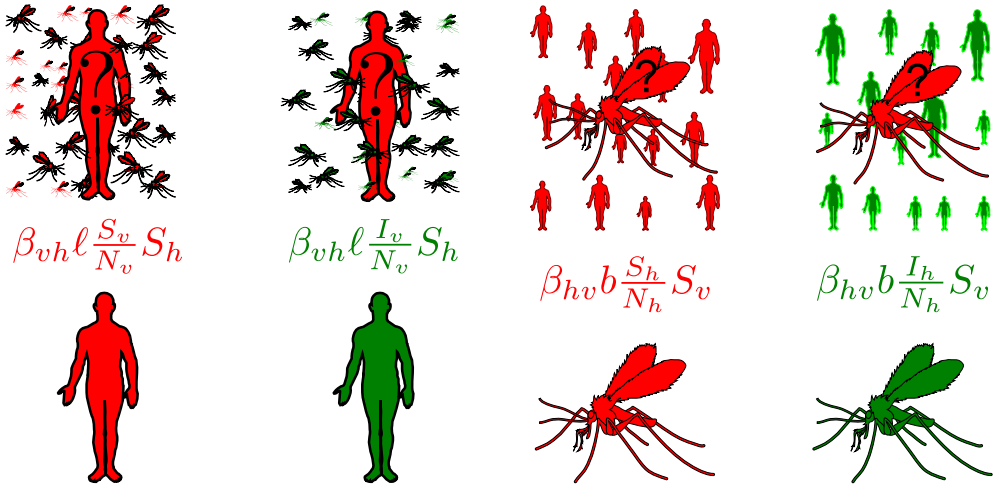

(a) Sandfly on Humans (b) Human to Sandflies

Figure 2.2: Illustration of the Possibilities of Success and Failure of Transmission of VL Infection: 2.2a From Sandfly to Humans and 2.2b From Human To Sandflies. Green Depicts Infection While Red Depicts Non-Infection. Human In (A) And Sandfly (B) Represent Missing Transmission Rates.

The assumption that ρ is constant is customary in the literature because the host vector ratio is not, in general, constant over time (but see (150)). We further assume that the average total number of bites received by a human per unit time is directly proportional to the sandfly landing rate ℓ ($\rho \propto \ell$). Based on the fact that contacts between susceptible host and susceptible vector populations do not result in infection, we consider only the terms where the contacts are between susceptible host/vector and infected vector/host populations. Because the total effective landing/feeding of vectors on a susceptible human is a function of the total vector population, which includes both susceptible and infected vectors, we can assume that the transmission rate is given by

$$\beta_{vh}\ell\left(\frac{S_v}{N_v}+\frac{I_v}{N_v}\right)S_h, \tag{2.6}$$

where β_{vh} is the per-person transmission efficiency (i.e., probability that infection is successfully transmitted from vector to human given an infected bite). Note that

$\beta_{vh}\ell$ is the number of effective landings per unit time, while $\beta_{vh}\ell\frac{I_v}{N_v}$ is the proportion of bites that result in infection. Therefore, $\beta_{vh}\ell\frac{S_v}{N_v}$ is the proportion of bites that get "wasted" since they cannot generate infections, as illustrated in Figure 2.2a. Similarly, we can derive the infection rate in the vector population generated by infected humans. If we let β_{hv} be the per-person transmission efficiency from human to vector (i.e., transmission probability per bite on infectious humans that leads to infection in a susceptible sandfly), then, given that the average number of landings of susceptible vectors on the susceptible and infectious humans, we can conclude that the transmission rate is

$$b\beta_{hv}\left(\frac{S_h}{N_h}+\frac{I_h}{N_h}\right)S_v, \tag{2.7}$$

where $b\beta_{vh}S_v\frac{I_h}{N_h}$ is the proportion of bites that result in infection and $b\beta_{vh}S_v\frac{S_h}{N_h}$ is the proportion that do not, and therefore, $\beta_{vh}bS_v$ is the total effective landing/feeding rate per unit of time (day), as illustrated in Figure 2.2b.

2.2.3 Data Sources

Several data sources are used to generate point estimates and ranges for the model parameters needed to calibrate our model, which is later used to assess and compare the potential of VL outbreaks in two hyperendemic areas: India and Sudan. The epidemiological data, used in calculating the number of yearly cases and deaths, was obtained from the World Health Organization, the Bihar State Health Society, and Rajendra Memorial Research Institute of Medical Sciences. Epidemiological and demographic parameter estimates were taken from the literature and census reports when available (4; 5; 101). The review of the literature led to two distinct sets of estimates for some of the VL epidemiological quantities. The parameter estimations in this chapter are carried out by region involving two data sets (A and B).

2.3 Analysis

In this section, we derive from the model an expression for the average number of secondary infections generated by an infected individual (referred here as the control reproduction number), as well as expressions for the prevalence of different types of the populations. We also discuss the procedures used for estimating model parameters.

2.3.1 Control Reproduction Number ($\mathcal{R}_C$) of VL

The control reproduction number ($\mathcal{R}_C$) is defined as the average number of secondary infections caused by a single infective individual (assumed infectious) when introduced into a wholly susceptible population of size $N \approx S_0$ in a system where treatment (θ_h) is continuously available (20; 149; 42; 89).

$\mathcal{R}_C$ is calculated using the next generation operator approach (149; 21; 20) a process that requires the computation of the matrix of new infection terms $\mathbf{F}$ and the matrix of transition between compartments $\mathbf{V}$. The $\mathcal{R}_C$ is the spectral radius of the next generation matrix, $\rho\left(\mathbf{F}\mathbf{V}^{-1}\right)$ (see Appendix A for a derivation). The control reproduction number of the model in terms of treatment θ_h is given by

$$\mathcal{R}_C\left(\theta_h\right) = \sqrt{\left(\frac{\phi_h}{(\mu_h+\phi_h)} \times \frac{\beta_{vh}\ell}{(\mu_h+\theta_h)}\right) \times \left(\frac{b\beta_{hv}}{\mu_v}\right)} \tag{2.8}$$

where ℓ is the landing rate on a human, b is the biting rate per sandfly, and β_{vh} is the number of infections generated by one infected vector per unit of time. The expression in Equation 2.8 is referred to as the control reproduction number because it depends on treatment control, given by the parameter θ_h. $\mathcal{R}_C\left(\theta_h\right)$ is the geometric mean of two reproduction numbers

$$\mathcal{R}^{hv}\left(\theta_h\right) = \tfrac{\phi_h}{(\phi_h+\mu_h)} \cdot \tfrac{\ell\beta_{vh}}{(\theta_h+\mu_h)} \quad \text{and} \quad \mathcal{R}^{vh} = \tfrac{b\beta_{hv}}{\mu_v} \tag{2.9}$$

where $\mathcal{R}^{hv}(0)$ is the number of secondary infections caused in humans by a single typical infectious sandfly when accessing an entirely susceptible population and $\mathcal{R}^{vh}$ denotes the number of secondary infections caused in female sandflies by a typical infected human. $\mathcal{R}_C$ is the expected number of secondary infections caused by an infectious human or infectious sandfly over the course of the entire infectious period in a wholly susceptible population of size $N_h \approx S_h$ and $N_v \approx S_v$, with access to treatment. From point onward we will denote $\mathcal{R}_{CI}$ and $\mathcal{R}_{CS}$ as the control reproduction numbers for set A and B respectively.

The analysis of Model (2.1)–(2.2) shows that the model has two equilibria (the Disease-Free Equilibrium (DFE) and Endemic Equilibrium (EE)).

Remark 2.3.1. The DFE of Model (2.1)–(2.2) always exists and is locally and globally asymptotically stable (LAS) if $\mathcal{R}_C < 1$ and unstable if $\mathcal{R}_C > 1$ (see Appendix A.2.3 for proof).

Remark 2.3.2. The EE exists and is locally and globally asymptotically stable only when $\mathcal{R}_C > 1$ (see Appendix A.2.3 for proof).

2.3.2 Parameter Robustness Analysis

We assess risk using $\mathcal{R}_C$ and endemic prevalences. Studying the sensitivity of $\mathcal{R}_C$ with respect to model parameters is critical if we wish to identify the pressure points of the system; that is, the parameters that are most sensitive, i.e., those that generate the largest changes in the dynamics sensitive parameters represent the ideal target points for intervention. Parameter uncertainty (UA) and sensitivity (SA) analyses are used to assess the robustness of the model results as a function of the lack of precision in the estimated model parameters. The analyses rely on Latin Hypercube Sampling (LHS) (Mckay et al., 1979; Blower and Dowlatabadi 1994; Marino et al., 2008 (94; 17; 92)) and require the computation of the Partial Rank

Correlation Coefficient (PRCC), a sensitivity index of the output quantities with respect to each parameter (Marino et al., 2008 (92)). The LHS scheme includes the generation of a stratified random sampling that ensures a complete exploration of the feasible parameter space. In the sampling, an input parameter X with a pre-defined probability distribution function (PDF) is divided into N equiprobable subintervals. From each subinterval, a value is sampled. The N values for this parameter are randomly paired with the corresponding N values of every other parameter generated in the same way. The PRCC is used to measure the degree of linear association between two parameters from a set of parameters, after the influence of linearity from all other parameters of the set has been eliminated (92). The calculated PRCCs and corresponding p-values are used to identify the input parameters sensitivity rank of the input parameter to the output variable. The PRCC value of each inputed parameter is considered statistically significant, with p-value < 0.05 if it satisfies $|\text{PRCC}| > 0.5$.

Multiple data sources and reports were considered as we proceeded to obtain point estimates for each parameter associated with $\mathcal{R}_C$ and prevalence expressions from the model. These point estimates were later used to obtain parameter values for the pre-selected theoretical distribution used for generating random parameter samples. We assess the impact of variation in each of the uncertain model parameters and its level of influence on the estimates of $\mathcal{R}_C$ as well as its prevalence of different populations.

2.3.3 Parameter Estimation

A thorough review of the literature and field studies on the epidemiology of VL was conducted and used to identify model parameter estimates and their possible ranges; we use this information to pre-select a reasonable distribution for each parameters (87; 54; 138; 155; 45). Because of significant variations in data from the literature,

two sets of data for parameters were used in this study. We refer to the two sets of parameters as data set A and data set B (Table 2.2). We developed an estimation procedure for calibrating parameters (includes parameters related to transmission probabilities) for which precise data could not be obtained from the literature. In Section 2.3.4 we provide a detailed discussion that uses the procedures for estimating transmission probabilities of the model for the two data sets.

2.3.4 Estimating the Transmission Probabilities

Lack of effective surveillance case identification and case management results in under-reporting and adds to the uncertainties associated with parameter estimates. A survey of the literature on mathematical epidemiology studies on VL revealed that data to estimate transmission probabilities of VL is limited. Hence, we derived two different approaches to estimate transmission probabilities. The two estimation approaches depend on model-generated expressions for the endemic components of the endemic equilibrium and the control reproduction number($\mathcal{R}_C$). The endemic equilibrium is given by

$$E^* = \left(\frac{\Lambda_h \left(b\phi_h \, \beta_{hv} \mu_h + G_1 G_2 \mu_v \right)}{b\phi_h \, \left(\ell \, \beta_{vh} + \mu_h \right) \beta_{hv} \mu_h}, \frac{\Lambda_h \left(\mathcal{R}_C^2 - 1 \right) G_2 \mu_v}{b\phi_h \, \left(\ell \, \beta_{vh} + \mu_h \right) \beta_{hv}}, \frac{A_h^* \phi_h}{G_2}, \frac{A_h^* \phi_h \, \theta_h}{G_2 G_3}, \frac{\Lambda_h \Lambda_v}{S_h^* \mu_h \mu_v \mathcal{R}_C^2}, \right.$$
$$\left. \frac{A_h^* \phi_h \, \theta_h \, \gamma_h}{G_2 G_3 \mu_h}, \frac{\mu_h \beta_{hv} b I_h^* S_v^*}{\mu_v \Lambda_h} \right) \tag{2.10}$$

where $G_1 = \phi_h + \mu_h$, $G_2 = \theta_h + \mu_h$, and $G_3 = \gamma_h + \mu_h$. The VL infected components of the endemic equilibrium are:

$$\mathcal{A}_h^* = \frac{\Lambda_h \left(b\ell \beta_{hv} \beta_{vh} \phi_h - G_2 G_3 \mu_v \right)}{\beta_{hv} \left(\ell \beta_{vh} + \mu_h \right) G_2 b \phi_h} \geq 0 \tag{2.11}$$

$$\mathcal{I}_h^* = \frac{\Lambda_h \left(b\ell \beta_{hv} \beta_{vh} \phi_h - G_2 G_3 \mu_v \right)}{\beta_{hv} \left(\ell \beta_{vh} + \mu_h \right) G_3 G_2 b} \geq 0 \tag{2.12}$$

$$\mathcal{I}_v^* = \frac{\Lambda_v \left(b\ell \beta_{hv} \beta_{vh} \phi_h - G_2 G_3 \mu_v \right) \mu_h}{\ell \beta_{vh} \left(b \beta_{hv} \mu_h \phi_h + G_2 G_3 \mu_v \right) \mu_v} \geq 0 \tag{2.13}$$

Table 2.2: Parameter Estimates for Human and Phlebotomus in Data Sets A and B

Parameter	Defination	Units	Mean (ranges)	References	Mean (ranges)	References
Human Population			**Data set A Estimates**		**Data set B Estimates**	
β_{vh}	Transmission probability when infected sandflies bite susceptible human	Dimensionless	0.0004 (0.0007–0.001)	Estimated	0.0001 (0.00004–0.00016)	Estimated
μ_h	Human daily per capita natural mortality rate	day^{-1}	4.302e-5 (4.08e-5–4.55e-5)	Est. (see App. B)	4.3e-5 (4e-5–4.54e-5)	Est. (see App. B)
ϕ_h	Per capita development rate of clinical symptoms	day^{-1}	0.0098 (0.006–0.0167)	(105; 147; 103; 29; 140)	0.0098 (0.0042–0.0167)	(62; 22; 29; 65)
θ_h	Per capita treatment rate of infectious humans	day^{-1}	0.0351 (0.0067–0.0597)	(1; 12; 13)	0.0143 (0.0027–0.0408)	(3; 127; 31; 100; 95; 78)
$\mathcal{P}_{\mathcal{I}_h}$	Point prevalence in humans	number	(0.0024–0.0027)	(136)	(0.0006–0.0013)	Est. (see App. B)
Sandfly Population			**P. Argentipes**		**P. orientalis**	
β_{hv}	Transmission probability when susceptible sandfly bite infected humans	Dimensionless	0.397 (0.13–0.49)	(138; 139)	0.25 (0.12–0.4)	Estimated
b	Average number of bites per sandfly	day^{-1}	0.7997 (0.1667–2.083)	(45; 87)	1.6208 (0.35–3.3583)	(54)
ℓ	Sandfly landing rate on human	day^{-1}	6.21 (3.47–9.9)	(77)	32 (15.7–48.3)	(54)
μ_v	Adult sandfly daily per capita mortality rate	day^{-1}	0.0833 (0.0667–0.1)	(128; 74; 84; 109; 138)	0.0857 (0.1–0.0714)	(59; 68)
$\mathcal{P}_{\mathcal{I}_v}$	Point prevalence in sandflies	number	(0.0085–0.0284)	(146)	(0.019–0.05)	(59)

The data sets A and B for known parameters, prevalence data from the literature, and expressions $\mathcal{I}_h^*$ (3.3) and $\mathcal{I}_v^*$ (3.4) are used to generate estimates (distribution) for the transmission probabilities (β_{vh} and β_{vh}). The expressions of the components of the endemic equilibrium (the infectious components, $\mathcal{I}_h^*$ (3.3) and $\mathcal{I}_v^*$ (3.4) of the equilibrium E^*(2.10))

$$\begin{aligned}\mathcal{P}_{\mathcal{I}_h} &= \frac{\mathcal{I}_h^*}{N_h^*} \\ &= \frac{\left(b\ell\beta_{hv}\beta_{vh}\phi_h - G_2G_3\mu_v\right)\mu_h}{\beta_{hv}\left(\ell\beta_{vh}+\mu_h\right)G_3G_2b}\end{aligned} \tag{2.14a}$$

$$\begin{aligned}\mathcal{P}_{\mathcal{I}_v} &= \frac{I_v^*}{N_v^*} \\ &= \frac{\left(b\ell\beta_{hv}\beta_{vh}\phi_h - G_2G_3\mu_v\right)\mu_h}{\ell\beta_{vh}\left(b\beta_{hv}\mu_h\phi_h + G_2G_3\mu_v\right)}\end{aligned} \tag{2.14b}$$

are used in developing the estimation procedures.

Approach 1

Fixing all model parameters and assuming that the human and vector prevalences are known, we isolate β_{hv} and β_{vh} from the equations (2.14a) and (2.14b) and obtain estimates of the transmission probabilities:

$$\beta_{hv} = \frac{\mu_v\mathcal{P}_{\mathcal{I}_v}}{b\mathcal{P}_{\mathcal{I}_h}\left(1-\mathcal{P}_{\mathcal{I}_v}\right)} \tag{2.15a}$$

$$\beta_{vh} = \frac{G_1G_2\mathcal{P}_{\mathcal{I}_h}\mu_h}{\ell\,\mathcal{P}_{\mathcal{I}_v}\left(\phi_h\,\mu_h - G_1G_2\mathcal{P}_{\mathcal{I}_h}\right)} \tag{2.15b}$$

where β_{vh} is well-defined iff $\frac{\phi_h\,\mu_h}{G_1G_2} > \mathcal{P}_{\mathcal{I}_h}$.

Approach 2

Now suppose the estimate of $\mathcal{R}_C$ is known. Rewriting the equations 2.14a and 2.14b in terms of $\mathcal{R}_C$, we obtain:

$$\mathcal{P}_{I_h} = \frac{\mu_h\left(\mathcal{R}_0^2-1\right)}{\mu_h\mathcal{R}_0^2+\ell\beta_{vh}} \tag{2.16a}$$

$$\mathcal{P}_{I_v} = \frac{\left(\mathcal{R}_0^2-1\right)\mu_h}{\mu_h\mathcal{R}_0^2+\ell\beta_{vh}} \tag{2.16b}$$

.

Isolating β_{vh} and β_{hv} from (2.16a) and (2.16b) leads to

$$\beta_{hv} = \frac{\mu_v\mathcal{P}_{\mathcal{I}_v}}{b\mathcal{P}_{\mathcal{I}_h}\left(1-\mathcal{P}_{\mathcal{I}_v}\right)} \tag{2.17a}$$

$$\beta_{vh} = \frac{\mu_h\left(1+\left(1-\mathcal{P}_{\mathcal{I}_v}\right)\mathcal{R}_0^2\right)}{\ell\mathcal{P}_{\mathcal{I}_v}} \tag{2.17b}$$

.

	Data set A			Data set B		
Parameters	Min	Mean	Max	Min	Mean	Max
Fixed						
b	-	2.08	-	-	1.6208	-
μ_h	-	4.54e-5	-	-	4.3e-5	-
μ_v	-	0.0833	-	-	0.0857	-
ϕ_h	-	0.00975	-	-	0.0098	-
θ_h	-	0.0083	-	-	0.0143	-
Varied						
$\mathcal{P}_h$	0.0024	-	0.0027	0.0013	-	0.0015
$\mathcal{P}_v$	0.0054	-	0.0157	0.054	-	0.037
ℓ	8.68	12.15	17	15.7	32	48.3
$\mathcal{R}_C$	1.3	2.0	2.1	1.1	1.3	1.5
Estimates using Approach 1						
β_{hv}	0.13	0.3	0.49	0.12	0.25	0.4
β_{vh}	0.0003	0.0008	0.003	4.8e-05	0.00013	0.0005
Estimates using Approach 2						
β_{hv}	0.13	0.397	0.49	0.12	0.25	0.4
β_{vh}	0.0004	0.0007	0.001	0.00004	0.00013	0.00016

Table 2.3: Summary of Estimates of the Transmission Probabilities, β_{hv} and β_{vh}, Using the Two Approaches with Mean and Ranges for Other Parameters (Table 2.2) for data sets A and B were fixed. Empty cells indicates vlues not used in the procesure.

2.4 Results from Global Uncertainty and Sensitivity Analyses

Parameter uncertainty and sensitivity analyses are performed on the reproduction number ($\mathcal{R}_C$) and the prevalence of the infected populations ($\mathcal{P}_{\mathcal{A}_h}$, $\mathcal{P}_{\mathcal{I}_h}$, and $\mathcal{P}_{\mathcal{I}_v}$).

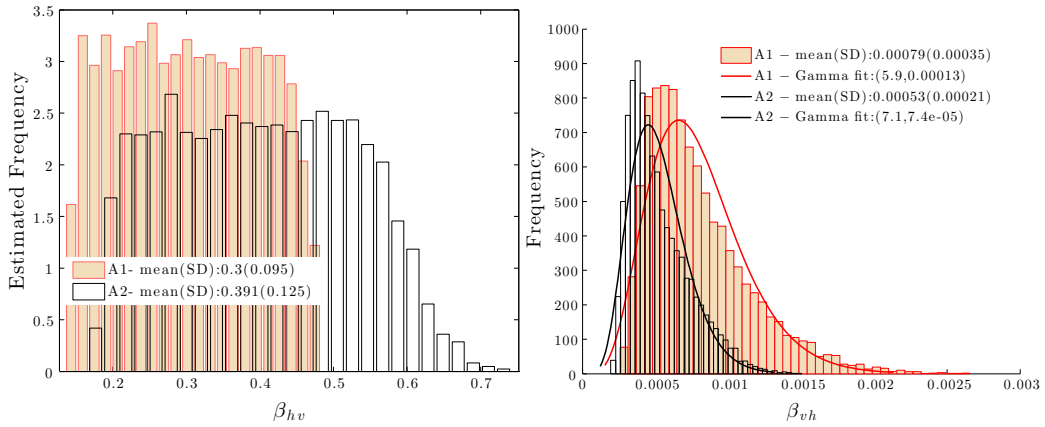

(a) Data Set A Estimate: β_{hv} (b) Data Set A Estimate: β_{vh}

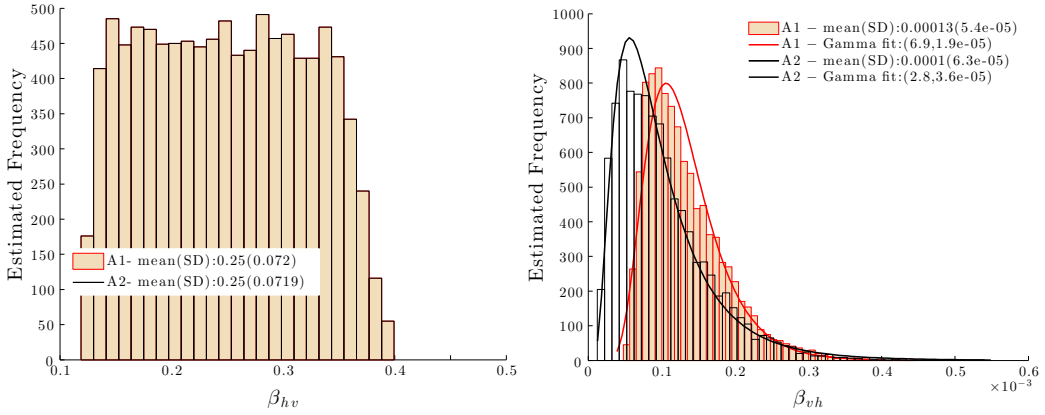

(c) Data Set B Estimates: β_{hv} (d) Data Set B Estimates: β_{vh}

Figure 2.3: Estimated Distribution of β_{vh} and β_{hv}, Respectively, for Data Set A, (a–b) and Data Set B, (c–d). A1(A2) Represent The Distribution Obtained Using Approach 1(Approach 2). A Visual Comparison of the Fitted Gamma Curve Together with the Model Obtained Estimated Transmission Probabilities Transmission Probabilities β_{vh}

The analyses used to assess which of the eight input parameters (b, ℓ, β_{hv}, β_{vh}, μ_h, μ_v, ϕ_h, and θ_h) are most relevant for disease dynamics. We assign a PDF to each of the eight parameters (See Table 2.4). For landing and biting rate of sandflies, denoted by b and ℓ, respectively, we obtained a triangular distribution by fitting to field data (shown in the Appendix B). The parameters, β_{vh} and ϕ_h were assigned a gamma distribution based on prior experience (Mubayi et al. (97)). The gamma distribution was found to be a best fit to the sample estimates of β_{vh} obtained using

our estimation procedure and an expression in Equation 3.5a (Figure 2.3b). In the case of the parameters β_{hv}, θ_h, μ_h, and μ_v we chose a uniform distribution, using the minimum and maximum estimates from the literature to determine their ranges. Similarly, for β_{hv}, the sample point estimates generated using Equation 2.15b are used to obtain a best-fit uniform distribution (Figure 2.3a). For each of the eight parameters with assigned probability distributions, sample sizes of $10,000$ values were randomly generated over ten independent realizations. Using LHS technique, for each of the realizations, we paired the first N samples of the first column with N samples from the second parameter randomly. After all, eight parameters were paired without replacement; an LHS matrix was generated with its rows and columns corresponding to samples and parameters, respectively. Each row of the LHS matrix was considered to generate one estimate of $\mathcal{R}_C$ using Equation 2.8. Thus, an $N \times p$ matrix was generated by the LHS method (where p represents number of parameters on which $\mathcal{R}_C$ depends), resulting in N samples for $\mathcal{R}_C$ in each realization.

2.4.1 Assessment of VL Related Parameters for Data Set A

We performed uncertainty and sensitivity analysis on the control reproductive number $\mathcal{R}_C$, the endemic prevalences, $\mathcal{P}_{\mathcal{A}_h}$, $\mathcal{P}_{\mathcal{I}_h}$, $\mathcal{P}_{\mathcal{I}_v}$ for data set A.

Uncertainty and Sensitivity Analysis on $\mathcal{R}_{C_I}$ Using Data Set A

The estimated distribution of $\mathcal{R}_{C_I}$ from the uncertainty analysis, is shown in Figure 2.5a. The mean estimate of $\mathcal{R}_{C_I}$ is found to be 2.1, with a standard deviation of 1.14. The sensitivity analysis of $\mathcal{R}_{C_I}$ provides the ranking of parameters based on their influence on $\mathcal{R}_{C_I}$. The parameter ranking in decreasing order of influence shows that θ_h, is the most sensitive, followed by ℓ, β_{hv}, β_{vh}, and b; the least sensitive are ϕ_h, followed by μ_v (Figure 2.5e).

Uncertainty and Sensitivity Analysis on the Endemic Infected Prevalence Using Data Set A

We perform uncertainty and sensitivity analyses on the point endemic prevalence for the infected populations $\mathcal{P}_{\mathcal{A}_h}$, $\mathcal{P}_{\mathcal{I}_h}$, and $\mathcal{P}_{\mathcal{I}_v}$. The estimated distributions of prevalence are shown in Figures 2.5b–2.5d. The mean estimate of $\mathcal{P}_{\mathcal{A}_h}$ was found to be 0.0038, with a standard deviation of 0.0025. The parameter ϕ_h was found to be the most influential parameter on the prevalence of asymptomatic individuals, $\mathcal{P}_{\mathcal{A}_h}$. The remaining parameters in descending order of magnitude of PRCC are, θ_h, ℓ, β_{hv}, β_{vh}, and μ_v and μ_h being the least sensitive parameters to $\mathcal{P}_{\mathcal{A}_h}$. The sensitivity analysis performed on $\mathcal{P}_{\mathcal{I}_h}$ reveal that the treatment rate θ_h is the most influential parameter when the goal is to change disease prevalence. The mean estimates of vector prevalence were found to be 0.0054, with a standard deviation of 0.0053. From our sensitivity analysis of $\mathcal{P}_{\mathcal{I}_v}$ we observe in Table 2.5 and Figure 2.5h, the four most influential parameters. These parameters, in decreasing order of rank, are θ_h, β_{vh}, b,

Parameter	Data set A	Data set B
b	$\mathcal{T}\,(0.8, 1.6, 2.5)$	$\mathcal{T}\,(0.35, 1.8, 3.4)$
ℓ	$\mathcal{T}\,(0.55, 8.3, 17)$	$\mathcal{T}\,(16, 32, 48)$
ϕ_h	$\mathcal{G}\,(5.5470, 0.0021)$	$\mathcal{G}\,(5.2727, 0.0018)$
β_{vh}	$\mathcal{G}(7e^{-5}, 7.5e^{-5})$	$\mathcal{G}(6.3e^{-5}, 3.7e^{-5})$
β_{hv}	$\mathcal{U}\,(0.16, 0.73)$	$\mathcal{U}\,(0.12, 0.42)$
θ_h	$\mathcal{U}\,(0.0014, 0.0167)$	$\mathcal{U}\,(0.0082, 0.0329)$
μ_h	$\mathcal{U}\,(4.1e^{-5}, 4.5e^{-5})$	$\mathcal{U}\,(4e^{-5}, 4.5e^{-5})$
μ_v	$\mathcal{U}\,(0.0667, 0.1250)$	$\mathcal{U}\,(0.071, 0.1)$

Table 2.4: Initial Assigned Distributions of the Model Parameters for Data Sets A and B. Where Triangular: $\mathcal{T}(min, mode, max)$, Gamma: $\mathcal{G}(shape, scale)$, and Uniform: $\mathcal{U}\,(min, max)$.

and μ_v.

Output	$\mathcal{R}_{C_I}$		$\mathcal{P}_{\mathcal{A}_h}$		$\mathcal{P}_{\mathcal{I}_h}$		$\mathcal{P}_{\mathcal{I}_v}$	
Rank	*Parameter*	*PRCC*	*Parameter*	*PRCC*	*Parameter*	*PRCC*	*Parameter*	*PRCC*
1	θ	−0.88	ϕ	−0.87	θ	−0.95	θ	−0.96
2	ℓ	0.83	θ	−0.66	ℓ	0.56	β_{vh}	0.89
3	β_{hv}	0.80	ℓ	0.57	β_{hv}	0.55	b	0.77
4	β_{vh}	0.76	β_{hv}	0.55	β_{vh}	0.49	μ_v	−0.69
5	b	0.58	β_{vh}	0.50	b	0.33	μ_h	0.17
6	μ_v	−0.49	b	0.34	μ_v	−0.27	ℓ	−0.03
7	μ_h	0.01	μ_v	−0.27	μ_h	0.11	ϕ	−0.01
8	ϕ	0.004	μ_h	0.13	ϕ	−0.01	β_{hv}	−0.01

Table 2.5: Shows the PRCCs by Rank of Importance for the Input Parameters of the Output Value $\mathcal{R}_C$, $\mathcal{P}_{\mathcal{A}_h}$, $\mathcal{P}_{\mathcal{I}_h}$, and $\mathcal{P}_{\mathcal{I}_v}$ for Data Set A. (*) Denotes PRCCs that are Non-Significant.

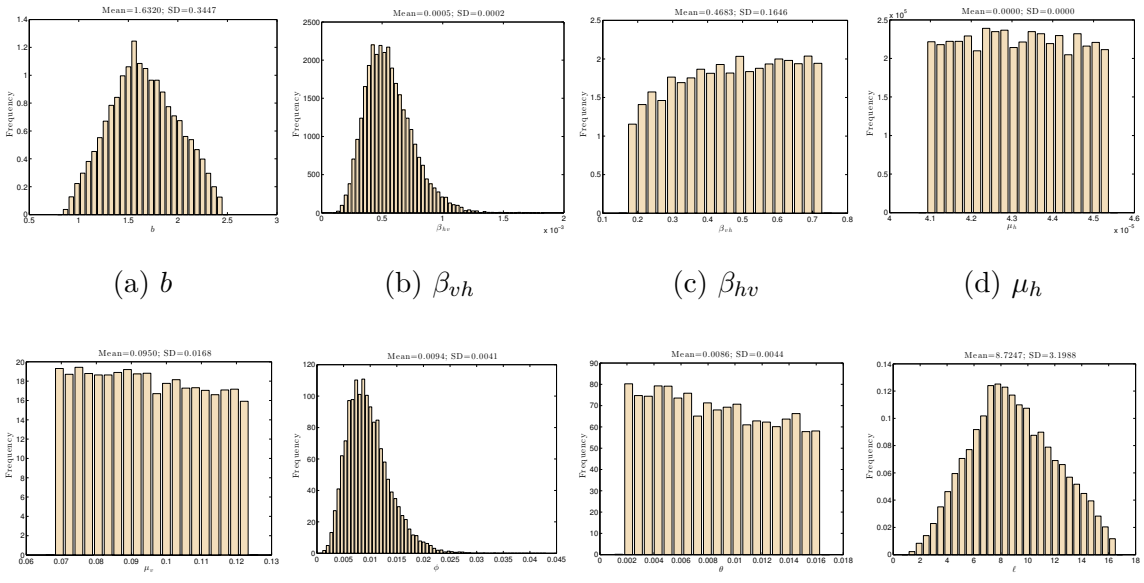

(a) b (b) β_{vh} (c) β_{hv} (d) μ_h

(e) μ_v (f) ϕ_h (g) θ_h (h) ℓ

Figure 2.4: Parameter Distributions Conditional on $\mathcal{R}_C > 1$ for Data set A Obtained from Uncertainty Analysis of the Prevalence

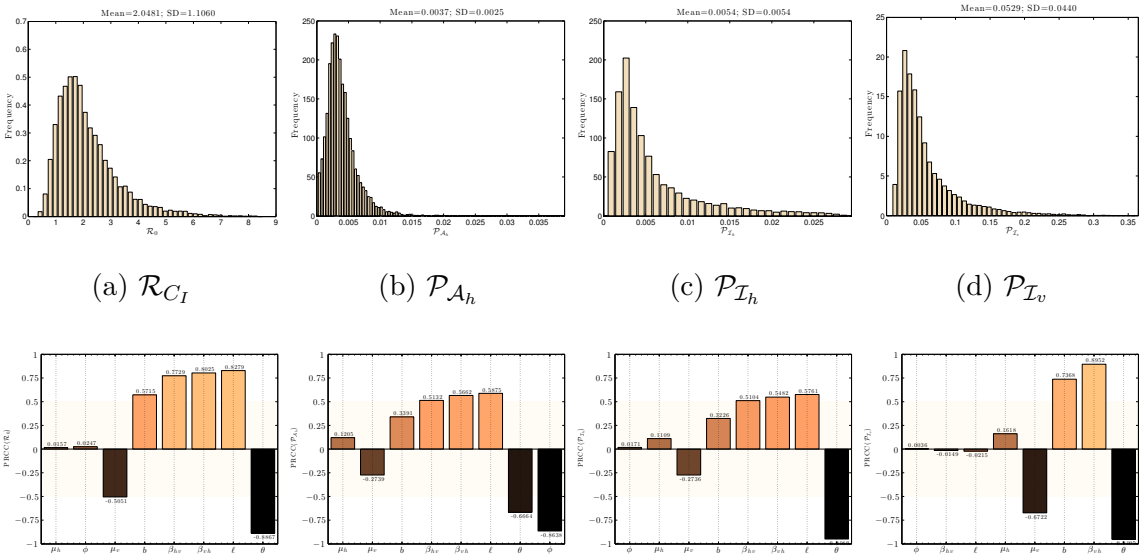

(a) $\mathcal{R}_{C_I}$ (b) $\mathcal{P}_{\mathcal{A}_h}$ (c) $\mathcal{P}_{\mathcal{I}_h}$ (d) $\mathcal{P}_{\mathcal{I}_v}$

(e) PRCCs($\mathcal{R}_{C_I}$) (f) PRCCs($\mathcal{P}_{\mathcal{A}_h}$) (g) PRCCs($\mathcal{P}_{\mathcal{I}_h}$) (h) PRCCs($\mathcal{P}_{\mathcal{I}_v}$)

Figure 2.5: Uncertainty Analysis of the (2.7a) Reproduction Number and the (2.7b –2.7d) Prevalence of Asymptomatics, Infectious Humans and Infectious Sandflies, Respectively. Tornado Plot Showing Partial Rank Correlation Coefficients (PRCCs) of the (2.7e) Reproduction Number and the (2.7f –2.7h) Prevalence in Asymptomatics, Infectious Humans and Infectious Sandflies, Respectively.

2.4.2 Assessment of VL-Related Parameters for Data Set B

Similarly, we performed uncertainty and sensitivity analysis on the control reproductive number $\mathcal{R}_{C_S}$ and the endemic prevalences $\mathcal{P}_{\mathcal{A}_h}$, $\mathcal{P}_{\mathcal{I}_h}$, $\mathcal{P}_{\mathcal{I}_v}$ for data set B.

Uncertainty and Sensitivity Analysis on the Control Reproduction Number ($\mathcal{R}_{C_S}$) Using Data Set B

The results of the uncertainty analysis on $\mathcal{R}_{C_S}$ are shown in Figure 2.7a, where the mean estimate of $\mathcal{R}_{C_S}$ is 1.45, and the standard deviation is 0.57. From Table 2.6 and Figure 2.7a, we observe ranking of each parameter based on its sensitivity on $\mathcal{R}_{C_S}$. In decreasing order: b, β_{hv}, θ_h, β_{vh}, and ℓ. The first negatively correlated parameter was θ_h, which indicated that measure in estimates of treatment will result in a decrease

in $\mathcal{R}_{C_S}$ estimates. The top two most positively sensitive parameters to $\mathcal{R}_{C_S}$ were β_{hv} and b.

Output	$\mathcal{R}_{C_S}$		$\mathcal{P}_{\mathcal{A}_h}$		$\mathcal{P}_{\mathcal{I}_h}$		$\mathcal{P}_{\mathcal{I}_v}$	
Rank	*Parameter*	*PRCC*	*Parameter*	*PRCC*	*Parameter*	*PRCC*	*Parameter*	*PRCC*
1	b	0.88	ϕ	−0.83	θ	−0.92	θ	−0.92
2	β_{hv}	0.87	β_{hv}	0.66	β_{hv}	0.72	b	0.91
3	θ	−0.86	θ	−0.65	b	0.71	β_{vh}	0.90
4	β_{vh}	0.85	b	0.64	β_{vh}	0.69	μ_v	−0.56
5	ℓ	0.72	β_{vh}	0.63	ℓ	0.53	μ_h	0.21
6	μ_v	−0.43	ℓ	0.47	μ_v	−0.29	β_{hv}	−0.04
7	μ_h	−0.02	μ_v	−0.25	μ_h	0.12	ℓ	−0.01
8	ϕ	0.01	μ_h	0.09	ϕ	0.02	ϕ	−0.01

Table 2.6: The PRCCs by Rank of Importance for the Input Parameters of the Output Values of $\mathcal{R}_{C_S}$, $\mathcal{P}_{\mathcal{A}_h}$, $\mathcal{P}_{\mathcal{I}_h}$, and $\mathcal{P}_{\mathcal{I}_v}$ for Data set B. (*) Denotes $p < 0.01$.

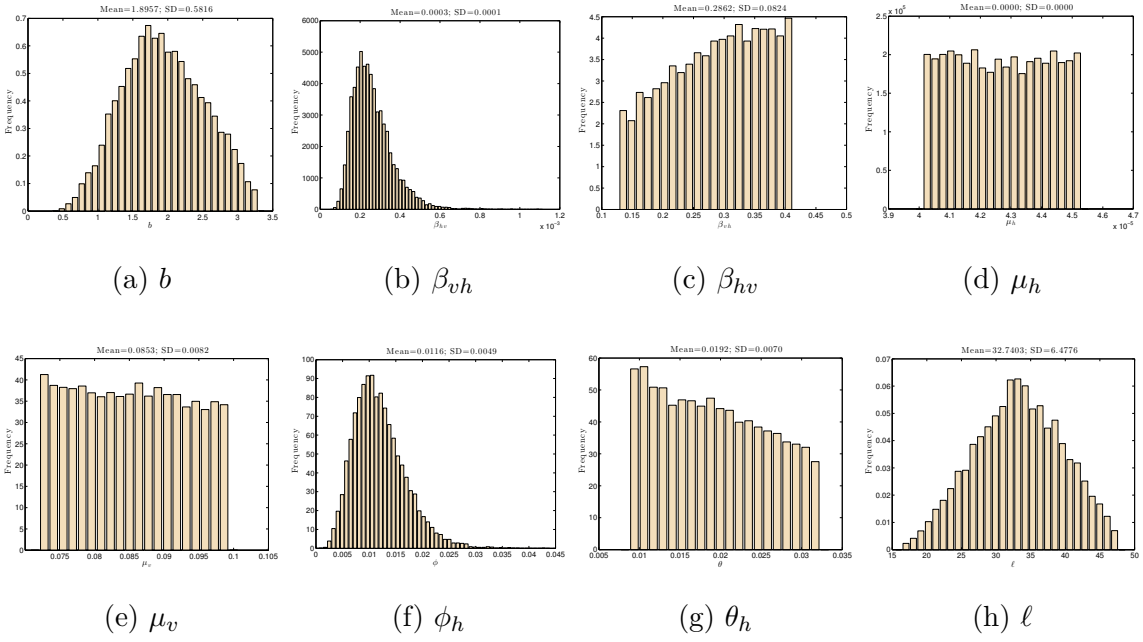

(a) b (b) β_{vh} (c) β_{hv} (d) μ_h

(e) μ_v (f) ϕ_h (g) θ_h (h) ℓ

Figure 2.6: Estimated Distributions of the Model Parameters Conditional on $\mathcal{R}_{C_S} > 1$ for Data set B Obtained from Uncertainty Analysis of the Prevalence

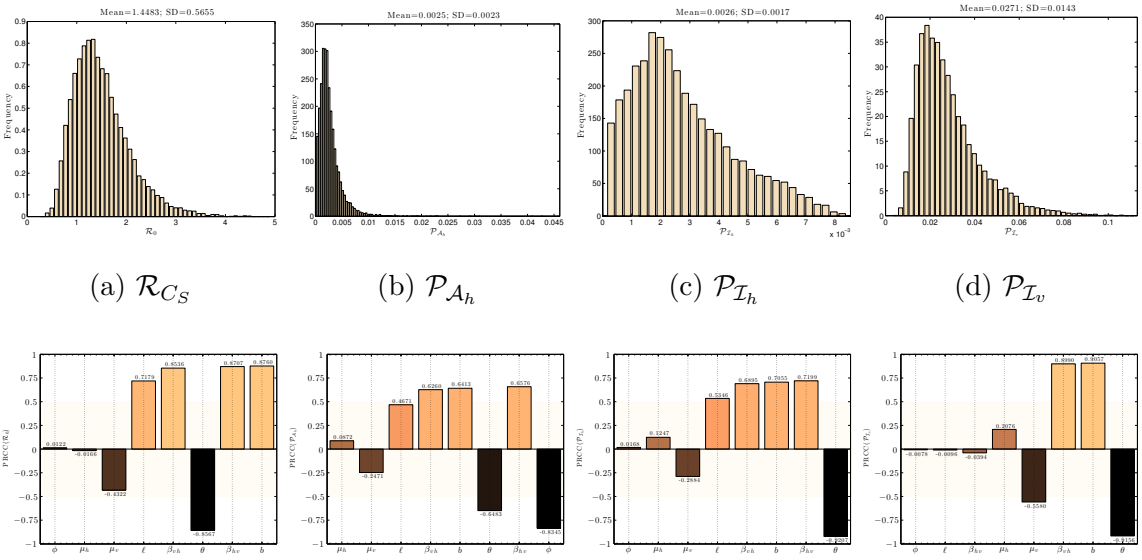

(a) $\mathcal{R}_{C_S}$ (b) $\mathcal{P}_{\mathcal{A}_h}$ (c) $\mathcal{P}_{\mathcal{I}_h}$ (d) $\mathcal{P}_{\mathcal{I}_v}$

(e) PRCCs($\mathcal{R}_{C_S}$) (f) PRCCs($\mathcal{P}_{\mathcal{A}_h}$) (g) PRCCs($\mathcal{P}_{\mathcal{I}_h}$) (h) PRCCs($\mathcal{P}_{\mathcal{I}_v}$)

Figure 2.7: Results for Data set B: Uncertainty Analysis of the (2.7a) Reproduction number and the (2.7b –2.7d) Prevalence of Asymptomatics, Infectious Humans and Infectious Sandflies, Respectively. Tornado Plot Showing Partial Rank Correlation Coefficients (PRCCs) of the (2.7e) Reproduction Number and the (2.7f–2.7h) Prevalence of Asymptomatics, Infectious Humans and Infectious Sandflies, Respectively.

Uncertainty and Sensitivity Analysis on the Endemic Infected Prevalence Using Data Set B

In the case of the asymptomatic prevalence $\mathcal{P}_{\mathcal{A}_h}$, we estimated its mean value as 0.0024 with a standard deviation 0.0018. The estimated distribution of $\mathcal{P}_{\mathcal{A}_h}$ for data set B is shown in Figure 2.7b. From Table 2.6 and Figure 2.7f, we observe that the $\mathcal{P}_{\mathcal{A}_h}$ is negatively correlated and most sensitive to ϕ_h, followed by β_{hv}, θ_h, b, β_{vh}, and ℓ. The natural death rates, μ_h and μ_v in humans and sandflies, respectively, were the least sensitive input parameters to $\mathcal{P}_{\mathcal{A}_h}$. From uncertainty analysis on $\mathcal{P}_{\mathcal{I}_h}$ (Figure 2.7c), we found the average prevalence estimate to be 0.0026, with a standard deviation of 0.0017. The results of our sensitivity analysis are summarized in Table 2.6 and displayed in Figure 2.7g, shows that the treatment rate of infectious humans is most sensitive to changes in θ_h, which is not surprising. The infection related parameters

β_{hv}, b, β_{vh}, and ℓ also play a dominant role on disease persistence. Finally, the results of the uncertainty analysis on the prevalence of infection in sandflies, $\mathcal{P}_{\mathcal{I}_v}$, are shown in Figure 2.7d. The estimated sample mean of $\mathcal{P}_{\mathcal{I}_v}$ is 0.0271, with a standard deviation of 0.0143. Our analysis identified the parameter's sensitivity to changes in $\mathcal{P}_{\mathcal{I}_v}$ (Table 2.6 and Figure 2.7h). The results show that the treatment rate, θ_h is the most dominant parameters, followed by b, β_{vh}, and μ_v. The less influential parameters on $\mathcal{P}_{\mathcal{I}_v}$ are μ_h, ℓ, ϕ_h, and β_{vh}.

2.5 Discussion

The risk factors associated with VL are complex and ambiguous. In the face of this uncertainty, the systematic evaluation of ongoing VL elimination programs is essential. Literature searches were carried out using public health databases, cross-sectional and cohort studies, government reports, and information from patients at Rajendra Memorial Institute of Medical Sciences. There was limited available longitudinal data due to a lack of regional publications with information. Further, because most data studies in the literature did not provide information on participant selection criteria, did not for confounding variables, and fail to make use of a single diagnostic test as proof of infection, modeling was our only choice. We used multiple data sets to get a plausible guess estimate on the ranges of the parameters.

To the best of our knowledge, this is the first study that reviews, evaluates, and makes use of an extensive collection of available data on epidemiological and ecological parameters in the context dynamics of Visceral Leishmaniasis (VL), a project that identifies risk factors using mathematical models. The objectives of this systematic modeling analysis are to detect and classify risk factors for VL use of the best available field evidence and data. This research may help reduce knowledge gaps of VL transmission dynamics. The sources of data were used to estimate parameters

and uncertainty and to address sensitivity light of the selected model. The dynamics of the model depend on the VL control reproductive number ($\mathcal{R}_C$), which measures the likelihood and severity of an outbreak. The estimated value of the VL control reproductive number was found to be 2.01 data set A and 1.14 data set B. Uncertainty analysis on $\mathcal{R}_C$ also showed that there were eight parameters (see Table 2.2) that should be taken into consideration when assessing the uncertainty associated with the risk of increasing levels of VL. The parameter sensitivity analysis on $\mathcal{R}_C$ suggests that the biting rate, the average number of vectors per person in a given day, the probability of infection transmission between vector and humans, and the treatment rate are the most influential parameters associated with the complex disease transmission cycle involving sandflies and humans for both countries.

The results are based on the model's parameter estimates that were collected or estimated from current and available VL data reports. The study was limited by available data as well as by the period used to collect the data. Several of the parameter value we found in the literature.

Chapter 3

COMPARISON OF RISKS ASSOCIATED WITH VL IN INDIA AND SUDAN

This chapter presents a comparative analysis using our model and available data of the hyperendemic VL regions in India and Sudan. Specifically, parameter estimates are used to assess and compare the VL burden in regions in India and Sudan. The most recent report estimates that there are between 200,000 and 400,000 annual cases of VL in six countries, with India supporting between 146,700 to 282,000 cases per year, and Sudan supporting between 15,700 and 30,300 cases per year (14).

In this chapter, we study the impact of risk factors that are critical for surveillance of VL for India and Sudan. In India, the sandfly species *Phlebotomus argentipes* is primarily responsible for transmitting the *L. donovani* parasite (116). The Indian state of Bihar is one of the worse affected by VL. In Bihar, cross-sectional studies have shown that annual patterns of high VL incidence are driven by factors that include seasonal fluctuations of the sandfly population, lack of health care resources and extreme poverty (97; 80); Malnutrition has also been shown to be a factor, with VL outbreaks, verified by studying deviations from the endemic level, occurring in regions in India where catastrophic events (such as flooding) resulted in food shortages (5). In Sudan, a variety of studies on vector entomology and epidemiology have been used to establish that *Phlebotomus orientalis* is the dominant sandfly vector associated with anthroponotic *L. donovani* transmission (155; 126; 68; 69; 55; 58). Typically, *P. Orientalis* is considered a forest species, and its abundance is frequently associated with the presence of the savanna woodland tree species *Acacia Seyal* and *Balanites aegyptiaca* as well as deeply cracked vertisols (black cotton soil) (55; 56). Primary risk factors for VL infection in Sudan include genetic factors (e.g., some indigenous

individuals may be more susceptible (5)), age, ethnicity, and poverty (23). Outbreaks also seem connected to the dynamics of massive population movements in endemic regions or areas facing war or political instability, accompanied by labor migrations for economic security reasons (118; 5).

In Bihar, where 90% of India's VL cases occur, aggressive attempts at improving vector control programs via the distribution of insecticide-treated bed nets and insecticide spraying are being carried out (5). India's Kala-Azar Elimination Programs (KAEP) aims at reducing VL morbidity and is tied into government-funded VL diagnosis and drug treatment programs. Pentavalent antimonial drugs, wherever effective, purchased by the public sector are barely sufficient to cover half of the infected patients (97; 4). The State of Bihar in India reports approximately 270,900 cases every year with an incidence rate of 21 cases per 1000 (72). The state of Bihar includes 21 districts among the 38 that are most affected in India.

VL is also endemic in southern, central, and eastern Sudan, with 6,957 cases reported in the state of Gedaref (near the Ethiopian border) during 2010 (82). Limited drug availability and drug resistance are growing problems in East Africa, particularly in Sudan, where antimonials are still the primary method of VL medical treatment. The poor must travel long distances to gain access to drugs and, consequently, the effectiveness of intervention policies are limited. Infected Sudanese often must wait extended periods of time before receiving minimal medical care (104). In a field study conducted by Burza, et al. in 2014, access to treatment was fund to be crucial in controlling VL (24). In both India and Sudan, the presence of livestock near or in the household was high risk for VL transmission. The materials used for building homes in both countries, such as mud and straws, serve as the natural sites for sandfly breeding.

There are four primary drugs available for VL treatment in Asia and East and

West Africa. In India and Sudan, the effectiveness of these drugs varies if measured by treatment outcome, efficiency, and availability (29). The primary drugs for VL treatment in India are liposomal amphotericin B after the first line treatment; pentavalent antimonial drugs, over the years, became drug resistant to the Leishmania parasite (86). In Sudan, the two primary drugs for VL are sodium antimony gluconate (SAG) and Liposomal Amphotericin B (86). In India, a single dose of Liposomal Amphotericin B is sufficient for treatment, but in Sudan higher dose is needed for complete treatment (29).

The most effective drugs for treating VL require cold storage facilities that are either missing or only available in limited numbers in VL-affected areas. Poor access to medical services often translates into low treatment rates in some regions (24). Additional, factors associated with disease transmission are landing rate, the average daily biting rate per human, and the transmission probabilities between human and sandflies. In India, houses with mud-plastered walls, straw houses, and the ownership and rearing of livestock (such as goats, cattle, buffalo, etc.) are all considered as high-risk factors for VL (134). The risk may be greater when a large number of individuals lived with animals (e.g., when animals are kept indoors to avoid theft(134). Livestock plays a crucial role in attracting sandflies and the increase in VL transmission probabilities (10). Staying with a family member who had a previous history of VL has also been shown to be a risk factor (134; 115). One of the major contributing factors for VL infection in Sudan is living and playing in the dark or in proximity to forested trees. In Sudan, the *P. Orientalis*, the primary vector for *L. Donovani* transmission, is closely associated with the presence of the *Acacia Seyal* and *Balanites Aegyptiaca*, tree species commonly found in the region (11; 53; 100). Additional risk factors include houses in proximity to caves, crevices, animal burrows, and termite mounds where *P. Orientalis* usually breeds (96).

$\mathcal{R}_C$ estimates for India and Sudan, a rough attempt at integrating reported biological and ecological field data to VL transmission in both countries, are used in the analysis presented in this chapter. The goal is to compare and contrast quantitative differences of VL in two ecologically distinct regions of the world, India and Sudan. The section collects the mathematical tools employed for comparative assessment for understanding VL dynamics.

3.1 Methods and Material

A model capturing VL transmission dynamics between human and sandfly populations is used to compare the risks associated with VL in India and Sudan. The model includes human and vector epidemiological states and the transition between states (shown in Figure 3.1). The model variables and parameters are defined in Table 2.2. The model control reproduction number in terms of treatment θ_h is

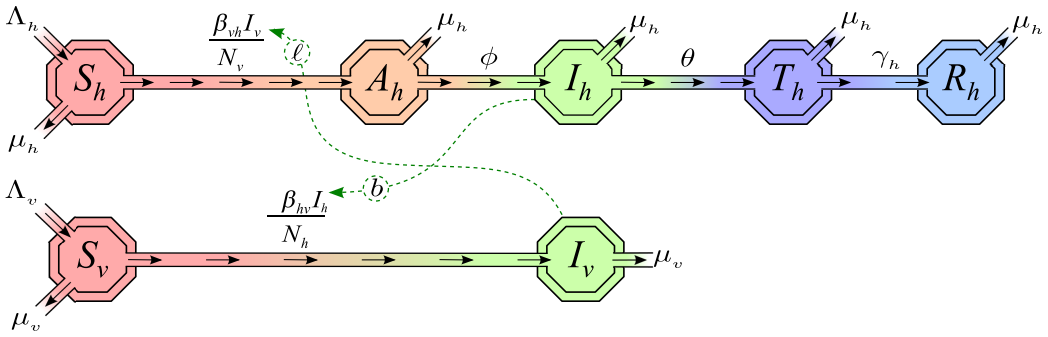

Figure 3.1: A Schematic Representation of the Mathematical Modeling Framework Consisting of Interacting Human(N_H) And Sandfly(N_V) Population. Arrows Represents Transition Between Different Infection Stages in the Two Populations.

$$\mathcal{R}_C^2(\theta_h) = \left(\frac{\phi_h}{(\mu_h+\phi_h)} \cdot \frac{\beta_{vh}\ell}{(\mu_h+\theta_h)}\right) \cdot \left(\frac{b\beta_{hv}}{\mu_v}\right) \tag{3.1}$$

The expression $\frac{\phi_h}{(\mu_h+\phi_h)} \cdot \frac{\beta_{vh}\ell}{(\mu_h+\theta_h)}$ is the average number of new cases vectors generated by one infected human and $\frac{b\beta_{hv}}{\mu_v}$ represents the average number of new cases in humans produced by one infected vector. The expression in Equation 4.7 is referred to as the

control reproduction number because it depends on the parameter θ_h. The model has two equilibria: the disease free state and the endemic equilibrium. When $\mathcal{R}_C > 1$, the model has stable endemic states that depend on other model parameters.

In the current hyperendemic regions of India and Sudan, we have, at the current estimated levels of treatment, that $\mathcal{R}_{C_I}(\theta_h) > \mathcal{R}_{C_S}(\theta_h) > 1$. That is, estimates of the control reproductive number for India $\mathcal{R}_{C_I}(\theta_h)$ are in general greater than those of Sudan $\mathcal{R}_{C_S}(\theta_h)$.

3.1.1 Endemic Equilibrium

The three infected components of our endemic equilibrium derived from our model express the prevalence of asymptotic humans, symptomatic humans and infected vectors:

$$A_h^* = \frac{b\ell\,\Lambda_h\Lambda_v\beta_{hv}\beta_{vh}\phi_h - G_1G_2N_hN_v\mu_h{\mu_v}^2}{\beta_{hv}\,\phi_h\,(\ell\,\Lambda_v\beta_{vh} + N_v\mu_h\mu_v)\,G_1b} \geq 0 \tag{3.2}$$

$$I_h^* = \frac{b\ell\,\Lambda_h\Lambda_v\beta_{hv}\beta_{vh}\phi_h - G_1G_2N_hN_v\mu_h{\mu_v}^2}{\beta_{hv}\,(\ell\,\Lambda_v\beta_{vh} + N_v\mu_h\mu_v)\,G_2G_1b} \geq 0 \tag{3.3}$$

$$I_v^* = \frac{b\ell\,\Lambda_h\Lambda_v\beta_{hv}\beta_{vh}\phi_h - G_1G_2N_hN_v\mu_h{\mu_v}^2}{\ell\,\beta_{vh}\,(b\Lambda_h\beta_{hv}\phi_h + G_1G_2N_h\mu_v)\,\mu_v}. \geq 0 \tag{3.4}$$

Using the infectious components of the endemic states, and the control reproduction number, we get (as in Chapter 2):

$$\beta_{hv} = \frac{\mu_v\mathcal{P}_{\mathcal{I}_v}}{b\mathcal{P}_{\mathcal{I}_h}\,(1-\mathcal{P}_{\mathcal{I}_v})} \tag{3.5a}$$

$$\beta_{vh} = \frac{G_1G_2\mathcal{P}_{\mathcal{I}_h}\mu_h}{\ell\,\mathcal{P}_{\mathcal{I}_v}\,(\phi_h\,\mu_h - G_1G_2\mathcal{P}_{\mathcal{I}_h})}. \tag{3.5b}$$

These expressions of the transmission probabilities are used to obtain their estimates using estimates of $\mathcal{R}_C$ and estimates of prevalences from literature.

3.1.2 Data Sources and Sensitivity Analysis

Data on the number of cases for Sudan and India for the 1989 to 2010 period (4; 5) are shown in Figure 3.2. Data sources on the sandflies' biting rate were taken from field studies concentrated on the landing and biting behavior of the *P. Argentipes* and *P. orientalis* (87; 45; 54). In the case of the species of *Phlebotomus* sandflies, most of the parameter estimates were taken from data collected via field studies in parasitology and ecology found in the literature (87; 45; 54). Other epidemiological data was also collected for India and Sudan.

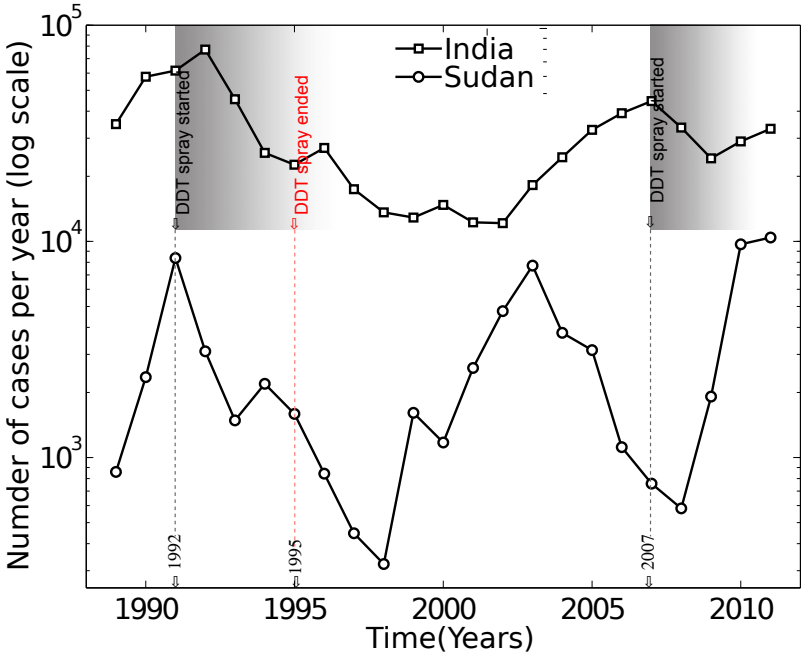

Figure 3.2: Trends of Visceral Leishmaniasis Cases in India and Sudan Over the Past 23 Years (4; 5). The Trends In India is Order In Magnitude Higher Than the Trends in Sudan. Also Shows Implementation of Major Intervention at Various Time Points.

Global parameter uncertainty and sensitivity analyses are performed on the Control reproduction number $\mathcal{R}_C$ and on the prevalences of symptomatic affected populations to assess which of the eight input parameters (b, $m_{h:v}$, β_{hv}, β_{vh}, μ_h, μ_v, ϕ_h, and θ_h) are most important for disease dynamics and control. We assign a probabil-

ity density function (PDF) to each of the eight parameters using available data. A uniform distribution was used along with data from the literature to sample values for the parameters b, μ_v, $m_{h:v}$, β_{vh}, β_{hv}, μ_h, and μ_v. The parameters ϕ_h, and θ_h were sampled from a gamma distribution based on prior experience (Mubayi, et al. (97)). For each of the eight parameters with assigned probability distributions, sample sizes of $10,000$ values were generated using LHS technique and randomly paired. For each 8-tuplets of 10,000 sample sets, the outcome variables $\mathcal{R}_C$, $\mathcal{P}_{A_h}$, $\mathcal{P}_{I_h}$, and $\mathcal{P}_{I_v}$ were computed using data from the respective countries. The estimated mean value of $\mathcal{R}_C$ for India was found to be approximately 2; the average value for Sudan was 1.4. Determine that India has the highest estimated incidence in the world (146,700 to 282,800/year) doubles Sudan having the highest in Africa (15,700 to 30,300/year) (5; 4), is not enough unless we can re-scale them appropriately to make any conclusions on differences in $\mathcal{R}_C$ values. These estimates of $\mathcal{R}_C$ confirm the current status of VL in India and Sudan. The difference in the magnitude of $\mathcal{R}_C$ may be attributable to the fact that India carries a much greater burden of all new VL cases (almost 50%).

The PRCCs were calculated for each country to quantify the sensitivity of model parameters on the $\mathcal{R}_C$ estimates. PRCC values above $+5$ or below -5 were considered significant. The parameters b, m_{hv}, β_{vh}, and β_{hv} with positive PRCC values indicate positive impact the value of $\mathcal{R}_C$. The parameter θ_h plays a negative role on the value of $\mathcal{R}_C$; that is, an increase in θ_h results in a decrease in $\mathcal{R}_C$ estimate.

3.1.3 Statistical Tests

The 2-sample t-test (Two–sample t-test, ttest2, Matlab routine $ttest2(x1, x2)$) was used to test if mean estimated values representing various VL-related quantities for the two countries are associated with each other. Following the 2-sample t-test, non-parametric analysis was conducted to compare estimated distributions of param-

eters for the two countries using the Kolmogorov–Smirnov test (Kolmogorov–Smirnov (KS)–test, Matlab routine $kstest2(x1, x2)$). In both tests, the $P - value < 0.05$ was considered significant.

3.2 Results from Comparative Assessment of VL in India and Sudan

Parameter estimates were obtained either from the literature or estimated from field data, and were used for an evaluation of country-specific risks. The risk quantified differences and similarities in VL disease burden in India and Sudan. In this section, we conduct the comparative assessment by studying the impact of the change in parameter estimations on VL disease burden in two countries when risk is measured either regarding $\mathcal{R}_C$ or in terms of the prevalence of infection. The final assessment took into account uncertainty and sensitivity analyses.

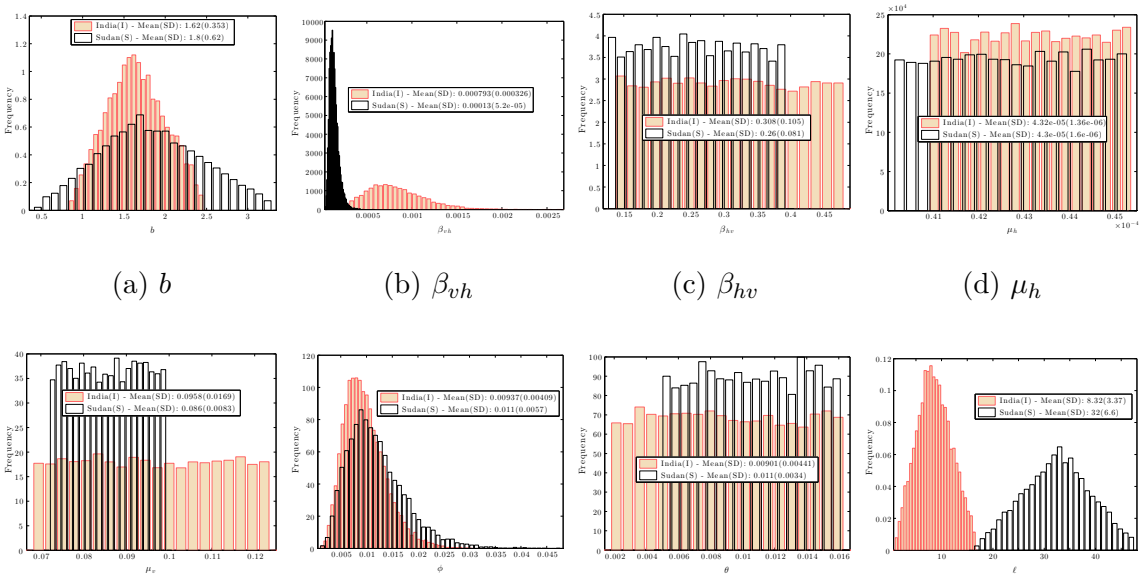

(a) b (b) β_{vh} (c) β_{hv} (d) μ_h

(e) μ_v (f) ϕ_h (g) θ_h (h) ℓ

Figure 3.3: A Comparison of Initially Assigned Distributions in Table 2.4 for Model Parameters (a) b, (b) β_{vh}, (c) β_{hv}, (d) μ_h, (e) μ_v, (f) ϕ_h, (g) θ_h and (h) ℓ Used in the Sensitivity and Uncertainty Analyses for the Indian and Sudan Populations

3.2.1 *Comparison When Risk is Defined Based on the Control Reproduction Number*

The observed difference in the mean estimate of $\mathcal{R}_{C_I}$ (≈ 2.01) and $\mathcal{R}_{C_S}$ (≈ 1.45) supports the observed higher levels of endemicity (almost more than 40%) in India compared to Sudan. Statistical tests were carried out to identify any significant differences in estimated means of $\mathcal{R}_C$ for India and Sudan ($H_0 : \mu(\mathcal{R}_{C_S}) = \mu(\mathcal{R}_{C_I})$ against $H_1 : \mu(\mathcal{R}_{C_S}) \neq \mu(\mathcal{R}_{C_I})$, where the μ represents mean of $\mathcal{R}_{C_I}$ and $\mathcal{R}_{C_S}$). The analysis suggested rejection of the null hypothesis (Table 3.1); that is, the obtained point estimates of $\mathcal{R}_C$ between India and Sudan are statistically different. We also performed the Kolmogorov-Smirnov test on empirical distributions of $\mathcal{R}_C$ for both countries and found that the estimated empirical distributions are not the same.

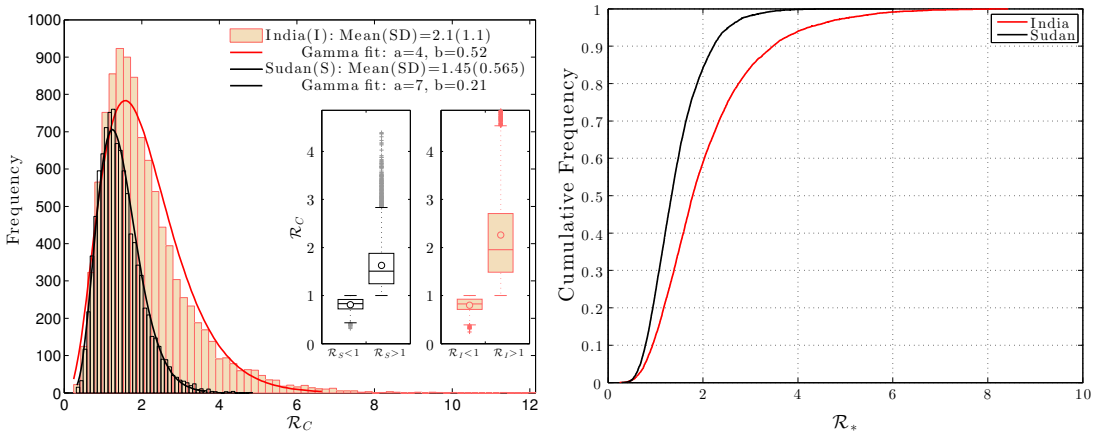

(a) (b)

Figure 3.4: (a) The Comparison Estimated Distributions of $\mathcal{R}_C$ for India and Sudan. The Box Plot Compares the Mean(∘), Median, Minimum, and Maximum of $\mathcal{R}_C$ Estimates for Both Countries. It is Found That the Gamma, is a Best-Fitted Distribution for the Samples From the Uncertainty Analysis. Table 2.2 Summarizes the Parameter Fitting for the Gamma Distribution for Both Countries. (b) The Empirical Cumulative Distributions of the $\mathcal{R}'s$ for India and Sudan

The outcome of the sensitivity analysis (shown in Table 3.2 and Figure 3.5) highlights differences in the influence of parameters for India and Sudan. In Figures 3.5,

Output	India(I)		Sudan(S)		Comparison between India(I) and Sudan(S)		
					2-Sample-t-test		K–S test
	Mean	SD	Mean	SD	t–statistic	95% CI	KS–statistic
$\mathcal{R}_C$	2.10	1.14	1.45	0.56546	50.906	(0.624, 0.67397)	0.2858
$\mathcal{P}_{\mathcal{A}_h}$	0.0038	0.0025	0.0025	0.0023	36.8400	(0.0012, 0.0013)	0.3046
$\mathcal{P}_{\mathcal{I}_h}$	0.0054	0.0053	0.0026	0.0017	50.3570	(0.0027, 0.0029)	0.2390
$\mathcal{P}_{\mathcal{I}_v}$	0.0372	0.0315	0.0271	0.0143	29.2950	(0.0094, 0.0108)	0.1431

Table 3.1: Statistical Estimates of Quantities, $\mathcal{R}_C$, $\mathcal{P}_{\mathcal{A}_h}$, $\mathcal{P}_{\mathcal{I}_h}$, and $\mathcal{P}_{\mathcal{I}_v}$, for VL in Sudan and India Using the 2 Sample T-Test and Two-Sample Kolmogorov–Smirnov Test. All Analysis were Found to be Significant, i.e. $p < 0.05$.

India			**Sudan**	
Parameter	PRCC($\mathcal{R}_C$)	*Rank*	*Parameter*	PRCC($\mathcal{R}_C$)
θ	-0.8849	1	β_{hv}	0.8760
ℓ	0.8265	2	b	0.8707
β_{vh}	0.8002	3	θ	-0.8567
β_{hv}	0.7610	4	β_{vh}	0.8536
b	0.5841	5	ℓ	0.7179
μ_v	-0.4898	6	μ_v	-0.4322
ϕ	0.0093*	7	ϕ	-0.0166*
μ_h	-0.0040	8*	μ_h	0.0122*

Table 3.2: A Comparison of the Partial Rank Correlation Coefficients for Input Parameters of the Output Value ($\mathcal{R}_C$). Where (*) Denotes $p < 0.01$ for India and Sudan.

the sign and the magnitude of the PRCC values for each parameter are included. We observe that the parameters b, ℓ, β_{hv}, β_{vh}, and θ_h are the most important in both countries for $\mathcal{R}_C$. The parameters b, ℓ, β_{vh}, and β_{hv} with positive PRCC values indicate positive impact on $\mathcal{R}_C$ for both countries, while θ_h plays a negative role.

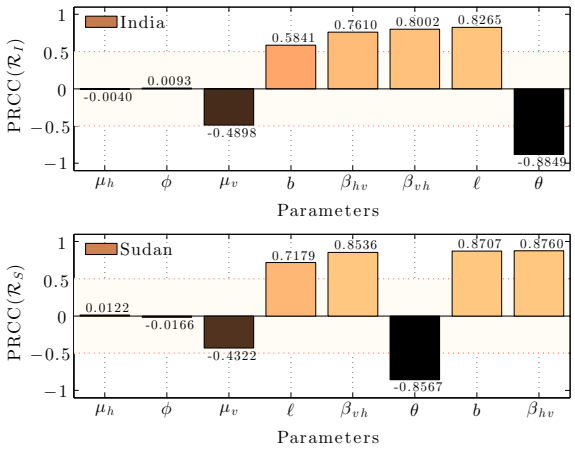

Figure 3.5: Tornado Diagrams of Partial Rank Correlation Coefficients, Indicating the Importance of all Eight Input Parameter's that Influence the Threshold Quantity $\mathcal{R}_C$. Figure Shows a Comparison of Sensitivity Indices for India and Sudan. In Both Regions, the Parameters that have $PRCC > 0$ Indicates an Increasing Influence on $\mathcal{R}_C$ Values and Those Having $PRCC < 0$ will Decrease $\mathcal{R}_C$ Values.

3.2.2 Comparison When Risk is Defined Based on the Prevalences

Point Prevalence of Asymptomatic Humans ($\mathcal{P}_{\mathcal{A}_h}$)

Although the level of $\mathcal{P}_{\mathcal{A}_h}$ can be determined when $\mathcal{R}_C$ is greater than unity, it is useful to understand the risk associated with increases in the number of asymptomatic individuals. We show that there is a significant difference between the point prevalence of asymptomatics for India (Mean(SD)=0.0038(0.0025)) and Sudan (Mean(SD)=0.0025(0.0023)). There was also a significant difference between the two distributions of parameters (two-sample Kolmogorov–Smirnov test, $p < 0.050$). Combining the results in Sections 2.4.1 and 2.4.2 allows us to compare the results of sensitivity analysis on $\mathcal{P}_{\mathcal{A}_h}$ for both countries. We observe from Figure 3.6c that the most sensitive parameters in both countries, in descending order, are ϕ_h, θ_h, ℓ, β_{vh}, β_{hv}, b, μ_v, and μ_h with the least sensitive being μ_v and μ_h.

From Table 3.3 and Figure 3.6c, we observed that both countries differ in the parameter ranking order, with the most sensitive parameter being ϕ_h in both. In

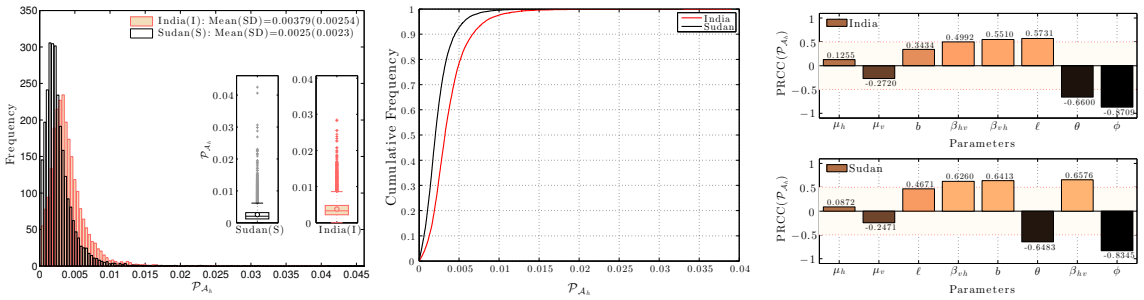

(a) (b) (c)

Figure 3.6: Comparison of Uncertainty and Sensitivity Analysis Results on the Equilibrium Prevalence of Asymptomatics Humans ($\mathcal{P}_{\mathcal{I}_h}$): (a) Frequency Distributions for Contributions, (b) Empirical Cumulative Distributions, and (c) Tornado Diagrams of Partial Rank Correlation Coefficients

India			**Sudan**	
Parameter	PRCC($\mathcal{P}_{\mathcal{A}_h}$)	*Rank*	*Parameter*	PRCC($\mathcal{P}_{\mathcal{A}_h}$)
ϕ	−0.8709	1	ϕ	−0.8345
θ	−0.6600	2	β_{hv}	0.6576
ℓ	0.5731	3	θ	−0.6483
β_{vh}	0.5510	4	b	0.6413
β_{hv}	0.4992	5	β_{vh}	0.6260
b	0.3434*	6	ℓ	0.4671
μ_v	−0.2720*	7	μ_v	−0.2471
μ_h	0.1255*	8	μ_h	0.0872*

Table 3.3: A Comparison of The Partial Rank Correlation Coefficients for Input Parameters of the Output Value ($\mathcal{P}_{\mathcal{A}_h}$). Where (*) Denotes $p < 0.01$ for India and Sudan.

descending order for India, we have θ_h, ℓ, β_{vh}, β_{hv}, and b, and for Sudan, we have β_{vh}, θ_h, b, β_{hv}, and ℓ.

Point Prevalence of Infected humans ($\mathcal{P}_{\mathcal{I}_h}$)

There are significant differences between the point prevalence of infected humans for India (Mean(SD)=0.0054(0.0053)) and Sudan (Mean(SD)=0.0026(0.0017)). For p-value < 0.05, the two-sample Kolmogorov–Smirnov test concludes that there is a significant difference between the two distributions (see Figure 3.7a–3.7b). We found that $\mathcal{P}_{\mathcal{I}_h}$ is most sensitive to θ_h, ℓ, b, β_{vh}, and β_{hv} and least sensitive to μ_h, μ_v and ϕ_h for both countries (Table 3.4 and Figure 3.7c). Both countries have in common the treatment rate as the most important parameter and μ_v, μ_h, and ϕ_h (in the same descending order) as least influential. For both countries, parameter sensitivities are as follows: For India, in descending order, we have ℓ, β_{vh}, β_{hv}, and b and for Sudan we have β_{vh}, b, β_{hv}, and ℓ.

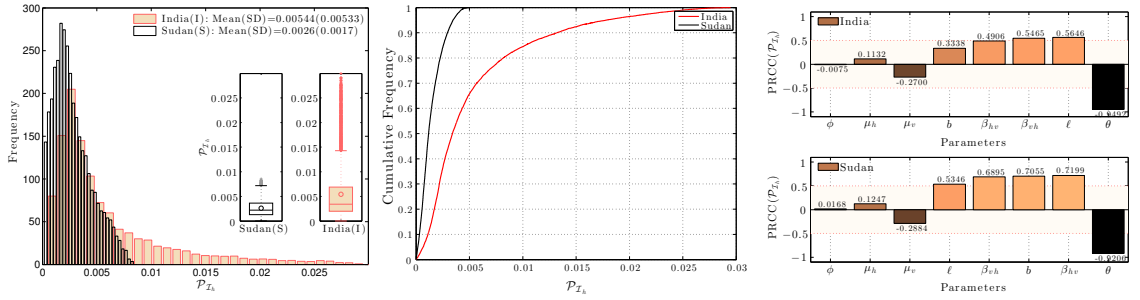

(a) (b) (c)

Figure 3.7: Comparison of Result From Uncertainty and Sensitivity Analysis Results on the Equilibrium Prevalence of Infected Humans ($\mathcal{P}_{\mathcal{I}_h}$): (a) Frequency Distributions for Contributions, (b) Empirical Cumulative Distributions, and (c) Tornado Diagrams of Partial Rank Correlation Coefficients.

Point Prevalence of of Infected sandflies ($\mathcal{P}_{\mathcal{I}_v}$)

There is a significant difference between the prevalence of infected sandflies for India (Mean(SD)=0.0372(0.0315)) and Sudan (Mean(SD)=0.0271(0.0143)). There was no significant difference between the two distributions, (Figure 3.8a - 3.8b, two-sample Kolmogorov–Smirnov test, $p < 0.05$). Parameters b, θ_h, μ_v, and β_{vh} were most sensi-

India			Sudan	
Parameter	PRCC($\mathcal{P}_{\mathcal{I}_h}$)	*Rank*	*Parameter*	PRCC($\mathcal{P}_{\mathcal{I}_h}$)
θ	−0.9492	1	θ	−0.9206
ℓ	0.5646	2	β_{hv}	0.7199
β_{vh}	0.5465	3	b	0.7055
β_{hv}	0.4906	4	β_{vh}	0.6895
b	0.3338*	5	ℓ	0.5346
μ_v	−0.2700*	6	μ_v	−0.2884
μ_h	0.1132*	7	μ_h	0.1247*
ϕ	−0.0075*	8	ϕ	0.0168*

Table 3.4: A Comparison of the Partial Rank Correlation Coefficients for Input Parameters of the Output Value ($\mathcal{P}_{\mathcal{I}_h}$). Where (*) Denotes $p < 0.01$ for India and Sudan.

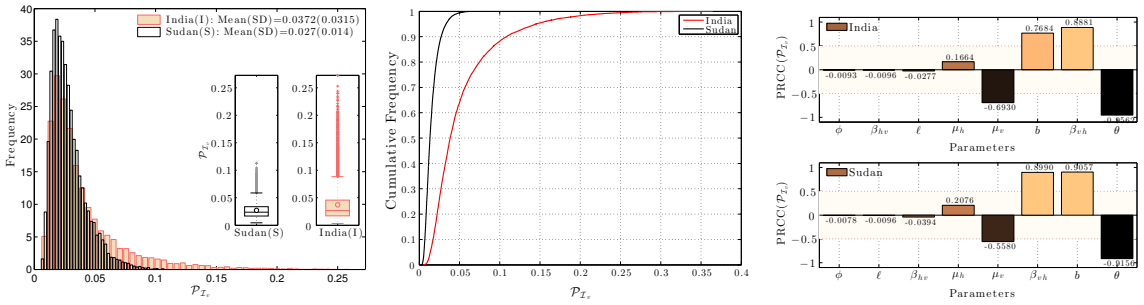

(a) (b) (c)

Figure 3.8: Comparison of Uncertainty and Sensitivity Analysis Results on the Equilibrium Prevalence of Infected Sandfies ($\mathcal{P}_{\mathcal{I}_v}$): (a) Frequency Distributions for Contributions, (b) Empirical Cumulative Distributions, and (c) Tornado Diagrams of Partial Rank Correlation Coefficients.

tive to the prevalence of infection in sandflies($\mathcal{P}_{I_v}$) for both countries (see Table 3.5 and Figure 3.8c). β_{hv} is more sensitive for India than for Sudan, and b is more sensitive for Sudan than for India. The least important parameters were μ_h, ℓ, ϕ_h, and β_{hv}.

India			Sudan	
Parameter	PRCC($\mathcal{P}_{\mathcal{I}_v}$)	*Rank*	*Parameter*	PRCC($\mathcal{P}_{\mathcal{I}_v}$)
θ	-0.9562	1	θ	-0.9156
β_{vh}	0.8881	2	b	0.9057
b	0.7684	3	β_{vh}	0.8990
μ_v	-0.6930	4	μ_v	-0.5580
μ_h	0.1664	5	μ_h	0.2076*
ℓ	-0.0277	6	β_{hv}	-0.0394*
β_{hv}	-0.0096	7	ℓ	-0.0096
ϕ	-0.0093	8	ϕ	-0.0078

Table 3.5: A Comparison of the Partial Rank Correlation Coefficients for Input Parameters of the Output Value ($\mathcal{P}_{\mathcal{I}_v}$). Where (*) Denotes $p < 0.01$. for India and Sudan.

3.3 Discussion

VL has received much less attention by researchers and policy makers as compared to many other tropical diseases and, hence, is classified as one of the neglected diseases by WHO. There are a limited number of studies that collect data to study VL patterns and even fewer studies that use specific data in a dynamical model for evaluating control programs. In this research, we carry out an analysis via a thorough literature review to identify what data is available and what is missing so that we can understand VL dynamics comprehensively for the two most VL-affected countries (India and Sudan) in the world.

A dynamic model was then used to capture data-driven VL epidemiological factors and identify risks associated with frequent VL outbreak. We develop approaches to estimate model parameters for which data was unavailable and performed parametric uncertainty and sensitivity analysis on metrics that define risk based on four differ-

ent definitions. The uncertainty and sensitivity analyses resulted in quantifying the impact of changes in less precise parameter estimates on the risk for VL, where risk is measured based on the control reproductive number, prevalences of asymptomatic, and symptomatic humans, or the prevalence of infectious vectors.

For both countries, we identify similarities and differences in parameter ranking associated with each of the four definitions of risk for VL. When risk was defined based on the control reproduction number, the treatment rate was found to be the most important factor in reducing VL cases in India, whereas in Sudan the transmission probability from sandfly to human was more important. Many studies have identified the abundance of *P. Orientalis* Sandflies in villages with the high density of *Acacia Seyal* and *Balanites aegyptiaca* vegetation, which is assumed to be one of the major environmental risk factors in Sudan (23; 93; 53; 100). The presence of an infected individual in these areas increases the likelihood of transmission between human and sandfly. The presence of domesticated animals also can serve as an attractant for sandflies in and near homes.

If the risk is defined using the prevalence of asymptomatic VL, the results indicate that the asymptomatic rate is the most sensitive parameter in both countries. Many public health researchers recognize that asymptomatic *L. Donovani* infected individuals as a substantial reservoir of the resurgence of VL infection in the 1970s, following the Global Malaria Eradication Program in the 1950s and 1960s (19; 10; 35).

One of the most efficient ways to control vector-borne diseases is to identify and treat infected individuals promptly. Treatment reduces the prevalence of illness in humans thereby reducing the chance of secondary infection in the vector. Our result is that the treatment rate, which relates to control, is the most important parameter in reducing the prevalence in sandflies and humans. Our results support an established notion that reducing the prevalence in humans through early identification of

asymptomatics and prompt treatment integrated with effective vector control can significantly decrease the prevalence of VL in the sandfly population.

Few modeling studies, on other Neglected tropical diseases, have only evaluated the role of environmental and socioeconomic risk factors on the transmission dynamics of diseases. Black, et al., (16), studied the environmental factors and the likelihood of transmission for *Trypanosoma Cruzi* (*T. Cruz*) seropositivity in two different geographic regions of Ecuador. Within these two regions, there are distinct insect vector species responsible for the transmission of *T. Cruzi*. Poorly structured housing with cracks and holes provided an ideal breeding area for the triatominae insect (the vector of T. Cruz) (16). A study by Bergquist and Tanner, 2010, (9), on the burden of Schistosomiasis japonica among the top two countries in the world (China and the Philippines) found that in China around 5 million individuals are at risk of Schistosomiasis and 1 million are currently infected, whereas in the Philippines, 560,000 were reported infected in 2008. In India the *P. Argentipes* is the main sandfly species responsible for transmission of VL to human populations. During the 1960s, the man-biting rate of sandflies was significantly reduced from DDT spraying applications that were employed in the malaria eradication campaign and designed to kill mosquito vectors. This campaign reduced the number of VL cases during this period (1962-1963), showing no new prorated cases. It was observed that soon after the DTT spraying campaign stopped the number of VL cases elevated to higher epidemic levels (4).

High treatment rate is also found to be a critical factor in impacting the dynamics of VL but, primarily in India. However, we assumed effective treatment for all individuals in the model and did not consider efficacy and toxicity of available drugs. These assumptions may influence our future findings.

Chapter 4

ANALYSIS OF VISCERAL LEISHMANIASIS TRANSMISSION DYNAMICS MODEL

This chapter collects some mathematical details for the VL model. The model considered here is modified to incorporate disease-induced mortality when treatment is not made widely available to everyone.

4.0.1 Model Derivation

The *Leishmania donovani* transmission cycle is anthroponotic and takes place from human to human via the bite of an infective female Phlebotominae sandfly. Hence, a compartmental dynamical model for the transmission of VL infection between the human (host) and sandfly (vector), is considered. The model has five epidemiological stages: susceptible individuals (S_h), asymptomatic individuals (A_h), individuals infected with VL (I_h), hospitalized individuals (T_h), and individuals who have recovered and are immune to reinfection (R_h), where $N_h = S_h + A_h + I_h + T_h + R_h$. Similarly, the sandfly population is assumed to be divided into susceptible sandflies $S_v(t)$ and infectious sandflies $I_v(t)$, so that $N_v = S_v + I_v$.

The dynamics of *Leishmania donovani* transmission in humans and sandflies are modeled by the system of equations given below:

Human Population

$$\begin{aligned}
\frac{dS_h}{dt} &= \Lambda_h - \lambda_{vh} S_h - \mu_h S_h \\
\frac{dA_h}{dt} &= \lambda_{vh} S_h - (\phi_h + \mu_h) A_h \\
\frac{dI_h}{dt} &= \phi_h A_h - (\delta_{h_1} + \theta_h + \mu_h) I_h \\
\frac{dT_h}{dt} &= \theta_h I_h - (\gamma_h + \delta_{h_2} + \mu_h) T_h \\
\frac{dR_h}{dt} &= \gamma_h T_h - \mu_h R_h
\end{aligned} \tag{4.1}$$

Sand fly Population

$$\begin{aligned}
\frac{dS_v}{dt} &= \Lambda_v - \lambda_{hv} S_v - \mu_v S_v \\
\frac{dI_v}{dt} &= \lambda_{hv} S_v - \mu_v I_v
\end{aligned} \tag{4.2}$$

where

$$\lambda_{hv} = b\beta_{hv}\frac{I_h}{N_h}, \tag{4.3}$$

$$\lambda_{vh} = b\beta_{vh}\frac{I_v}{N_h}, \tag{4.4}$$

and $S_{h_1} \geq S_{h_2}$

Parameter	***Definition***	***Unit***	**Value**	**Source**
b	Average number of bites per sandfly	day^{-1}	0.7997	(45)
β_{vh}	Transmission probability when infected sandfly bitessusceptible human	Dimensionless	0.0001	Estimated
β_{hv}	Transmission probability when susceptible sandfly bites infected humans	Dimensionless	0.3	Estimated
δ_{h_1}, δ_{h_2}	Disease-induced death rate for infect humans VL	day^{-1}	0.011	(141)
γ_h	Per capita treatment-induced recovery rate from VL infection	day^{-1}	0.0016	(142)
Λ_h	Human recruitment rate	day^{-1}	0.004	(60)
Λ_v	Sandfly daily recruitment rate	day^{-1}	0.0213	(129)
μ_h	Human daily per capita natural mortality rate	day^{-1}	4.08e-5	Est. (see App. B)
μ_v	Adult Sand fly daily per capita mortality rate	day^{-1}	0.0909	(138)
ϕ_h	Per capita development rate of clinical symptoms of VL infection	day^{-1}	0.0086	(140)
θ_h	Per capita treatment rate of infectious humans	day^{-1}	0.0439	(97)

Table 4.1: Parameter Notation, Biological Meaning, Values and Sources.

4.1 Mathematical Analysis

The state variables of the Model (4.1) are non-negative for all time. That is, all solutions are positively-invariant in the (feasible) parameter and initial condition regions $\Omega = \Omega_h \times \Omega_v \in \mathbb{R}^5_+ \times \mathbb{R}^2_+$ for $t \geq 0$.

4.1.1 Basic Qualitative Features

The basic qualitative properties of System (4.1)–(4.2) are collected in a series of results.

Theorem 4.1.1. *The system (4.1)–(4.2) preserves positivity of solutions. In other words, the solutions of the model (4.1)–(4.2) with positive initial data remain positive for all $t > 0$. Furthermore,*

$$\limsup_{t\to\infty} N_h(t) \leq \frac{\Lambda_h}{\mu_h} \quad \text{and} \quad \limsup_{t\to\infty} N_v(t) \leq \frac{\Lambda_v}{\mu_v}.$$

Proof. It is clear from the first equation of the model (4.1)–(4.2) that

$$\frac{dS_h}{dt} = \Lambda_h - \lambda_{vh} S_h - \mu_h S_h \geq -(\lambda_{vh} + \mu_h) S_h,$$

so by a (comparison) theorem from Birkhoff and Rota (see (15)) on differential inequality, we get

$$S_h(t) \geq S_h(0) \exp\Big\{ - \int_0^t [\lambda_{vh}(u)] du + \mu_h t \Big\} > 0.$$

for each t. This is because $S_h(0) > 0$, and exponential functions are also positive for any t. Using a similar approach, it can be shown that all other state variables of the model remain positive for all $t > 0$. Furthermore, adding the first five equations of (4.1), gives:

$$\frac{dN_h}{dt} = \Lambda_h - \mu_h N_h - \delta_{h_1} I_h - \delta_{h_2} T_h. \tag{4.5}$$

Thus,

$$\Lambda_h - (\mu_h + \delta_{h_1} + \delta_{h_2}) N_h(t) \leq \frac{dN_h(t)}{dt} \leq \Lambda_h - \mu_h N_h(t)$$

and

$$\frac{\Lambda_h}{\mu_h + \delta_{h_1} + \delta_{h_2}} \leq \liminf_{t\to\infty} N_h(t) \leq \limsup_{t\to\infty} N_h(t) \leq \frac{\Lambda_h}{\mu_h}$$

so that,

$$\limsup_{t\to\infty} N_h(t) \leq \frac{\Lambda_h}{\mu_h}.$$

Hence, we have that N_h is a bounded solution of system (4.1) and is trapped in the region

$$\Omega_h = \left\{(S_h, A_h, I_h, T_h, R_h) \in \mathbb{R}^5_+ : 0 \leq S_h + A_h + I_h + T_h + R_h \leq \frac{\Lambda}{\mu}\right\}.$$

Similarly, adding the two equations of model System (4.2)

$$\frac{dN_v}{dt} = \Lambda_v - \mu_v N_v.$$

Let $(S_v, I_v) \in \mathbb{R}^2_+$ be a solution with non-negative initial conditions. Now $\underset{t\to\infty}{lim\, sup} S_v = \frac{\Lambda_v}{\mu_v}$. Taking the time derivative along sum the of all solutions curves of system (4.2) gives

$$\begin{aligned} \dot{N}_v &= \Lambda_v - N_h\mu_h \\ &\leq \Lambda_v - N_h\mu_h. \end{aligned}$$

By differential inequality theorem (15) we find

$$0 \leq N_v(t) \leq \tfrac{\Lambda_v}{\mu_v} + \left(N_v(0) - \tfrac{\Lambda_v}{\mu_v}\right) \mathrm{e}^{-\mu_v t},$$

where $N_v(0)$ represents the initial sandfly population at the initial phase of the disease process. So as $t \to \infty$, the inequality becomes

$$0 \leq N_v(t) \leq \tfrac{\Lambda_v}{\mu_v}.$$

Hence we have that N_v is a bounded solution of System (4.2) and is trapped in the region

$$\Omega_v = \left\{(S_v, I_v) \in \mathbb{R}^2_+ : 0 \leq S_v + I_v \leq \frac{\Lambda_v}{\mu_v}\right\}.$$

□

Lemma 4.1.2. *The following epidemiology feasible region of System (4.1)–(4.2), defined by* $\Omega = \Omega_h \times \Omega_v$*, is positively invariant and attracting.*

Proof. It follows from 4.1.1 that $\frac{dN_h(t)}{dt} \leq \Lambda_h - \mu_h N_h(t)$ and $\frac{dN_v(t)}{dt} = \Lambda_v - \mu_v N_v(t)$, so that $\frac{dN_h}{dt} < 0$ and $\frac{dN_v}{dt} < 0$ if $N_h(t) > \frac{\Lambda_h}{\mu_h}$ and $N_v(t) > \frac{\Lambda_v}{\mu_v}$. Thus, by a standard comparison theorem (15), we find $N_h(t) \leq N(0)e^{-\mu_h t} + \frac{\Lambda_h}{\mu_h}(1 - e^{-\mu_h t})$ and $N_v(t) \leq N(0)e^{-\mu_v t} + \frac{\Lambda_v}{\mu_v}(1 - e^{-\mu_v t})$. In particular, $N_h(t) \leq \Lambda_h/\mu_h$ and $N_v(t) \leq \Lambda_v/\mu_v$ if $N_h(0) \leq \Lambda_h/\mu_h$ and $N_v(0) \leq \Lambda_v/\mu_v$, respectively. Thus, Ω is positively invariant. Further, if $N_h(t) > \frac{\Lambda_h}{\mu_h}$ and $N_v(t) > \frac{\Lambda_v}{\mu_v}$, then either the solution enters Ω in finite time, or $N_h(t)$ approaches Λ_h/μ_h and $N_v(t)$ approaches Λ_v/μ_h, and the infected variables approach zero. Hence, Ω is attracting (i.e., all solutions in $\mathbb{R}^7_+$ eventually approach, enter or stay in Ω).

Hence, the model system (4.1)–(4.2) is epidemiologically and mathematically well-posed in Ω (71). □

4.1.2 Infection-Free Equilibrium and the Basic Reproduction Number

In the rest of this chapter, we will assume for simplicity, that $S_{h_1} = S_{h_2}$. Model (4.1 – 4.2) has the infection-free equilibrium $E_0 = (\Lambda_h/\mu_h, 0, 0, 0, 0, \Lambda_v/\mu_v, 0)$, where the $'$ means vector transpose. In order to evaluate the basic reproductive number, we apply the method shown in (149). We compute the matrices $\mathcal{F}$ (for the new infection terms) and $\mathcal{V}$ (for the transition terms):

$$\mathcal{F} = \begin{bmatrix} 0 & 0 & \frac{b\beta_{vh}S_h\mu_v}{\Lambda_v} \\ 0 & 0 & 0 \\ 0 & \frac{b\beta_{hv}S_v\mu_h}{\Lambda_h} & 0 \end{bmatrix} \quad \text{and} \quad \mathcal{V} = \begin{bmatrix} G_1 & 0 & 0 \\ -\phi_h & G_2 & 0 \\ 0 & 0 & \mu_v \end{bmatrix}. \tag{4.6}$$

where G_2 modifies to $G_2 = \theta_h + \mu_h + \delta_{h_1}$ The basic reproduction number $\mathcal{R}_0$ is the spectral radius of the matrix $\mathcal{F}\mathcal{V}^{-1}$, and

$$\mathcal{R}_0 = \rho\left(\mathcal{F}\mathcal{V}^{-1}\right) = \sqrt{\frac{b\beta_{hv}}{\mu_v} \cdot \frac{\phi_h}{(\phi_h + \mu_h)} \cdot \frac{b\beta_{vh}}{(\theta_h + \mu_h + \delta_{h_1})} \cdot \frac{N_h^*}{N_v^*}} \tag{4.7}$$

4.1.3 Local Asymptotic Stability of the IFE

Theorem 4.1.3. *The disease-free equilibrium point, E_0, of model system (4.1- 4.2) is locally asymptotically stable (LAS) if $\mathcal{R}_0 < 1$ and unstable if $\mathcal{R}_0 > 1$.*

Proof. Linearization at DFE gives

$$J_{E_0} = \begin{bmatrix} -\mu_h & 0 & 0 & 0 & 0 & 0 & -b\beta_{vh} \\ 0 & -G_1 & 0 & 0 & 0 & 0 & b\beta_{vh} \\ 0 & \phi_h & -G_2 & 0 & 0 & 0 & 0 \\ 0 & 0 & \theta_h & -G_3 & 0 & 0 & 0 \\ 0 & 0 & 0 & \gamma_h & -\mu_h & 0 & 0 \\ 0 & 0 & -\frac{b\beta_{hv}\Lambda_v\mu_h}{\mu_v\Lambda_h} & 0 & 0 & -\mu_v & 0 \\ 0 & 0 & \frac{b\beta_{hv}\Lambda_v\mu_h}{\mu_v\Lambda_h} & 0 & 0 & 0 & -\mu_v \end{bmatrix}, \tag{4.8}$$

where G_2 modifies to $G_2 = \theta_h + \mu_h + \delta_{h_1}$. The characteristic polynomial of the Jacobian matrix is given by

$$P(\lambda) = (\lambda + \mu_v)(\lambda + \mu_h)^2(\lambda + G_3)\left(\lambda^3 + h_2\lambda^2 + h_1\lambda + h_0\right) \tag{4.9}$$

where $h_0 = \mu_v(\phi_h + \mu_h)(\theta_h + \mu_h)(1 - \mathcal{R}_0^2)$, $h_1 = (G_1 + G_2)\mu_v + G_1G_2$ and $h_2 = G_2 + G_1 + \mu_v$. We observe that four eigenvalues for this polynomial have negative real parts, and are given by $\lambda = \{-\mu_v, -G_3, -\mu_h, -\mu_h\}$ with geometric multiplicity of two. The remaining expression is a cubic polynomial, $P(\lambda) = \lambda^3 + h_2\lambda^2 + h_1\lambda + h_0$.

Applying the Routh-Hurwitz criteria (73), we find the conditions for all eigenvalues to have negative real parts, that is $H_1 = h_1 > 0$, $H_2 = h_0 > 0$, and $H_3 = h_2 h_1 - h_0 > 0$. Thus, by Routh-Hurwitz criteria, E_0 is locally asymptotically stable for $\mathcal{R}_0 < 1$ and is unstable for $\mathcal{R}_0 > 1$. □

4.1.4 Existence of Backward Bifurcation

At $R_0 = 1$, the term-free of λ in equation (4.9) vanishes, which implies that the matrix J_0, and therefore J_{E_0}, has a trivial eigenvalue in addition to six more (negative) eigenvalues. Center manifold analysis near the trivial equilibrium E_0 (see Castillo-Chavez and Song (27)) can be applied here. The approach is based on computing the two expressions

$$a_1 = \sum_{i,j,k=1}^{7} v_i w_j w_k \frac{\partial^2 f_i}{\partial x_j \partial x_k}(E_0, b_0),$$
$$b_1 = \sum_{i,j=1}^{7} v_i w_j \frac{\partial^2 f_i}{\partial x_j \partial b}(E_0, b_0)$$

where $x_1 = S_h, x_2 = A_h, x_3 = I_h, x_4 = T_h, x_5 = R_h, x_6 = S_v, x_7 = I_v$ and $f_i(x) = \dot{x_i}, i = 1, 2, , .., 9$, is the right hand side of model (4.1–4.2). The parameter b_0 represents the biting rate at $R_0 = 1$, which implies that

$$b_0 = \sqrt{\frac{G_1 G_2 \mu_v N_h^*}{\phi_h \beta_{hv} \beta_{vh} N_v^*}}.$$

The components v_i are those of the left eigenvector v of the Jacobian matrix $J_{E_0}(R_0 = 1)$ and are given by

$$v_1 = v_4 = v_5 = v_6 = 0,$$
$$v_2 = b_0 \beta_{hv} \phi_h \mu_h \Lambda_v,$$
$$v_3 = \frac{G_1}{\phi_h} v_2,$$
$$v_7 = \frac{G_1 G_2 N_h^*}{b_0 \beta_{hv} \phi_h N_v^*} v_2.$$

The components w_i represent those of the right eigenvector w of the Jacobian matrix $J_{E_0}(R_0 = 1)$ and are given by

$$\begin{aligned}
w_1 &= -\frac{G_1}{\mu_h} w_2, \\
w_2 &= b_0 \beta_{vh} G_2 G_3 \mu_h \mu_v N_h^*, \\
w_3 &= \frac{\phi_h}{G_2} w_2, \\
w_4 &= \frac{\theta_h \phi_h}{G_2 G_3} w_2, \\
w_5 &= \frac{\gamma_h \theta_h \phi_h}{G_2 G_3 \mu_h} w_2, \\
w_6 &= -\frac{b_0 \phi_h \beta_{hv} N_v^*}{G_2 \mu_v N_h^*} w_2, \\
w_7 &= \frac{G_1}{b_0 \beta_{vh}} w_2.
\end{aligned}$$

After some calculation, we get

$$\begin{aligned}
a_1 &= -\frac{2b_0}{N_h^*}(w_2 + w_3 + w_4 + w_5)\left(v_2 w_7 \beta v h + v_7 w_3 \beta_{hv} \frac{N_v^*}{N_h^*}\right) + 2 v_7 w_3 \frac{b_0 \beta_{hv}}{N_h^*}\left(w_6 - w_1 \frac{N_v^*}{N_h^*}\right) \\
&= -\frac{2G_1 v_2 w_2^2}{G_2 G_3 \mu_v \mu_h N_h^*}\{2\mu_v[\mu_h G_3(G_2 + \phi_h) + \phi_h \theta_h(\gamma_h + \mu_h)] + G_3(b_0 \phi_h \mu_h \beta_{hv} - G_1 G_2 \mu_v)\}, \\
&= -\frac{2G_1 v_2 w_2^2}{G_2 G_3 \mu_v \mu_h N_h^*}\{2\mu_v[G_1 G_2 G_3 - \phi_h \delta_{h_1}(G_3 + \theta_h)] + b_0 \beta_{hv} \phi_h \mu_h G_3 - G_1 G_2 G_3 \mu_v\}, \qquad (4.10) \\
b_1 &= \frac{2G_1}{b_0} v_2 v_3 > 0. \qquad (4.11)
\end{aligned}$$

As the expression b_1 is positive, then according to theorem 4.1 of Castillo-Chavez and Song (27), the model (4.1–4.2) undergoes backward bifurcation at $\mathcal{R}_0$ if and only if the expression a_1 is positive, i.e., if

$$2\mu_v[G_1 G_2 G_3 - \phi_h \delta_{h_1}(G_3 + \theta_h)] + b_0 \beta_{hv} \phi_h \mu_h G_3 - G_1 G_2 G_3 \mu_v < 0. \qquad (4.12)$$

If $\delta_{h_1} = 0$, then the inequality cannot be true. Hence, we have forward bifurcation. We show the following proposition.

Proposition 4.1.4. *Model (4.1–4.2) exhibits backward bifurcation if and only if the inequality (4.12) holds.*

4.1.5 *Endemic Equilibria and Critical Basic Reproduction Number*

To find the endemic equilibrium, we set the derivatives in the left hand side of the model (4.1–4.2) equal to zero and solve the resulting algebraic system, for the case $i_v \neq 0$ and $i_h \neq 0$ at equilibrium to get the state variables. Thus,

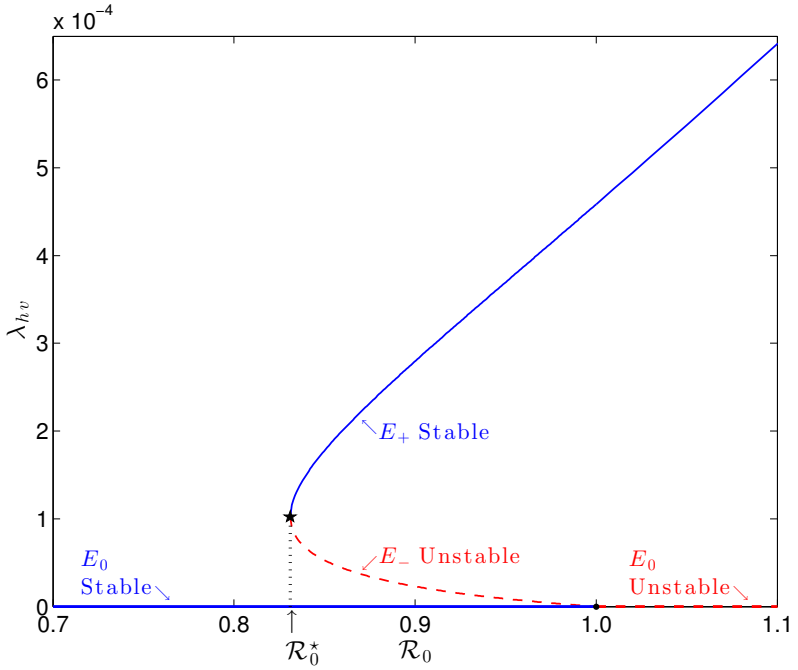

Figure 4.1: Bifurcation Diagrams for Mean Parameters in India: $\beta_{vh} = 0.0821$, $\beta_{hv} = 0.025$, $\delta_{h_1} = 0.011$, $\mu_h = 4.08 \times 10^{-5}$, $\mu_v = 0.0909$, $\phi_h = 0.0086$, $\theta_h = 0.0439$, $\Lambda_h = 0.0016$, $\Lambda_v = 0.0213$, $\gamma_h = 0.004$. Backward Bifurcation: The Solid Curves (-) Denotes Stable Endemic Equilibrium with Higher Infection Level; The Dashed Curves (- -) Denote Instable Branch.

$$
\begin{aligned}
S_h^* =& \frac{\Lambda_h}{\lambda_{vh}+\mu_h},\\
A_h^* =& \frac{\Lambda_h\lambda_{vh}}{G_1(\lambda_{vh}+\mu_h)},\\
I_h^* =& \frac{\Lambda_h\lambda_{vh}\phi_h}{G_1G_2(\lambda_{vh}+\mu_h)},\\
T_h^* =& \frac{\Lambda_h\lambda_{vh}\phi_h\theta_h}{G_1G_2G_3(\lambda_{vh}+\mu_h)},\\
R_h^* =& \frac{\Lambda_h\gamma_h\lambda_{vh}\phi_h\theta_h}{G_1G_2G_3\mu_h(\lambda_{vh}+\mu_h)},\\
S_v^* =& \frac{\Lambda_v}{\lambda_{hv}+\mu_v},\\
I_v^* =& \frac{\Lambda_v\lambda_{hv}}{\mu_v(\lambda_{hv}+\mu_v)}.
\end{aligned}
\tag{4.13}
$$

Now, we substitute equations 4.13 in equations (4.3) and (4.4), to get an equation in the endemic force of infection λ_{vh} as

$$
f(\lambda_{vh}) = A_0\lambda_{vh}^2 + B_0\lambda_{vh} + C_0 = 0 \tag{4.14}
$$

where

$$
\begin{aligned}
A_0 &= \mu_v\Lambda_h\{G_1G_2G_3 - \delta_{h_1}\phi_h(G_3+\theta_h)\}\{\mu_v[G_1G_2G_3 - \delta_{h_1}\phi_h(G_3+\theta_h)] + bG_3\beta_{hv}\mu_h\phi_h\}\\
B_0 &= G_1G_2G_3\mu_h\{2\mu_v^2\Lambda_h[G_1G_2G_3 - \delta_{h_1}\phi_h(G_3+\theta_h)] + bG_3\Lambda_h\beta_{hv}\mu_h\mu_v\phi_h - b^2G_3\Lambda_v\beta_{hv}\beta_{vh}\mu_h\phi_h\}\\
C_0 &= G_1G_2G_3^2\mu_h^2[G_1G_2\Lambda_h\mu_v^2 - \Lambda_v\beta_{hv}\beta_{vh}\mu_h\phi_hb^2].
\end{aligned}
$$

We notice that the expression

$$
G_1G_2G_3 - \delta_{h_1}\phi_h(G_3+\theta_h) = (\gamma_h+\delta_{h_1}+\mu_h)[\phi_h(\theta_h+\mu_h)+\mu_h(\theta_h+\delta_{h_1}+\mu_h)] - \delta_{h_1}\phi_h\theta_h > 0.
$$

Because all model parameters are strictly positive, except δ_{h_1} representing the Visceral Leishmaniasis disease-induced mortality rate, then the expression A_0 is positive. However, both B_0 and C_0 can be positive or negative, depending on parameter values. This implies that Equation (4.14) may have up to two feasible solutions (a solution that satisfies $\lambda_{vh} \in [0,\infty)$). It is clear that $C_0 < 0$ corresponds to $R_0 > 1$, while

$C_0 > 0$ corresponds to $R_0 < 1$. If $R_0 > 1$, then there are two solutions of equation (4.14), of which only one is feasible (positive) while the other is not feasible. This solution is given by

$$\lambda_{hv}^{+} = \frac{-B_0 + \sqrt{B_0^2 - 4A_0C_0}}{2A_0}. \tag{4.15}$$

However, if $R_0 = 1$, then $C_0 = 0$ and therefore a positive solution of (4.14) exists only if $B_0 < 0$. This solution is given by $-B_0/A_0$. If $R_0 < 1$ then $C_0 > 0$, and therefore positive solutions of (4.14) exist only if $B_0 < 0$ and $B_0^2 - 4A_0C_0 > 0$, while otherwise no feasible solutions exists. One of the two feasible solutions is given by (4.15) while the other is given by

$$\lambda_{hv}^{-} = \frac{-B_0 - \sqrt{B_0^2 - 4A_0C_0}}{2A_0}. \tag{4.16}$$

Hence, in addition to the infection-free equilibrium, if:

- $C_0 < 0$, then a unique endemic equilibrium exists and corresponds to a value of the endemic force of infection λ_{hv} given by (4.15).
- $C_0 = 0$, then an endemic equilibrium exists only if $B_0 < 0$ and corresponds to the solution given by (4.15).
- $C_0 > 0, B_0 < 0$ and $B_0^2 - 4A_0C_0 \geq 0$, then two endemic equilibria exist and correspond to the two feasible solutions of equation (4.14) which are given by (4.15) and (4.16).
- otherwise, no endemic equilibrium exists.

The conditions in the third bullet are of great interest, as they show the possible existence of backward bifurcation for values of $R_0 < 1$. To find the backward bifurcation range, in terms of R_0, we set the discriminant $B_0^2 - 4A_0C_0$ equal to zero and solve for the critical value of R_0 (which we call $R_0^{\star}$), where

$$R_0^\star = \frac{\sqrt{\phi_h}(Q_1 + 2\sqrt{Q_2})}{Q_3}, \tag{4.17}$$

$$Q_1 = \beta_{hv}\Lambda_h\mu_h[2\delta_{h_1}\phi_h(G_3+\theta_h) - G_1G_2G_3],$$

$$Q_2 = \beta_{hv}\Lambda_h\mu_h\delta_{h_1}(G_3+\theta_h)(G_1G_2\Lambda_v\beta_{vh} - \Lambda_h\mu_h\phi_h\beta_{hv})(G_1G_2G_3 - \delta_{h_1}\phi_h(G_3+\theta_h)),$$

$$Q_3 = G_1G_2G_3\sqrt{\beta_{hv}\beta_{vh}G_1G_2\mu_h\Lambda_h\Lambda_v}.$$

Thus, two endemic equilibria exist for values of $R_0^\star < R_0 < 1$. This phenomenon is known as backward bifurcation (121; 122; 75; 47) (ee bifurcation diagram in Fig 4.1). Simulations are done for parameter values as estimated in Table 4.1, except δ_{h_1}, which has been chosen to be $\delta_{h_1} = 0.011$ day^{-1}.

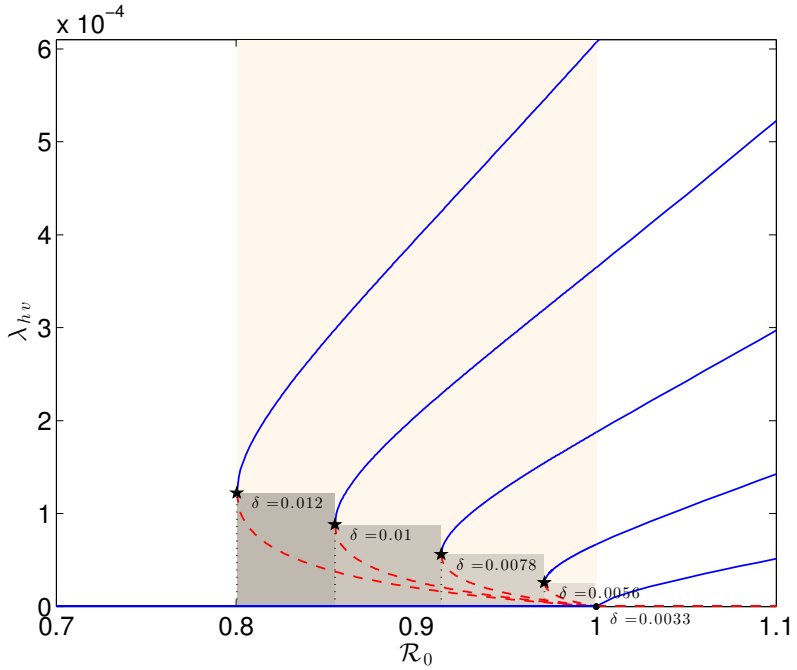

Figure 4.2: Changes in the Qualitative Behavior of the Model Under Effective Treatment. Observe that the Bifurcation Diagram in Figure 4.1 Collapses to a Forward Bifurcation as Disease Mortality (δ_{h_1}) Decrease as a Result of Perfect Treating of Humans.

4.2 Conclusion

In this Chapter, we studied and analyzed a vector-borne model and showed the existence of multiple endemic equilibria when the basic reproduction number is less than one. Under perfect treatment, there exists (unique) disease-free and an endemic equilibria. The dynamical scenarios shown via the model analysis, have also been observed in VL prevalence trends for some countries. For example, extensive DDT insecticide spraying in India in 2007 (91) resulted in the elimination of VL from some districts in India, whereas in some other district, VL came back after few years without any local cases and became endemic. These two distinct scenarios might be because of varying migration patterns, i.e., different levels of influx of infected individuals in the two types of districts.

Chapter 5

DISCUSSION AND LIMITATIONS

In this dissertation, we have investigated the role of regional risk factors on the transmission dynamics of Visceral Leishmaniasis (VL) via novel mathematical estimation methods in the face of limited data. The study has contributed significantly, via development and implementation of model parameterization procedure, to the field of mathematical epidemiology for vector-borne infectious diseases. We showed how to collect and compile consistent data from the literature, to estimate model parameters using such data, and to use parameter estimates to assess dynamics of VL.

The literature is reviewed thoroughly to gather relevant data for the model in Chapter 2. The review of the literature resulted in two distinct sets of data for estimating the model parameters. However, an attempt to find data on transmission probabilities was not successful, and, hence, a two model based novel estimation procedures were developed in the study. The first procedure makes use of the data on the VL prevalence in humans and sandflies, whereas the second estimation method uses the estimates of the control reproduction number. Having obtained estimates of model parameters, the risks associated with VL for the two data sets were assessed. The risk of VL was evaluated based on the four different output metrics (reproduction number, the prevalence of asymptomatic human hosts, the prevalence of symptomatic infectious humans, and the prevalence of infected sandflies) obtained from the model analysis.

Using the methodology developed in Chapter 2, a comparative VL risk analysis is performed in Chapter 3 for the two highly VL-endemic countries in the world: India

and Sudan. A comparative assessment was conducted to identify differences in risk factors associated with VL. From the analysis, we concluded that there are varying risks factors (environmental, ecological and socio-economic) for VL and the sensitivity of these factors depends on the structures of the community.

In Chapter 4, we provided some mathematical details of the model (2.1)–(2.2). The analytical results suggest derivation of the two threshold expression (R_c and R_c^*), estimates of which led to either disease extinction or disease persistence. The parameter space is divided into three regions with distinct dynamics: (i) disease extinction is the only possibility if $0 \leq R_c < R_c^*$, (ii) disease persistence at an endemic level is the only possibility when $1 \leq R_c$, and (iii) disease extinction or persistence both can happen in the long run but the eventual state depends on the initial size of the infectious individuals in the population if $R_c^* \leq R_c < 1$. This type of qualitative behavior in the literature is referred to as backward bifurcation. Furthermore, if treatment rate is assumed to be zero in the model, then the region (iii) vanishes, resulting in a typical forward bifurcation scenario as shown by numerous studies in the literature (75; 30; 121; 122).

Limitation: Throughout the development of this study, we encountered several challenges. Initially, in an attempt to gather parameter estimates for the respective countries from field data, we found that much of the data in the literature is either outdated or from different time periods. For example, the human landing collection is considered unethical, because study worker/participant in VL-endemic areas may be at risk of being bitten by an infected sandfly during the data collection process (135). Many of the empirical studies, were conducted in the 1980s and 1990s, during which only limited development had taken place to reduce the exposure of sandflies through vector control and effective treatment. To get a measure of the human landing catch of sandflies, field scientists now rely on new and novel methods including indoor Cen-

ters for Disease Control (CDC) light trap, sticky oil traps, rodent-baited traps, and human bait catches (90; 59; 44). Second, this study made use of many empirical studies conducted in varying geographic locations where data may have originated and employed different technics of data collection. Compiling these estimates together may introduce uncertainties in parameter estimates when paired in a model. The prevalence of VL was approximated using estimates for a per-population sample size of 10000 and was then used to estimate the prevalence for the entire population.

Future Work: In my future work, I would like to consider all six major VL-affected geographic regions (India, Bangladesh, Sudan, South Sudan, Brazil, and Ethiopia) and perform the comparative analysis between them to identify the risk factors in each of the countries. The implications for such studies would provide health organizations with a globally coordinated perspective on VL and help with the design of better control or eradication programs. Additionally, I will modify the model to include more disease compartments to allow different types of field diagnostic methods used in the various countries as well as reservoir hosts. The study will eventually increase our understanding of the role of disease complication when partially treated recovery individuals develop a complication.

REFERENCES

[1] Indu B IB Ahluwalia, Caryn C Bern, Cristiane C Costa, Tangin T Akter, Rajib R Chowdhury, Mustakim M Ali, Didarul D Alam, Eben E Kenah, Josef J Amann, Meghla M Islam, Yukiko Y Wagatsuma, Rashidul R Haque, Robert F RF Breiman, and James H JH Maguire. Visceral leishmaniasis: consequences of a neglected disease in a Bangladeshi community. *The American Journal of Tropical Medicine and Hygiene*, 69(6):624–628, December 2003.

[2] Jorge Alvar. Interventions for visceral leishmaniasis. *Cochrane Database of Systematic Reviews*, 6, June 2010.

[3] Jorge Alvar, Seife Bashaye, Daniel Argaw, Israel Cruz, Pilar Aparicio, Askal Kassa, Giannos Orfanos, Fernando Parreño, Olusegan Babaniyi, Nigussu Gudeta, Carmen Cañavate, and Caryn Bern. Kala-azar outbreak in libo kemkem, ethiopia: Epidemiologic and parasitologic assessment. *The American Journal of Tropical Medicine and Hygiene*, 77(2):275–282, 2007.

[4] Jorge Alvar, Iván D. Vélez, Caryn Bern, Mercé Herrero, Philippe Desjeux, Jorge Cano, Jean Jannin, Margriet den Boer, and the WHO Leishmaniasis Control Team. Leishmaniasis worldwide and global estimates of its incidence: Text s43. leishmaniasis country profiles, india. *PLoS ONE*, 7(5):e35671, 05 2012.

[5] Jorge Alvar, Iván D. Vélez, Caryn Bern, Mercé Herrero, Philippe Desjeux, Jorge Cano, Jean Jannin, Margriet den Boer, and the WHO Leishmaniasis Control Team. Leishmaniasis worldwide and global estimates of its incidence: Text s81, leishmaniasis country profiles, south sudan. *PLoS ONE*, 7(5):e35671, 05 2012.

[6] Jorge Alvar, Sergio Yactayo, and Caryn Bern. Leishmaniasis and poverty. *Trends in Parasitology*, 22(12):552 – 557, 2006.

[7] Jorge Alvar, Sergio Yactayo, and Caryn Bern. Leishmaniasis and poverty. *Trends Parasitol*, 22(12):552–557, December 2006.

[8] Karthik Bathena. A mathematical model of cutaneous leishmaniasis. Master's thesis, Rochester Institute of Technology, Rochester, NY 14623, 6 2009.

[9] Robert Bergquist and Marcel Tanner. Controlling schistosomiasis in southeast asia: A tale of two countries. In Remigio Olveda Xiao-Nong Zhou, Robert Bergquist and Jürg Utzinger, editors, *Important Helminth Infections in Southeast Asia: Diversity and Potential for Control and Elimination, Part A*, volume 72 of *Advances in Parasitology*, chapter 5, pages 109–144. Academic Press, Ingerod, Brastad, Sweden, July 2010.

[10] Caryn Bern, Orin Courtenay, and Jorge Alvar. Of cattle, sand flies and men: a systematic review of risk factor analyses for south asian visceral leishmaniasis and implications for elimination. *PLoS Negl Trop Dis*, 4(2):e599, 2010.

[11] Caryn Bern, Rashidul Haque, Rajib Chowdhury, Mustakim Ali, Katie M Kurkjian, Louise Vaz, Josef Amann, M A Wahed, Yukiko Wagatsuma, Robert F Breiman, John Williamson, W Evan Secor, and James H Maguire. The epidemiology of visceral leishmaniasis and asymptomatic leishmanial infection in a highly endemic bangladeshi village. *Am J Trop Med Hyg*, 76(5):909–914, May 2007.

[12] Caryn Bern, Allen W Hightower, Rajib Chowdhury, Mustakim Ali, Josef Amann, Yukiko Wagatsuma, Rashidul Haque, Katie Kurkjian, Louise E Vaz, Moarrita Begum, Tangin Akter, Catherine B Cetre-Sossah, Indu B Ahluwalia, Ellen Dotson, W Evan Secor, Robert F Breiman, and James H Maguire. Risk factors for kala-azar in bangladesh. *Emerging infectious diseases*, 11(5):655–662, 00 2005.

[13] Caryn Bern, James H Maguire, and Jorge Alvar. Complexities of assessing the disease burden attributable to leishmaniasis. *Plos Neglected Tropical Diseases*, 2(10):e313, 2008.

[14] Tapan Bhattacharyya, Duncan E. Bowes, Sayda El-Safi, Shyam Sundar, Andrew K. Falconar, Om Prakash Singh, Rajiv Kumar, Osman Ahmed, Marleen Boelaert, and Michael A. Miles. Significantly lower anti-*Leishmania* igg responses in sudanese versus indian visceral leishmaniasis. *PLoS Negl Trop Dis*, 8(2):e2675, 02 2014.

[15] Garrett Birkhoff and Gian-Carlo Rota. *Ordinary Differential Equations*. John Wiley & Sons, 4 edition, January 1989.

[16] Carla L. Black, Sofia Ocaña, Diana Riner, Jaime A. Costales, Mauricio S. Lascano, Santiago Davila, Laura Arcos-Teran, J. Richard Seed, and Mario J. Grijalva. Household risk factors for trypanosoma cruzi seropositivity in two geographic regions of ecuador. *Journal of Parasitology*, 93(1):12–16, 2016/01/27 2007.

[17] S M Blower and H Dowlatabadi. Sensitivity and Uncertainty Analysis of Complex Models of Disease Transmission: An HIV Model, as an Example. *International Statistical Review / Revue Internationale de Statistique*, 62(2):229, August 1994.

[18] M Boelaert, F Meheus, A Sanchez, S P Singh, V Vanlerberghe, A Picado, B Meessen, and S Sundar. The poorest of the poor: a poverty appraisal of households affected by visceral leishmaniasis in bihar, india. *Tropical Medicine & International Health*, 14(6):639–644, 00 2009.

[19] D Bora. Epidemiology of visceral leishmaniasis in india. *The National Medical Journal of India*, 12(2):62–68, 1999.

[20] Fred Brauer and Carlos Castillo-Chavez. *Mathematical Models in Population Biology and Epidemiology*, volume 40 of *Texts in Applied Mathematics*. Springer New York, 2nd edition, November 2012.

[21] Fred Brauer, Carlos Castillo-Chávez, Elmer De La Pava, Kamal Barley, Carlos W Castillo-Garsow, Diego Chowell, Baltazar Espinoza, Gonzalez Paula Parra, Carlos Hernandez Suarez, and Victor M Moreno. *Modelos De La Propagación De Enfermedades Infecciosas*. Universidad Autónoma de Occidente, Cali, Colombia, 12 2014.

[22] RS Bray, KP Chang, et al. Immunodiagnosis of leishmaniasis. *Leishmaniasis.(Human Parasitic Diseases Vol. 1.)*, pages 177–182, 1985.

[23] Bruno Bucheton, Musa Mohamed Kheir, Sayda Hassan El-Safi, Awad Hammad, Adil Mergani, Charles Mary, Laurent Abel, and Alain Dessein. The interplay between environmental and host factors during an outbreak of visceral leishmaniasis in eastern sudan. *Microbes and Infection*, 4(14):1449 – 1457, November 2002.

[24] Sakib Burza, Prabhat K. Sinha, Raman Mahajan, María Angeles Lima, Gaurab Mitra, Neena Verma, Manica Balasegarem, and Pradeep Das. Five-year field results and long-term effectiveness of 20 mg/kg liposomal amphotericin b (ambisome) for visceral leishmaniasis in bihar, india. *PLoS Negl Trop Dis*, 8(1):e2603, 01 2014.

[25] C Castillo-Chavez and H Thieme. Asymptotically autonomous epidemic models. In Ovide Arino, David E. Axelrod, and Marek Kimmel, editors, *Mathematical Population Dynamics: Analysis of Heterogeneity*, volume 1 of *Theory of Epidemics*, pages 33–50. Wuerz, Winnipeg, 1995.

[26] Carlos Castillo-Chavez and Sunmi Lee. Epidemiology modeling. In Björn Engquist, editor, *Encyclopedia of Applied and Computational Mathematics*, pages 427–439. Springer Berlin Heidelberg, Berlin, Heidelberg, 1 edition, 2015.

[27] Carlos Castillo-Chavez and Baojun Song. Dynamical Models of Tuberculosis and Their Applications. *Mathematical Biosciences and Engineering (MBE)*, 1(2):361–404, 11 2004.

[28] Jaya Chakravarty and Shyam Sundar. Drug resistance in leishmaniasis. *Journal of Global Infectious Diseases*, 2(2):167–176, May-Aug 2010.

[29] François Chappuis, Shyam Sundar, Asrat Hailu, Hashim Ghalib, Suman Rijal, Rosanna W Peeling, Jorge Alvar, and Marleen Boelaert. Visceral leishmaniasis: what are the needs for diagnosis, treatment and control? *Nature reviews. Microbiology*, 5(11):873–882, 00 2007.

[30] Nakul Chitnis, J. M. Cushing, and J. M. Hyman. Bifurcation analysis of a mathematical model for malaria transmission. *SIAM Journal on Applied Mathematics*, 67(1):24–45, 2006.

[31] Simon Collin, Robert Davidson, Koert Ritmeijer, Kees Keus, Yosef Melaku, Sammy Kipngetich, and Clive Davies. Conflict and kala-azar: determinants of adverse outcomes of kala-azar among patients in southern Sudan. *Clinical Infectious Diseases*, 38(5):612–619, March 2004.

[32] Kenneth L. Cooke and James A. Yorke. Some equations modelling growth processes and gonorrhea epidemics. *Mathematical Biosciences*, 16(1–2):75 – 101, 1973.

[33] Simon L Croft, Karin Seifert, and Vanessa Yardley. Current scenario of drug development for leishmaniasis. *Indian Journal of Medical Research*, 123(3):399, 2006.

[34] David CV and Craft N. Cutaneous and mucocutaneous leishmaniasis. *Dermatologic Therapy*, 22(6):491–502, 2009.

[35] S.a Das, G.b Matlashewski, G.S.c Bhunia, S.c Kesari, and P.c Das. Asymptomatic leishmania infections in northern india: A threat for the elimination programme? *Transactions of the Royal Society of Tropical Medicine and Hygiene*, 108(11):679–684, 2014. cited By 2.

[36] V. N. R Das, N. A Siddiqui, R. B. Verma, R. K. Topno, D Singh, S. Das, A. Ranjan, K. Pandey, N. Kumar, and P Das. Asymptomatic infection of visceral leishmaniasis in hyperendemic areas of vaishali district, bihar, india: a challenge to kala-azar elimination programmes. *Trans R Soc Trop Med Hyg*, 105(11):661–6, 2011.

[37] O. Martin Sainz de la Maza. Leishmaniasis transmission biology: Role of promastigote secretory gel as a transmission determinant. http://researchonline.lshtm.ac.uk/1775854/, May 2014.

[38] C. B. Palatnik de Sousa, W. R. dos Santos, J. C. Franca-Silva, R. T. da Costa, A. B. Reis, M. Palatnik, W. Mayrink, and O. Genaro. Impact of canine control on the epidemiology of canine and human visceral leishmaniasis in brazil. *The American journal of tropical medicine and hygiene*, 65(5):510, 2001.

[39] P. Desjeux. Urbanization: an increasing risk factor for leishmaniasis. In *World Health Organization: Weekly Epidemiological Recordvol*, volume 77, pages 365–372. Geneva, Netherlands, 2002.

[40] P Desjeux. Leishmaniasis: current situation and new perspectives. *Comparative immunology, microbiology and infectious diseases*, 27(5):305–318, September 2004.

[41] Philippe Desjeux and V. Ramesh. Post-kala-azar dermal leishmaniasis: Facing the challenge of eliminating kala-azar from south asia. In T.K. Jha and E. Noiri, editors, *Kala Azar in South Asia*, pages 111–124. Springer Netherlands, 2011.

[42] O. Diekmann and J. A. P. Heesterbeek. *Mathematical Epidemiology of Infectious Diseases: Model Building, Analysis and Interpretation*, volume 5 of *Wiley series in mathematical and computational biology*. Chichester ; New York John Wiley, illustrated, reprint edition, 2000.

[43] Erin Dilger. *The effects of host-vector relationships and density dependence on the epidemiology of visceral leishmaniasis*. PhD thesis, University of Warwick, Coventry, CV4 7AL, UK, 01 2013.

[44] D. S. Dinesh, P. Das, A. Picado, C. Davies, N. Speybroeck, M. Boelaert, and M. Coosemans. The efficacy of indoor cdc light traps for collecting the sandfly phlebotomus argentipes, vector of leishmania donovani. *Medical and Veterinary Entomology*, 22(2):120–123, 2008.

[45] D S DS Dinesh, A A Ranjan, A A Palit, K K Kishore, and S K SK Kar. Seasonal and nocturnal landing/biting behaviour of Phlebotomus argentipes (Diptera: Psychodidae). *Annals of Tropical Medicine and Parasitology*, 95(2):197–202, March 2001.

[46] Diwakar S Dinesh, Pradeep Das, Albert Picado, Clive Davies, Niko Speybroeck, Bart Ostyn, Marleen Boelaert, and Marc Coosemans. Long-lasting insecticidal nets fail at household level to reduce abundance of sandfly vector phlebotomus argentipes in treated houses in bihar (india). *Trop Med Int Health*, 13(7):953–8, 2008.

[47] Jonathan Dushoff, Wenzhang Huang, and Carlos Castillo-Chavez. Backwards bifurcations and catastrophe in simple models of fatal diseases. *Journal of Mathematical Biology*, 36(3):227–248, 1998.

[48] C. Dye The logic of visceral leishmaniasis control. *The American journal of tropical medicine and hygiene*, 55(2):125–130, August 1996.

[49] C. Dye, R. Killick-Kendrick, M. M. Vitutia, R. Walton, M. Killick-Kendrick, A. E. Harith, M. W. Guy, M.-C. Cañavate, and G. Hasibeder. Epidemiology of canine leishmaniasis: prevalence, incidence and basic reproduction number calculated from a cross-sectional serological survey on the island of gozo, malta. *Parasitology*, 105:35–41, 7 1992.

[50] C. Dye and D M Wolpert. Earthquakes, influenza and cycles of Indian kala-azar. *Trans R Soc Trop Med Hyg*, 82(6):843–850, 1988.

[51] C. Dye Leishmaniasis epidemiology: the theory catches up. *Parasitology*, 104 Suppl:S7–18, January 1992.

[52] Ibrahim M. ELmojtaba, J. Y. T. Mugisha, and Mohsin H A Hashim. Mathematical analysis of the dynamics of visceral leishmaniasis in the Sudan. *Applied Mathematics and Computation*, 217(6):2567–2578, 2010.

[53] D. A. Elnaiem, S J Connor, M C Thomson, M M Hassan, H K Hassan, M A Aboud, and R W Ashford. Environmental determinants of the distribution of phlebotomus orientalis in sudan. *Ann Trop Med Parasitol*, 92(8):877–887, Dec 1998.

[54] D. A. Elnaiem, A. M. Elnahas, and M. A. Aboud. Protective efficacy of lambdacyhalothrin-impregnated bednets against phlebotomus orientalis, the vector of visceral leishmaniasis in sudan. *Medical and Veterinary Entomology*, 13(3):310–314, 1999.

[55] D. A. Elnaiem, H. K. Hassan, and R. D. Ward. Associations of phlebotomus orientalis and other sandflies with vegetation types in the eastern sudan focus of kala-azar. *Medical and Veterinary Entomology*, 13(2):198–203, 1999.

[56] D A Elnaiem, M M Hassan, R Maingon, G H Nureldin, A M Mekawi, M Miles, and R D Ward. The egyptian mongoose, herpestes ichneumon, is a possible reservoir host of visceral leishmaniasis in eastern sudan. *Parasitology*, 122(5):531–536, 2001.

[57] D A Elnaiem, R D Ward, H K Hassan, M A Miles, and I A Frame. Infection rates of Leishmania donovani in Phlebotomus orientalis from a focus of visceral leishmaniasis in eastern Sudan. *Annals of Tropical Medicine and Parasitology*, 92(2):229–232, March 1998.

[58] Dia-Eldin A. Elnaiem. Ecology and control of the sand fly vectors of leishmania donovani in east africa, with special emphasis on phlebotomus orientalis. *Journal of Vector Ecology*, 36:S23–S31, March 2011.

[59] Dia-Eldin A. E. Elnaiem, Hassan K. Hassan, Omran F. Osman, Rhayza Dc Maingon, Robert Killick-Kendrick, and Richard D. Ward. A possible role for phlebotomus (anaphlebotomus) rodhaini (parrot, 1930) in transmission of leishmania donovani. *Parasit Vectors*, 4:238, 2011.

[60] A. Gemperli, P. Vounatsou, N Sogoba, and T Smith. Malaria mapping using transmission models: application to survey data from Mali. *American journal of epidemiology*, 163(3):289–297, February 2006.

[61] Kamlesh Gidwani, Rajiv Kumar, Madhukar Rai, and Shyam Sundar. Longitudinal seroepidemiologic study of visceral leishmaniasis in hyperendemic regions of bihar, india. *The American journal of tropical medicine and hygiene*, 80(3):345–346, 2009.

[62] André Griekspoor, Egbert Sondorp, and Theo Vos. Cost-effectiveness analysis of humanitarian relief interventions: Visceral leishmaniasis treatment in the sudan. *Health Policy and Planning*, 14(1):70–76, 1999.

[63] "The World Bank Group". World databank: World development indicators - india. Online, May 2015.

[64] "The World Bank Group". World databank: World development indicators - sudan. Online, May 2015.

[65] A Hailu, M Gramiccia, and P A Kager. Visceral leishmaniasis in Aba-Roba, south-western Ethiopia: prevalence and incidence of active and subclinical infections. *Ann Trop Med Parasitol*, 103(8):659–670, December 2009.

[66] E. Handman. Leishmaniasis: current status of vaccine development. *Clinical microbiology reviews*, 14(2):229, 2001.

[67] Epco Hasker, Sangeeta Kansal, Paritosh Malaviya, Kamlesh Gidwani, Albert Picado, Rudra Pratap Singh, Ankita Chourasia, Abhishek Kumar Singh, Ravi Shankar, Joris Menten, Mary Edyth Wilson, Mary Elizabeth Wilson, Marleen Boelaert, and Shyam Sundar. Latent infection with leishmania donovani in highly endemic villages in bihar, india. *PLoS Negl Trop Dis*, 7(2):e2053, 2013.

[68] M. Hassan, Ahmed M Elhassan, Ahmed M Musa, Omran F Osman, Fathi MA El-Raba'a, Meshesha Balkew, and Ibrahim M Elhassan. Establishment and maintenance of a laboratory colony of the sandflyPhlebotomus orientalis (Diptera: Psychodidae), the vector of visceral leishmaniasis in Sudan. *Khartoum Medical Journal*, 3(2), 2010.

[69] M M Hassan, E M Elamin, and M M Mukhtar. Isolation and identification of Leishmania donovani from Phlebotomus orientalis, in an area of eastern Sudan with endemic visceral leishmaniasis. *Annals of Tropical Medicine and Parasitology*, 102(6):553–555, September 2008.

[70] M. M. Hassan, F. M. A. Elraba'a, R. D. Ward, R. D. C. Maingon, and D. A. Elnaiem. Detection of high rates of in-village transmission of leishmania donovani in eastern sudan. *Acta Tropica*, 92(1):77–82, 2004.

[71] Herbert W Hethcote. The mathematics of infectious diseases. *SIAM review*, 42(4):599–653, 2000.

[72] Moazzem Hossain and KaziM. Jamil. Geographical distribution of kala-azar in south asia. In T.K. Jha and E. Noiri, editors, *Kala Azar in South Asia*, chapter 1, pages 3–9. Springer Netherlands, 2011.

[73] Adolf Hurwitz. On the Conditions Under Which an Equation Has Only Roots With Negative Real Parts. In Robert Bellman and Richard Kalaba, editors, *Selected Papers on Mathematical Trends in Control Theory*, pages 273–284. Dover Publications, 1964.

[74] Ivy Hurwitz, Heidi Hillesland, Annabeth Fieck, Pradeep Das, and Ravi Durvasula. The paratransgenic sand fly: a platform for control of Leishmania transmission. *Parasit Vectors*, 4:82–82, January 2011.

[75] Hisashi Inaba. Backward Bifurcation in a Model for Vector Transmitted Disease. In Toshio Sekimura, Sumihare Noji, Naoto Ueno, and PhilipK Maini, editors, *Morphogenesis and Pattern Formation in Biological Systems*, pages 271–279–279. Springer Japan, Tokyo, 2003.

[76] T. K. Jha, E. Noiri, Moazzem Hossain, and KaziM. Jamil. *Pathology and Mechanism of Disease in Kala-Azar and Post-kala-azar Dermal Leishmaniasis*, pages 11–14. Springer Netherlands, 2011.

[77] Anand B. Joshi, Murari L. Das, Shireen Akhter, Rajib Chowdhury, Dinesh Mondal, Vijay Kumar, Pradeep Das, Axel Kroeger, Marleen Boelaert, and Max Petzold. Chemical and environmental vector control as a contribution to the elimination of visceral leishmaniasis on the Indian subcontinent: cluster randomized controlled trials in Bangladesh, India and Nepal. *BMC Medicine*, 7(1):54, 2009.

[78] C. L Karp, S. H el Safi, T. A. Wynn, M. M. Satti, A. M. Kordofani, F. A. Hashim, M. Hag-Ali, F. A. Neva, T. B. Nutman, and D. L. Sacks. In vivo cytokine profiles in patients with kala-azar. Marked elevation of both interleukin-10 and interferon-gamma. *The Journal of clinical investigation*, 91(4):1644–1648, April 1993.

[79] Ozge Erisoz Kasap and Bulent Alten. Comparative demography of the sand fly phlebotomus papatasi (diptera: Psychodidae) at constant temperatures. *Journal of vector ecology : journal of the Society for Vector Ecology*, 31(2):378–385, 00 2006.

[80] Shreekant Kesari, Gouri Sankar Bhunia, Vijay Kumar, Algarswamy Jeyaram, Alok Ranjan, and Pradeep Das. A comparative evaluation of endemic and non-endemic region of visceral leishmaniasis (Kala-azar) in India with ground survey and space technology. *Memórias do Instituto Oswaldo Cruz*, 106(5):515–523, 08 2011.

[81] E. A. G. Khalil, A. M. El Hassan, E. E. Zijlstra, M. M. Mukhtar, H. W. Ghalib, B. Musa, M. E. Ibrahim, A. A. Kamil, M. Elsheikh, A. Babiker, and F. Modabber. Autoclaved leishmania major vaccine for prevention of visceral leishmaniasis: A randomised, double-blind, bcg-controlled trial in sudan. *The Lancet*, 356(9241):1565–1569, 11 2000.

[82] E. A. G Khalil, A. M. Musa, S. H. H. Elgawi, A Meshasha, I. Gamar Eldawla, M. O. Elhassan, K. A. Eljaleel, B. M. Younis, M. E. E. Elfaki, and A. M. El-Hassan. Revival of a focus of visceral leishmaniasis in central sudan. *Ann Trop Med Parasitol*, 102(1):79–80, Jan 2008.

[83] R. Killick-Kendrick. The biology and control of phlebotomine sand flies. *Clinics in Dermatology*, 17(3):279 – 289, 1999.

[84] R. Killick Kendrick, William H. R. Lumsden, and D. A. Evans. Biology of leishmania in phlebotomine sandflies. In W. H. R. Lumsden and D. A. Evans, editors, *Biology of the Kinetoplastida*, volume 2, chapter 8, pages 395–460. Academic Press, London–New York, 1 edition, 1979.

[85] Awanish Kumar. Introduction. In Awanish Kumar, editor, *Leishmania and Leishmaniasis*, volume 3 of *SpringerBriefs in Immunology*, chapter 1, pages 1–11. Springer New York, 1 edition, 2013.

[86] Rajiv Kumar and Christian Engwerda. Vaccines to prevent leishmaniasis. *Clin Trans Immunol*, 3:e13–, 03 2014.

[87] R P Lane, M M Pile, and F P Amerasinghe. Anthropophagy and aggregation behaviour of the sandfly Phlebotomus argentipes in Sri Lanka. *Medical and Veterinary Entomology*, 4(1):79–88, January 1990.

[88] J. P. LaSalle and Z Artstein. *The Stability of Dynamical Systems*. CBMS-NSF Regional Conference Series in Applied Mathematics. Society for Industrial and Applied Mathematics, 1976.

[89] Alun L. Lloyd, Ji Zhang, and AMorgan Root. Stochasticity and heterogeneity in host–vector models. *Journal of the Royal Society Interface*, 4(16):851–863, 10 2007.

[90] Paritosh Malaviya, Epco Hasker, Albert Picado, Mukesh Mishra, Jean-Pierre Van Geertruyden, Murari Lal Das, Marleen Boelaert, and Shyam Sundar. Exposure to ¡italic¿phlebotomus argentipes¡/italic¿ (diptera, psychodidae, phlebotominae) sand flies in rural areas of bihar, india: The role of housing conditions. *PLoS ONE*, 9(9):e106771, 09 2014.

[91] Paritosh Malaviya, Albert Picado, Shri Prakash Singh, Epco Hasker, Rudra Pratap Singh, Marleen Boelaert, and Shyam Sundar. Visceral leishmaniasis in muzaffarpur district, bihar, india from 1990 to 2008. *PLoS ONE*, 6(3):e14751 EP –, 00 2011.

[92] Simeone Marino, Ian B Hogue, Christian J Ray, and Denise E Kirschner. A methodology for performing global uncertainty and sensitivity analysis in systems biology. *Journal of theoretical biology*, 254(1):178–196, September 2008.

[93] Laura-Isobel . I. McCall, Chetan E. Chitnis, Wen-Wei . W. Zhang, and Greg Matlashewski. Determinants for the development of visceral leishmaniasis disease. *PLoS Pathogens*, 9(1):e1003053, 1 2013.

[94] M D McKay, R J Beckman, and W J Conover. A Comparison of Three Methods for Selecting Values of Input Variables in the Analysis of Output from a Computer Code. *Technometrics*, 21(2):239, May 1979.

[95] Yosef Melaku, Simon M. Collin, Kees Keus, Francis Gatluak, Koert Ritmeijer, and Robert N. Davidson. Treatment of kala-azar in southern sudan using a 17-day regimen of sodium stibogluconate combined with paromomycin: A retrospective comparison with 30-day sodium stibogluconate monotherapy. *The American Journal of Tropical Medicine and Hygiene*, 77(1):89–94, 2007.

[96] Aviad Moncaz, Oscar Kirstein, Araya Gebresellassie, Wossenseged Lemma, Solomon Yared, Teshome Gebre-Michael, Asrat Hailu, Moshe Shenker, and Alon Warburg. Characterization of breeding sites of phlebotomus orientalis –the vector of visceral leishmaniasis in northwestern ethiopia. *Acta Tropica*, 139:5–14, 11 2014.

[97] Anuj Mubayi, Carlos Castillo-Chavez, Gerardo Chowell, Christopher Kribs-Zaleta, Niyamat Ali Siddiqui, Narendra Kumar, and Pradeep Das. Transmission dynamics and underreporting of kala-azar in the indian state of bihar. *Journal of Theoretical Biology*, 262(1):177–185, 00 2010.

[98] A. K. Mukhopadhyay and R. N. Mishra. Development of leishmania donovani in phlebotomus argentipes and ph. papatasi fed on kala-azar patients in bihar. *Indian Journal of Medical Research - Section A Infectious Diseases*, 93(MAY):152–154, 1991.

[99] Kumar Narendra, Siddiqui NA, Verma RB, and Das P. Knowledge about sandflies in relation to public and domestic control activities of kala-azar in rural endemic areas of bihar. *Journal of Communnity Disease*, 41(2):121–128, 2009.

[100] J. L. Nyungura, V. C. S. Nyambati, M. Muita, and E. Muchiri. Risk factors for the transmission of kala-azar in fangak, south sudan. *Southern Sudan Medical Journal*, 4(2):26–29, May 2011.

[101] Government of India. Census of india. Technical report, Office of the Registrar General and Census Commissioner, New Delhi, India, 2001.

[102] Piero L Olliaro, Philippe J Guerin, Sibylle Gerstl, Astrid Aga Haaskjold, John-Arne Rottingen, and Shyam Sundar. Treatment options for visceral leishmaniasis: a systematic review of clinical studies done in india, 1980–2004. *The Lancet infectious diseases*, 5(12):763–774, 2005.

[103] Ad Hoc Committee on Health Research Relating to Future Intervention Options. Investing in health research and development: Report of the ad hoc committee on health research relating to future intervention options, convened under the auspices of the world health organization. Technical Report TDR/ Gen/96.1, Cornell University, Geneva, Switzerland, September 1996.

[104] World Health Organization(WHO). Visceral leishmaniasis therapy: statement on the outcome of a meeting. *Madrid*, 9 2009.

[105] Bart Ostyn, Kamlesh Gidwani, Basudha Khanal, Albert Picado, François Chappuis, Shri Prakash Singh, Suman Rijal, Shyam Sundar, and Marleen Boelaert. Incidence of symptomatic and asymptomatic ¡italic¿leishmania donovani¡/italic¿ infections in high-endemic foci in india and nepal: A prospective study. *PLoS Negl Trop Dis*, 5(10):e1284, 10 2011.

[106] Bart Ostyn, Veerle Vanlerberghe, Albert Picado, Diwakar Singh Dinesh, Shyam Sundar, Francois Chappuis, Suman Rijal, Jean-Claude Dujardin, Marc Coosemans, Marleen Boelaert, and Clive Davies. Vector control by insecticide-treated nets in the fight against visceral leishmaniasis in the indian subcontinent, what is the evidence? *Tropical Medicine and International Health*, 13(8), August 2008.

[107] David Pace. Leishmaniasis. *Journal of Infection*, 69, Supplement 1:S10 – S18, 2014. Hot Topics in Infection and Immunity in Children - Papers from the 11th annual {IIC} meeting, Oxford, UK, 2013.

[108] B. R. Paiva, A. G. Oliveira, M. E. M. C. Dorval, E. A. B. Galati, and R. S. Malafronte. Species-specific identification of leishmania in naturally infected sand flies captured in mato grosso do sul state, brazil. *Acta Tropica*, 115(1-2):126–130, 2010.

[109] Anup Palit, Sujit Kumar Bhattacharya, and Sachinandan Kundu. Gonotrophic cycle and age gradation of phlebotomus argentipes in west bengal, india. In Prof. P. K. Bandyopadhyay, editor, *Proceedings Of The 22Nd National Congress On Parasitology*, Advances in Parasitology : A Novel Approach Towards a Disease Free World, pages 10–17, Kalyani–741235 West Bengal, India, 00 2011. Department Of Zoology University Of Kalyani.

[110] Thierry Passeron. Acquired hypomelanosis. In Thierry Passeron and Jean-Paul Ortonne, editors, *Atlas of Pigmentary Disorders*, pages 129–183. Springer International Publishing, Cham, 2016.

[111] A Picado, S P Singh, S Rijal, S Sundar, B Ostyn, F Chappuis, S Uranw, K Gidwani, B Khanal, M Rai, I S Paudel, M L Das, R Kumar, P Srivastava, J C Dujardin, V Vanlerberghe, E W Andersen, C R Davies, and M Boelaert. Longlasting insecticidal nets for prevention of Leishmania donovani infection in India and Nepal: paired cluster randomised trial. *BMJ*, 341(dec29 1):c6760–c6760, January 2010.

[112] Albert Picado, Aditya P. Dash, Sujit Bhattacharya, and Marleen Boelaert. Vector control interventions for visceral leishmaniasis elimination initiative in south asia, 2005-2010. *Indian J Med Res.*, 136(1):22–31, July 2012.

[113] Albert Picado, Bart Ostyn, Shri Prakash Singh, Surendra Uranw, Epco Hasker, Suman Rijal, Shyam Sundar, Marleen Boelaert, and François Chappuis. Risk factors for visceral leishmaniasis and asymptomatic ¡italic¿leishmania donovani¡/italic¿ infection in india and nepal. *PLoS ONE*, 9(1):e87641 EP –, 01 2014.

[114] D. M. Pigott, S. Bhatt, N. Golding, K. A. Duda, K. E. Battle, O. J. Brady, J. P. Messina, Y. Balard, P. Bastien, F. Pratlong, J. S. Brownstein, C. C. Freifeld, S. R. Mekaru, P. W. Gething, D. B. George, M. F. Myers, R. Reithinger, and S. I. Hay. Global distribution maps of the leishmaniases. *eLife Sciences Publications Limited*, 3, 06 2014.

[115] Alok Ranjan, Dipika Sur, Vijay P Singh, Niyamat A Siddique, Byomkesh Manna, Chandra S Lal, Prabhat K Sinha, Kamal Kishore, and Sujit K Bhattacharya. Risk factors for indian kala-azar. *The American Journal of Tropical Medicine and Hygiene*, 73(1):74–78, Jul 2005.

[116] Amber Read, Ivy Hurwitz, and Ravi Durvasula. Leishmaniasis: An Update on a Neglected Tropical Disease. In Vadrevu Sree Hari Rao and Ravi Durvasula, editors, *Dynamic Models of Infectious Diseases*, pages 95–138. Springer New York, 2013.

[117] Paul D Ready. Biology of phlebotomine sand flies as vectors of disease agents. *Annual Review of Entomology*, 58:227–250, 2013.

[118] Richard Reithinger, Simon Brooker, and Jan H. Kolaczinski. Visceral leishmaniasis in eastern africa – current status. *Transactions of The Royal Society of Tropical Medicine and Hygiene*, 101(12):1169–1170, 2007.

[119] L. S. Rocha, A. Falqueto, C. B. dos Santos, A. L. Ferreira, G. C. da Graça, G. Grimaldi, and E. Cupolillo. Survey of natural infection by leishmania in sand fly species collected in southeastern brazil. *Transactions of the Royal Society of Tropical Medicine and Hygiene*, 104(7):461–466, 2010.

[120] Juliany Cola Fernandes Rodrigues, Joseane Lima Prado Godinho, and Wanderley Souza. Biology of human pathogenic trypanosomatids: Epidemiology, lifecycle and ultrastructure. In L. S. André Santos, H. Marta Branquinha, M. Claudia d'Avila Levy, F. Lucimar Kneipp, and L. Cátia Sodré, editors, *Proteins and Proteomics of Leishmania and Trypanosoma*, volume 74 of *Subcellular Biochemistry*, chapter 1, pages 1–42. Springer Netherlands, 1 edition, 2014.

[121] Muntaser Safan and Klaus Dietz. On the eradicability of infections with partially protective vaccination in models with backward bifurcation. *Mathematical biosciences and engineering : MBE*, 6(2):395–407, April 2009.

[122] Muntaser Safan, Hans Heesterbeek, and Klaus Dietz. The minimum effort required to eradicate infections in models with backward bifurcation. *Journal of mathematical biology*, 53(4):703–718, October 2006.

[123] Nermin Sakru, Metin Korkmaz, Yusuf Ozbel, Hatice Ertabaklar, Mustafa Sengul, and Seray Ozensoy Toz. Investigation of asymptomatic visceral leishmaniasis cases using western blot in an endemic area in turkey. *The new microbiologica*, 30(1):13–18, 00 2007.

[124] L. Sánchez-García, M. Berzunza-Cruz, I. Becker-Fauser, and E. A. Rebollar-Téllez. Sand flies naturally infected by leishmania (l.) mexicana in the periurban area of chetumal city, quintana roo, méxico. *Transactions of the Royal Society of Tropical Medicine and Hygiene*, 104(6):406–411, 2010.

[125] Henk DFH Schallig, Marilene Canto-Cavalheiro, and Eduardo S da Silva. Evaluation of the direct agglutination test and the rk39 dipstick test for the sero-diagnosis of visceral leishmaniasis. *Memórias do Instituto Oswaldo Cruz*, 97(7):1015–1018, 2002.

[126] Judith A. Schorscher and Marga Goris. Incrimination of phlebotomus (larroussius) orientalis as a vector of visceral leishmaniasis in western upper nile province, southern sudan. *Transactions of The Royal Society of Tropical Medicine and Hygiene*, 86(6):622–623, 1992.

[127] J Seaman, A J Mercer, H E Sondorp, and B L Herwaldt. Epidemic visceral leishmaniasis in southern Sudan: treatment of severely debilitated patients under wartime conditions and with limited resources. *Annals of internal medicine*, 124(7):664–672, April 1996.

[128] G. S. Shukla and V. B. Upadhyay. *Economic Zoology*, chapter 5, pages 70–71. Rastogi Publications, Meerut, India, 4 edition, 2009.

[129] G S Shukla and V B Upadhyay. *Economic Zoology*. Rastogi Publications, Meerut, India, 2010.

[130] NA Siddiqui, Narendra Kumar, A Ranjan, K Pandey, VNR Das, RB Verma, and P Das. Awareness about kala-azar disease and related preventive attitudes and practices in a highly endemic rural area of india. *Southeast Asian Journal Tropical Medicine Public Health*, 41:1–12, January 2010.

[131] Dharmendra Singh, Krishna Pandey, Vidya Nand Rabi Das, Sushmita Das, Neena Verma, Alok Ranjan, Sekhar Chandra Lal, Kamal Roshan Topno, Shubhankar Kumar Singh, Rakesh Bihari Verma, Ashish Kumar, Abul Hasan Sardar, Bidyut Purkait, and Pradeep Das. Evaluation of rk-39 strip test using urine for diagnosis of visceral leishmaniasis in an endemic region of india. *The American Journal of Tropical Medicine and Hygiene*, 88(2):222–226, 2013.

[132] Sarman Singh. New developments in diagnosis of leishmaniasis. *Indian J Med Res*, 123(3):311–330, Mar 2006.

[133] Sarman Singh, Veena Kumari, and Niti Singh. Predicting kala-azar disease manifestations in asymptomatic patients with latent leishmania donovani infection by detection of antibody against recombinant k39 antigen. *Clinical and Diagnostic Laboratory Immunology*, 9(3):568–572, 2002.

[134] Shri P Singh, Albert Picado, Marleen Boelaert, Kamlesh Gidwani, Elisabeth W Andersen, Bart Ostyn, Filip Meheus, Madhukar Rai, François Chappuis, Clive Davies, and Shyam Sundar. The epidemiology of Leishmania donovani infection in high transmission foci in India. *Tropical Medicine & International Health*, 15:12–20, June 2010.

[135] R Srinivasan and K N Panicker. Biting rhythm & biting activity of phlebotomid sandflies. *Indian Journal of Medical Research*, 95:301–304–304, 00 1992.

[136] Narendra Srivastava, Brajesh Kumar Singh, and Archana Yadav. Survey report of visceral leishmaniasis based on serodiagnostic test in madhepura district of bihar, india. *National Academy Science Letters*, 37(6):487–492, 2014.

[137] Pankaj Srivastava, Anand Dayama, Sanjana Mehrotra, and Shyam Sundar. Diagnosis of visceral leishmaniasis. *Trans R Soc Trop Med Hyg*, 105(1):1–6, 2011.

[138] Anette Stauch, Ram Rup Sarkar, Albert Picado, Bart Ostyn, Shyam Sundar, Suman Rijal, Marleen Boelaert, Jean-Claude Dujardin, and Hans-Peter Duerr. Visceral leishmaniasis in the indian subcontinent: Modelling epidemiology and control. *PLoS Negl Trop Dis*, 5(11):e1405, 11 2011.

[139] Anette A Stauch, Hans-Peter HP Duerr, Jean-Claude JC Dujardin, Manu M Vanaerschot, Shyam S Sundar, and Martin M Eichner. Treatment of Visceral Leishmaniasis: Model-Based Analyses on the Spread of Antimony-Resistant L. donovani in Bihar, India. *PLoS Neglected Tropical Diseases*, 6(12):e1973–e1973, December 2012.

[140] A Sud, N Varma, R K Marwaha, F M Patel, A Trehan, S Singh, and S Varma. Visceral leishmaniasis in a non-endemic area of India. *Tropical doctor*, 34(4):247–249, October 2004.

[141] S Sundar, G Agrawal, M Rai, M K Makharia, and H W Murray. Treatment of indian visceral leishmaniasis with single or daily infusions of low dose liposomal amphotericin b: randomised trial. *BMJ (Clinical research ed.)*, 323(7310):419–422, 00 2001.

[142] Shyam Sundar, Himanshu Mehta, A V Suresh, Shri P Singh, Madhukar Rai, and Henry W Murray. Amphotericin b treatment for indian visceral leishmaniasis: conventional versus lipid formulations. *Clin Infect Dis*, 38(3):377–83, 2004.

[143] Shyam Sundar and M Rai. Laboratory diagnosis of visceral leishmaniasis. *Clinical and Diagnostic Laboratory Immunology*, 25(2), September 2002.

[144] M. Svobodová, B. Alten, L. Zídková, V. Dvořák, J. Hlavačková, J. Myšková, V. Šeblová, O. E. Kasap, A. Belen, J. Votýpka, and P. Volf. Cutaneous leishmaniasis caused by leishmania infantum transmitted by phlebotomus tobbi. *International Journal for Parasitology*, 39(2):251–256, 2009.

[145] C P Thakur. Socio-economics of visceral leishmaniasis in bihar (india). *Transactions of the Royal Society of Tropical Medicine and Hygiene*, 94(2):156–7, 2000.

[146] Puja Tiwary, Dinesh Kumar, Mukesh Mishra, Rudra Pratap Singh, Madhukar Rai, and Shyam Sundar. Seasonal variation in the prevalence of sand flies infected with *Leishmania donovani*. *PLoS ONE*, 8(4):e61370 EP –, 04 2013.

[147] Roshan K Topno, Vidya N R Das, Alok Ranjan, Krishna Pandey, Dharmender Singh, Nawin Kumar, Niyamat A Siddiqui, Vijay P Singh, Shreekant Kesari, Narendra Kumar, Sanjeev Bimal, Annadurai Jeya Kumar, Chetram Meena, Ranjeet Kumar, and Pradeep Das. Asymptomatic infection with visceral leishmaniasis in a disease-endemic area in bihar, india. *The American Journal of Tropical Medicine and Hygiene*, 83(3):502–506, 00 2010.

[148] Felipe Francisco Tuon, Vicente Amato Neto, and Valdir Sabbaga Amato. Leishmania: origin, evolution and future since the precambrian. *FEMS Immunology & Medical Microbiology*, 54(2):158–166, 2008.

[149] P. van den Driessche and James Watmough. Reproduction numbers and subthreshold endemic equilibria for compartmental models of disease transmission. *Mathematical Biosciences*, 180(1–2):29–48, 2002/12// 2002.

[150] Jorge X Velasco-Hernandez and Carlos Castillo-Chavez. Modelling vector-host disease transmission and food web dynamics through the mixing/pair formation approach. In V. Lakshmikantham, editor, *World Congress of Nonlinear Analysts '92*, volume 1 of *Proceedings of the First World Congress of Nonlinear Analysts, Tampa, Florida, August 19-26, 1992*, pages 3175–3186. Walter de Gruyter & Co., Berlin, Boston: DE GRUYTER, August 1996.

[151] World Health Organization (WHO). The world health assembly resolution on the "control of leishmaniasis". http://www.who.int/leishmaniasis/resolutions/en/, May 2007.

[152] World Health Organization (WHO). Control of the leishmaniasis: report of a meeting of the who expert committee on the control of leishmaniases, geneva, 22-26 march 2010. Online, Geneva, Switzerland, March 2010.

[153] World Health Organization (WHO). Leishmaniasis: worldwide epidemiological and drug access update. Online, 2012.

[154] World Health Organization (WHO). Who control of neglected tropical diseases(ntd). Oline, 2013.

[155] Sally Osman SO Widaa, Khalid Awadelkarim KA Ahmed, Amel Ahmed Elsheikh AA Bari, Mayada Mohmmedelhassan MM Ali, Mihad Abdelaal MA Ibrahim, Mohammed Ahmed MA Bashir, Ahmed Hamid Awadelkarim AH Mastour, Zakkiah Algali ZA Yagi, and Mo'awia Mukhtar MM Hassan. Sandflies (Diptera: Psychodidae) in a focus of visceral leishmaniasis in White Nile, Sudan. *Memorias do Instituto Oswaldo Cruz*, 107(4):470–475, June 2012.

[156] J A Yorke, H W Hethcote, and A Nold. Dynamics and control of the transmission of gonorrhea. *Sex Transm Dis*, 5(2):51–56, Apr-Jun 1978.

[157] EE Zijlstra, AM Musa, EAG Khalil, IM El Hassan, and AM El-Hassan. Post-kala-azar dermal leishmaniasis. *The Lancet Infectious Diseases*, 3(2):87–98, 2 2003.

APPENDIX A

MODEL DERIVATION AND COMPUTATIONS

A.1 Complete Model Derivation

The dynamics of *Leishmania donovani* transmission in humans and sandflies are modeled by the system of equations given by model (2.1)–(2.2) in wich the force of infection is modeled by Equation B.0.1. Newly infected but not yet infectious individuals move into the asymptomatic population (sub-clinical infection, exposed to VL but not yet infectious), who may exit the system through natural death or through progress to clinical VL. The change in A_h population is

$$\frac{dA_h}{dt} = \lambda_{vh} S_h - (\phi_h + \mu_h) A_h.$$

The asymptomatic can then progress to a VL clinical symptoms stage (I_h) at the rate ϕ_h:

$$\frac{dI_h}{dt} = \phi_h A_h - (\mu_h + \theta_h) I_h,$$

where θ_h is the per-capita treatment rate and μ_h is the per-capita departure rate. The infectious individuals with clinical symptoms may enter treatment (T_h) at the rate θ_h. Through successful treatment, individuals recover at the rate γ_h, and hence

$$\frac{dT_h}{dt} = \theta_h I_h - (\gamma_h + \mu_h) T_h.$$

The population of recovered individuals from VL (R_h) is increased following successful treatment, leading to permanent immunity into the R_h class (at the rate γ_h). The population is decreased by natural death and is given by

$$\frac{dR_h}{dt} = \gamma_h T_h - \mu_h R_h.$$

The population of new female sandflies (S_v) is increased by an adult recruitment rate (λ_v) and decrease by natural mortality (μ_v). The vector in this population can acquire the *L. Donovani parasite* from an infectious human at a rate λ_v and is modeled by Equation 2.4. The change in the susceptible population is described by

$$\frac{dS_v}{dt} = \Lambda_v - \lambda_{hv} S_v - \mu_v S_v.$$

The population of infected female sandflies is generated at the per-capita rate λ_{hv} and diminished by the natural death rate μ_v. Thus,

$$\frac{dI_v}{dt} = \lambda_{hv} S_v - \mu_v.$$

A.2 Details of the Analytical Results of VL Model

A.2.1 Derivation of the Basic Reproductive Number

For simplification, we let $G_1 = \phi_h + \mu_h, G_2 = \theta_h + \mu_h$ and $G_3 = \gamma + \mu_h$. Considering the infected sub-populations $I_h(t)$, $A_h(t)$, and $I_v(t)$, we let $\mathcal{F}$ be the rate of new

infections into the infected compartments and $\mathcal{V}$ be the rate of exit of humans into infected compartments:

$$\frac{d}{dt}\begin{bmatrix} A_h \\ I_h \\ I_v \end{bmatrix} = \mathcal{F} - \mathcal{V} = \begin{bmatrix} \frac{bm_{v:h}\beta_{vh}I_vS_h}{N_v} \\ 0 \\ \frac{b\beta_{hv}I_hS_v}{N_h} \end{bmatrix} - \begin{bmatrix} (\phi_h + \mu_h)\, A_h \\ -\phi_h A_h + (\theta_h + \mu_h)\, I_h \\ \mu_v I_v \end{bmatrix}. \tag{A.1}$$

We apply the next generation operator method presented in (149), where $\mathcal{F}$ is considered to be the vector of rates of inflow of new infections in each compartment and $\mathcal{V} = \mathcal{V}^+ + \mathcal{V}^-$ is the vector of rates transfer rates of individuals into and out of the infective compartments by all other processes. Taking the Jacobian matrix of each vector with respect to each of the infectious classes and evaluating at $E_0 = (\Lambda_h/\mu_h, 0, 0, 0, 0, \Lambda_v/\mu_v, 0)$ gives

$$\mathbf{F} = \begin{bmatrix} 0 & 0 & b\, m_{v:h}\beta_{vh} \\ 0 & 0 & 0 \\ 0 & \frac{b\beta_{hv}\Lambda_v\mu_h}{\Lambda_h\mu_v} & 0 \end{bmatrix} \quad \text{and} \quad \mathbf{V} = \begin{bmatrix} G_1 & 0 & 0 \\ -\phi_h & G_2 & 0 \\ 0 & 0 & \mu_v \end{bmatrix}. \tag{A.2}$$

Computing $\mathbf{F}\mathbf{V}^{-1}$, we obtain

$$\mathbf{F}\mathbf{V}^{-1} = \begin{bmatrix} 0 & 0 & \frac{b\, m_{v:h}\beta_{vh}}{\mu_v} \\ 0 & 0 & 0 \\ \frac{b\beta_{hv}\Lambda_v\mu_h\phi_h}{\mu_v\Lambda_h G_1 G_2} & \frac{b\beta_{hv}\Lambda_v\mu_h}{\mu_v\Lambda_h G_2} & 0 \end{bmatrix}. \tag{A.3}$$

Taking the spectral radius of the next generation matrix operator, $\rho\left(\mathbf{F}\mathbf{V}^{-1}\right)$, gives

$$\mathcal{R}_C = \rho\left(\mathbf{F}\mathbf{V}^{-1}\right) = \sqrt{\frac{b\beta_{hv}}{\mu_v} \cdot \frac{b\beta_{vh}\phi_h}{(\phi_h + \mu_h)\,(\theta_h + \mu_h)} \cdot m_{v:h}}. \tag{A.4}$$

A.2.2 Positivity and Boundedness of Solutions

Since this model is of epidemiologyical relevance, all its associated parameters are non-negative. Further, the following non-negativity result holds. The state variables of the model (2.1) are non-negative for all time, so solutions are positively invariant in $\Omega = \Omega_h \times \Omega_v$, where

$$\begin{aligned} \Omega_h &= \left\{(S_h, A_h, I_h, T_h, R_h) \in \mathbb{R}^5_+ : S_h + A_h + I_h + T_h + R_h \leq \frac{\Lambda_h}{\mu_h}\right\}, \\ \Omega_v &= \left\{(S_v, I_v) \in \mathbb{R}^2_+ : S_v + I_v \leq \frac{\Lambda_v}{\mu_v}\right\}. \end{aligned}$$

Remark A.2.1. If all initial conditions start in region $\Omega = \Omega_h \times \Omega_v$, then all corresponding solutions $(S_h, A_h, I_h, T_h, R_h, S_v, I_v)'$ are non-negative for all $t > 0$, where $'$ means vector transpose.

Proof. Because this model is of epidemiological relevance, we first show that the region Ω is positively invariant in $\mathbb{R}^7_+$, with respect to the system (1) and (2). It is easy to see that $\dot{S}_h \mid_{S_h=0} > 0, \dot{A}_h \mid_{A_h=0} > 0, \dot{I}_h \mid_{I_h=0} > 0, \dot{T}_h \mid_{T_h=0} > 0, \dot{R}_h \mid_{R_h=0} > 0, \dot{S}_v \mid_{S_v=0} > 0, \dot{I}_v \mid_{I_V=0} > 0$. Hence, all trajectories point to inside the region Ω (where the dot means derivative with respect to time). Also, the time derivative along all solutions of (1) is

$$\begin{aligned} \frac{dN_h}{dt} &= \Lambda_h - N_h\mu_h \\ &\leq \Lambda_h - N_h\mu_h. \end{aligned}$$

It is clear that $dN_h/dt < 0$ if $N_h > \Lambda_h/\mu_h$. Hence, on applying a (comparison) theorem from Birkhoff and Rota ((15)) on differential inequality, we get

$$0 \leq N_h(t) \leq \frac{\Lambda_h}{\mu_h} + \left(N_h(0) - \frac{\Lambda_h}{\mu_h}\right) \mathrm{e}^{-\mu_h t}.$$

When $t \to \infty$, then $N_h < \Lambda_h/\mu_h$. Thus, for initial conditions $N_h(0) < \Lambda_h/\mu_h$, we have $N_h(t) < \Lambda_h/\mu_h$. Similarly, let $(S_v, I_v) \in \mathbb{R}^2_+$ be the solution with non-negative initial solution. Taking the time derivative along the sum of all solutions curves of model (2) gives

$$\begin{aligned} \frac{N_v}{dt} &= \Lambda_v - N_h\mu_h \\ &\leq \Lambda_v - N_h\mu_h. \end{aligned}$$

By differential inequality theorem in (15), we find

$$0 \leq N_v(t) \leq \frac{\Lambda_v}{\mu_v} + \left(N_v(0) - \frac{\Lambda_v}{\mu_v}\right) \mathrm{e}^{-\mu_v t},$$

where $N_v(0)$ represents the initial sandfly population at the initial phase of the disease. As $t \to \infty$, the inequality becomes

$$0 \leq \lim_{t\to\infty} N_v(t) \leq \frac{\Lambda_v}{\mu_v}.$$

In particular, we have $N_v(t) < \Lambda_v/\mu_v$ if $N_v(0) < \Lambda_v/\mu_v$. Hence the region Ω is positively invariant. Furthermore, if we start with initial conditions $N_h(0) > \Lambda_h/\mu_h$ and $N_v(0) > \Lambda_v/\mu_v$, then either the solutions enter Ω in finite time or $N_h(t) \to \Lambda_h/\mu_h$ and $N_v(t) \to \Lambda_v/\mu_v$, as $t \to \infty$.

Hence, for the model (2.1–2.2), the compact set Ω is a positively invariant and absorbing set that attracts all solutions of model (2.1–2.2) starting in $\mathbb{R}^7_+$. □

A.2.3 Stability Analysis of the Disease-Free Equilibrium Point (DFE)

Local stability of the Endemic Equilibrium (DFE)

Remark A.2.2. The disease-free equilibrium point, E_0, of model system 2.1- 2.2 is locally asymptotically stable (LAS) if $\mathcal{R}_C < 1$, and unstable if $\mathcal{R}_C > 1$.

Proof. Linearization at DFE gives

$$J(E_0) = \begin{bmatrix} -\mu_h & 0 & 0 & 0 & 0 & 0 & -b\beta_{vh} \\ 0 & -G_1 & 0 & 0 & 0 & 0 & b\beta_{vh} \\ 0 & \phi_h & -G_2 & 0 & 0 & 0 & 0 \\ 0 & 0 & \theta_h & -G_3 & 0 & 0 & 0 \\ 0 & 0 & 0 & \gamma_h & -\mu_h & 0 & 0 \\ 0 & 0 & -\frac{b\beta_{hv}\Lambda_v\mu_h}{\mu_v\Lambda_h} & 0 & 0 & -\mu_v & 0 \\ 0 & 0 & \frac{b\beta_{hv}\Lambda_v\mu_h}{\mu_v\Lambda_h} & 0 & 0 & 0 & -\mu_v \end{bmatrix} \tag{A.5}$$

The characteristic polynomial of the Jacobian matrix $J(E_0)$ is given by

$$P(\lambda) = (\lambda + \mu_v)(\lambda + \mu_h)^2(\lambda + G_3)\left(\lambda^3 + h_2\lambda^2 + h_1\lambda + h_0\right) \tag{A.6}$$

where $h_0 = \mu_v(\phi_h + \mu_h)(\theta_h + \mu_h)(1 - \mathcal{R}_C^2)$, $h_1 = (G_1 + G_2)\mu_v + G_1G_2$ and $h_2 = G_2 + G_1 + \mu_v$. We observe that four eigenvalues for this polynomial have negative real parts, and are given by $\lambda = \{-\mu_v, -G_3, -\mu_h, -\mu_h\}$ with geometric multiplicity of two. The remaining expression is a cubic polynomial, $P(\lambda) = \lambda^3 + h_2\lambda^2 + h_1\lambda + h_0$. Applying the Routh-Hurwitz criteria (73), we find the conditions for all eigenvalues to have negative real parts, that is $H_1 = h_1 > 0$, $H_2 = h_0 > 0$, and $H_3 = h_2h_1 - h_0 > 0$. Thus by Routh-Hurwitz criteria, E_0 is locally asymptotically stable for $\mathcal{R}_C < 1$ and is unstable for $\mathcal{R}_C > 1$. □

Global Stability of the Disease-free Equilibrium (DFE)

Remark A.2.3. The disease-free equilibrium $E_0 = \left(\frac{\Lambda_h}{\mu_h}, 0, 0, 0, 0, \frac{\Lambda_v}{\mu_v}, 0\right)$ of model system 2.1- 2.2 is globally asymptotically stable in Ω whenever $\mathcal{R}_C < 1$ and unstable if $\mathcal{R}_C > 1$.

Proof. Consider a candidate Lyapunov function defined in Ω,

$$\begin{aligned} \mathcal{L}(t) =& L_1\left(S_h - S_h^* - S_h^*\log\left(\frac{S_h}{S_h^*}\right)\right) + L_2A_h + L_3I_h \\ &+ L_4\left(S_v - S_v^* - S_v^*\log\left(\frac{S_v}{S_v^*}\right)\right) + L_5I_v \end{aligned} \tag{A.7}$$

where the constants $L_i, i = 1...5$ are taken to be $L_1 = L_2 = \mu_h\mathcal{R}_C^2$, $L_3 = \frac{L_3}{\phi}$, and $L_4 = L_5 = \frac{\mu_v\mathcal{R}_C^2}{b\beta_{vh}}$. The function $\mathcal{L}$ is positive definite, in the sense that it vanishes

only at the disease-free equilibrium while otherwise it is positive in Ω. Moreover, taking the time derivative of the function in (A.7) along solutions of system 2.1–2.2 and then substituting the expression for the derivatives, gives

$$\begin{aligned}\dot{\mathcal{L}}=&L_1\left(1-\frac{S_h^*}{S_h}\right)\left(\Lambda_v-\frac{b\beta vhI_vS_h}{N_h^*}-\mu_hS_v\right)+L_2\left(\frac{b\beta_{vh}I_vS_h}{N_h^*}-G_1A_h\right)+L_3\left(\phi A_h-G_2I_h\right)\\&+L_4\left(1-\frac{S_v^*}{S_v}\right)\left(\Lambda_v-\frac{b\beta_{hv}S_vI_h}{N_h^*}-\mu_vS_v\right)+L_5\left(\frac{b\beta_{hv}S_vI_h}{N_h^*}-\mu_vI_v\right)\end{aligned} \tag{A.8}$$

Substituting the L_i constants in equation A.8 and then grouping and collecting terms, gives

$$\dot{\mathcal{L}}=\mu_h\mathcal{R}_C^2\left(2-\frac{S_h}{S_h^*}-\frac{S_h^*}{S_h}\right)+\frac{\mu_v\mathcal{R}_C^2}{b\beta_{vh}}\left(2-\frac{S_v}{S_v^*}-\frac{S_v^*}{S_v}\right)+\left(\mathcal{R}_0^2-1\right)\frac{\mu_v}{\phi}\left(G_1\mathcal{R}_C^2G_2K_h+b\beta_{vh}K_v\phi\right). \tag{A.9}$$

The first two terms are negative, as the arithmetic mean is greater than or equal to the geometrical mean. However, the third term is negative for values of $\mathcal{R}_0<1$. Therefore, by Lyapunov-LaSalle asymptotic stability (88), the disease-free equilibrium E_0 is globally asymptotically stable if $\mathcal{R}_0<1$ for all $t>0$. □

A.2.4 Stability Analysis of the Endemic Equilibrium Point, E^*

As a result of no disease deaths, observeD in Figure 4.2, the existence of a DFE and an Endemic Equilibrium (EE) that depends on $\mathcal{R}_C$. In this section, we show the local and global stability of the EE when $\mathcal{R}_C^*$ become 1.

Local Stability of the Endemic Equilibrium (EE)

Remark A.2.4. If $\mathcal{R}_C>1$, then the unique positive endemic equilibrium(EE), E^*, for Model system equations 2.1–2.2 is locally asymptotically stable.

Proof. The EE of the Model system equations 2.1–2.2 is given by E^*. The Jcobian matrix at EE gives by

$$J(E^*)=\begin{bmatrix}-b\beta_{vh}I_v^*-\mu_h & 0 & 0 & 0 & 0 & 0 & -b\beta_{vh}S^*\\ b\beta_{vh}I_v^* & -G_1 & 0 & 0 & 0 & 0 & b\beta_{vh}S^*\\ 0 & \phi_h & -G_3 & 0 & 0 & 0 & 0\\ 0 & 0 & \theta_h & -G_3 & 0 & 0 & 0\\ 0 & 0 & 0 & \gamma_h & -\mu_h & 0 & 0\\ 0 & 0 & -b\beta_{hv}S_v^* & 0 & 0 & -b\beta_{hv}I_h^*-\mu_v & 0\\ 0 & 0 & b\beta_{hv}S_v^* & 0 & 0 & b\beta_{hv}b\beta_{hv}I_h^* & -\mu_v\end{bmatrix}.$$

It's characteristic polynomial is given by

$$P(\lambda)=(\lambda+\mu_h)(\lambda+G_3)(\mu_v+\lambda)\left(\lambda^4+h_3\lambda^3+h_2\lambda^2+h_1\lambda+h_0\right),$$

where

$$
\begin{aligned}
h_3 =& b\beta_{vh}I_v^* + b\beta_{hv}I_h^* + G_2 + G_1 + \mu_v + \mu_h,\\
h_2 =& b^2\beta_{hv}I_h^*\beta_{vh}I_v^* + b\beta_{hv}I_h^*\mu_h + \mu_v b\beta_{vh}I_v^* + G_2 b\beta_{vh}I_v^* + b\beta_{hv}I_h^*G_2\\
&+ G_1 b\beta_{vh}I_v^* + b\beta_{hv}I_h^*G_1 + G_1\mu_h + \mu_v\mu_h + G_2\mu_h + \mu_v G_2 + \mu_v G_1 + G_2G_1,\\
h_1 =& \frac{\phi_h,\beta_{hv}b\Big(\beta_{vh}\mu_h\beta_{hv}\phi_h\left(G_1+G_2\right)b^2+\left(\left(G_2+\mu_v\right)G_1+\mu_v G_2\right)G_1G_2\beta_{vh}b+\mu_h {G_2}^2{G_1}^2\Big)\mu_h}{G_1(G_2G_1\mu_v+\mu_h b\beta_{hv}\phi_h)G_2}\\
&+ \frac{G_1G_2\mu_v\mu_h\left(\mathcal{R}_C^2-1\right)}{b\beta_{vh}+\mu_h},\\
h_0 =& \mu_v\mu_h G_1G_2\left(\mathcal{R}_C^2-1\right).
\end{aligned}
$$

We observe that the characteristic polynomial $P(\lambda)$ can be factored to roots $\lambda = -\mu_h, -\mu_v, -G_3$ and $\overline{P}(\lambda) = (\lambda^4 + h_3\lambda^3 + h_2\lambda^2 + h_1\lambda + h_0)$. Applying the Routh-Hurwitz conditions: $h_i > 0$, $(i = 0, ..., 4)$, $h_1h_2 - h_0h_3 > 0$, and $h_1h_2h_3 > h_1 + h_0h_3^2$, we find that

$$
\begin{aligned}
h_1h_2 - h_0h_3 =& I_hI_v\beta_{vh}\beta_{hv}\left(I_h\beta_{hv}+I_v\beta_{vh}\right)b^3+\Big(\left(I_h\beta_{hv}+I_v\beta_{vh}\right)^2G_1+\left(I_h\beta_{hv}+I_v\beta_{vh}\right)^2G_2\\
&+ {I_v}^2\mu_v{\beta_{vh}}^2 + 2\,I_hI_v\beta_{hv}\left(\mu_h+\mu_v\right)\beta_{vh} + {I_h}^2\mu_h{\beta_{hv}}^2\Big)b^2\\
&+\Big(\left(I_h\beta_{hv}+I_v\beta_{vh}\right){G_1}^2 + 2\,\left(I_h\beta_{hv}+I_v\beta_{vh}\right)\left(G_2+\mu_h+\mu_v\right)G_1\\
&+\left(I_h\beta_{hv}+I_v\beta_{vh}\right){G_2}^2 + 2\,\left(\mu_h+\mu_v\right)\left(I_h\beta_{hv}+I_v\beta_{vh}\right)G_2\\
&+2\,I_v\left(\mu_h+1/2\,\mu_v\right)\mu_v\beta_{vh} + I_h\mu_h\beta_{hv}\left(\mu_h+2\,\mu_v\right)\Big)a\\
&+\left(\left(G_2+\mu_h+\mu_v\right)G_1+\left(\mu_h+\mu_v\right)\left(G_2+\mu_h\right)\right)\left(G_1+G_2+\mu_v\right)\\
>& 0
\end{aligned}
\tag{A.10}
$$

and

$$
\begin{aligned}
h_1h_2h_3 - h_1^2 + h_0h_3^2 =& \Big(\beta_{hv}I_hI_v\beta_{vh}\left(G_1+G_2\right)b^2\\
&+\left(\left(\left(I_h\beta_{hv}+I_v\beta_{vh}\right)G_2+\mu_h\beta_{hv}I_h+\mu_v\beta_{vh}I_v\right)G_1\right.\\
&\left.+G_2\left(\mu_h\beta_{hv}I_h+\mu_v\beta_{vh}I_v\right)\right)a\\
&+\mu_h\left(\left(G_2+\mu_v\right)G_1+\mu_vG_2\right)\Big)\Big(\Big(b^2I_hI_v\beta_{vh}\beta_{hv}\\
&+\left(\left(I_h\beta_{hv}+I_v\beta_{vh}\right)G_1+\left(I_h\beta_{hv}+I_v\beta_{vh}\right)G_2+\mu_h\beta_{hv}I_h+\mu_v\beta_{vh}I_v\right)a\\
&+\left(G_2+\mu_h+\mu_v\right)G_1+\left(\mu_h+\mu_v\right)G_2+\mu_h\mu_v\Big)\left(b\left(I_h\beta_{hv}+I_v\beta_{vh}\right)\right.\\
&\left.+G_1+G_2+\mu_h+\mu_v\right)-\beta_{hv}I_hI_v\beta_{vh}\left(G_1+G_2\right)b^2\\
&-\left(\left(\left(I_h\beta_{hv}+I_v\beta_{vh}\right)G_2+\mu_h\beta_{hv}I_h+\mu_v\beta_{vh}I_v\right)G_1\right.\\
&\left.+G_2\left(\mu_h\beta_{hv}I_h+\mu_v\beta_{vh}I_v\right)\right)a-\mu_h\left(\left(G_2+\mu_v\right)G_1+\mu_vG_2\right)\Big)\\
&-\left(b\left(I_h\beta_{hv}+I_v\beta_h\right)+G_1+G_2+\mu_h+\mu_v\right)^2bG_1G_2\left(aI_hI_v\beta_{vh}\beta_{hv}\right.\\
&\left.+\mu_h\beta_vI_h+\mu_v\beta_{vh}I_v\right)\\
>& 0
\end{aligned}
\tag{A.11}
$$

hold when $\mathcal{R}_C > 1$. Thus, the endemic equilibrium, E^*, is locally asymptotically stable because all eigenvalues of the septic polynomial have all negative real parts for $\mathcal{R}_C > 1$. □

Global stability of the Endemic Equilibrium (EE)

Remark A.2.5. If $\mathcal{R}_C > 1$, then the unique positive endemic equilibrium, E^*, for Model (2.1–2.2) is globally asymptotically stable.

Proof. Consider a candidate Lyapunov function defined in Ω,

$$\begin{aligned}\mathcal{L}(t) = L_1 \left[S_h - S_h^* - S_h^* \log\left(\frac{S_h}{S_h^*}\right)\right] + L_2 \left[A_h - A_h^* - A_h^* \log\left(\frac{A_h}{A_h^*}\right)\right] \\ + L_3 \left[I_h - I_h^* - I_h^* \log\left(\frac{I_h}{I_h^*}\right)\right] + L_4 \left[S_v - S_v^* - S_v^* \log\left(\frac{S_v}{S_v^*}\right)\right] \\ + L_5 \left[I_v - I_v^* - I_v^* \log\left(\frac{I_v}{I_v^*}\right)\right],\end{aligned} \tag{A.12}$$

where the constants $L_i, i = 1...5$ are given by $L_1 = L_2 = \frac{N_h^*}{b\beta_{vh} I_v^* S_h^*}$, $L_3 = \frac{1}{\phi_h A_h^*}$, and $L_4 = L_5 = \frac{N_h^*}{b\beta_{hv} S_v^* I_h^*}$. Taking the time derivative of the Lyapunov function in (A.12) along solutions of system 2.1–2.2 and then substituting the expression for the derivatives gives

$$\begin{aligned}\dot{\mathcal{L}} = L_1 \left(1 - \frac{S_h^*}{S_h}\right)\left(\Lambda_h - \frac{b\beta vh I_v S_h}{N_h^*} - \mu_h S_v\right) + L_2 \left(1 - \frac{A_h^*}{A_h}\right)\left(\frac{b\beta_{vh} I_v S_h}{N_h^*} - G_1 A_h\right) \\ + L_3 \left(1 - \frac{I_h^*}{I_h}\right)(\phi_h A_h - G_2 I_h) + L_4 \left(1 - \frac{S_v^*}{S_v}\right)\left(\Lambda_v - \frac{b\beta_{hv} S_v I_h}{N_h^*} - \mu_v S_v\right) \\ + L_5 \left(1 - \frac{I_v^*}{I_v}\right)\left(\frac{b\beta_{hv} S_v I_h}{N_h^*} - \mu_v I_v\right).\end{aligned} \tag{A.13}$$

Substituting the L_i in A.13 and performing some algebra gives

$$\begin{aligned}\dot{\mathcal{L}} = \frac{\mu_h N_h^*}{b\beta_{vh} I_v^* S_h^*}\left(2 - \frac{S_h}{S_h^*} - \frac{S_h^*}{S_h}\right) + \frac{\mu_h N_h^*}{b\beta_{hv} S_v^* I_h^*}\left(2 - \frac{S_v}{S_v^*} - \frac{S_v^*}{S_v}\right) \\ + 5 - \frac{S_v^*}{S_v} - \frac{I_v^* S_v I_h}{S_v^* I_h^* I_v} - \frac{S_h^*}{S_h} - \frac{A_h^* I_v S_h}{I_v^* S_h^* A_h} - \frac{I_h^* A_h}{A_h^* I_h}\end{aligned} \tag{A.14}$$

The first two terms in parenthesis and the remaining expression are negative, as the arithmetic mean is greater than or equal to the geometrical mean. Therefore, by LaSalle's Invariable Principle (88), the endemic equilibrium point E^* is globally asymptotically stable in Ω for $\mathcal{R}_0 > 1$ for all $t > 0$. □

APPENDIX B

ESTIMATING MODEL PARAMETERS

B.0.1 Estimating Model Parameters

After extensive searching of the literature, annual reports, and census data, ecological and epidemiological parameter ranges for the respective human and sandfly populations in India and Sudan were gathered and estimated. See Table 2.2 for a summary of these estimates.

b: The per-capita daily biting rate on humans by female Phlebotomus sandflies species differ by geographical region.

P. Argentipes (India): On average, the biting rate of a sandfly on a human per night was estimated to be 0.85 *per day* and range from 0.2 to 2.5 per day (87). More current studies found a mean estimates biting density per day to be 0.7997 with a range of 0.1667 to 2.0833 per day (45). From these studies, we calculated the mean number of bites on a human to be 0.7997 with a range of 0.1667 to 2.083 bites per human.

P. Orientalis (Sudan): In a field investigations conducted by Elnaiem, et al., the average bites *per man-night* was estimated to range from 23.7 to 40.3 for no bed net and 4.2 to 9.6 for those using untreated bed nets over a period of 12 nights (54). In both studies, an average of 32 bites per *man-night* was established over a period of 12 nights. In our model we took the average biting rate to be 1.6208 per man-night with a range of 0.35 to 3.3583 per man-night.

β_{hv}**:** The transmission probability that an uninfected sandfly acquires a VL parasite from an infectious human.

India Parameter estimates were taken from a recent modeling study on VL in India by Stauch A, et al.(138; 139). From these, we took the mean transmission potential to be 0.025 with a range between 0.013 and 0.063.

Sudan We use the infection rate for sandflies, using an equation from our model to estimate β_{hv}. We first solve for β_{hv} in this expression and use average infection rates of 9.6% (126), 8.6% (69) and 6.9%, and 3.6% (57) and the average biting rates in Table 2.2. The average transmission potential in human for *P. Orientalis* was estimated to be 0.1275 with a range of 0.0640 to 0.1706.

β_{vh}**:** The transmission probability, is the probability that a VL-infectious sandfly transmits to a human.

India Parameter estimates were generated by solving for β_{vh} in our $\mathcal{R}_C$ expression

$$\beta_{vh} = \frac{\mathcal{R}_C^2 \mu_v \left(\mu_h + \theta\right)\left(\phi + \mu_h\right)}{\beta_{hv} \phi b^2 m_{V:h}} \tag{B.1}$$

and then pairing samples of known values in Table 2.2 together with an estimated $\mathcal{R}_C$ value of 2.01 by Mubayi, et al. (2010(97)). From this calculation, the mean transmission coefficients were estimated as 0.0694 with a range of 0.0266–0.1652.

Sudan A similar approach from India was taken and applied to Sudan using know parameter estimates from Table 2.2 and an estimated $\mathcal{R}_C$ value of 1.3 from ELmojtaba, et al, 2010 (52). The calculations yield an average estimate for β_{vh} as 0.0012 with a range of 0.0007–0.0020.

μ_v**:** The per-capita daily mortality rate of an adult sandfly, taken as 1/ (life expectancy of sandflies)

P. Argentipes (India) The mortality for this species of sandfly varies between 0.125 to 0.1 (128) and 0.0667 to 0.1 (109) per day. Some studies established the average lifespan to be, 0.0833 per day (74; 84) and 0.091 per day (138). For this species, the per-capita mortality rate was averaged out from these studies to be $\mu_v = 0.0833$ per day with a range of 0.0667 to 0.1 per day.

P. Orientalis (Sudan) The adult life span of this species has not been well studied. In one extensive study, the whole life cycle range was 48–60 days (68). From this study, the combine time of the four (4) different developmental larval stages and the pupation stage gives a range of 40 to 56 days. So, the life span of adult sandflies ranges from 10 to 14 days and average 12 days. For this species, the per-capita mortality rate was averaged out to be, $\mu_v = 0.0857$ per day and ranges from 0.1 to 0.0714 per day.

ℓ**:** The human landing rate of an adult female sandflies was used as a approximate measure of the human biting rate. Before the late 1990s, the human landing catches (HLC), was a common way for measuring the human landing rate of Phlebotomine sandflies. However, for ethical reasons, this method is less commonly used and has been replaced with the use of human baits and Centers for Disease Control light traps (CDCLT) to attract female sandflies. In a comparison study, Dilger, E. (2013) investigated the relationship between the number of sandflies caught by HLC and CDCLT upon humans and showed that CDCLT are appropriate for estimating the number of sandflies visiting humans (43). Various comparatives on HLC and CDCLT were used as measured to establish an appropriate parameter range for the human landing rate.

P. Argentipes (India) In this study conducted by Joshi B, et al. (2009) (77) on the collection of *P. Argentines* per house per night using CDC LT, we took the mean number of landing 12.15 with a range of 8.68 to17.

P. Orientalis (Sudan) From a studies conducted on the effectiveness of impregnated bed net on the landing/bite of female *P. Orientalis* human volunteers by Elnaiem et al. (1999, 2011), we took the mean number of human landing rate to be 32 landing/human/per day with a range 15.7 to 48.3 landing/human/per day (54; 59).

μ_h**:** For both India and Sudan, the average life expectancy at birth in a year was collected from multiple censored data sources. Using these sources, we estimate the per-person/day natural death rate as (average life expectancy $\times 365)^{-1}$. For

each of these respective regions, the mean and range of the natural death rates was estimated to be:

India From the mean data from multiple survey sites, we found the per-capita natural death rate to be 4.55e-5 (Census of India, 2001), 4.28e-5 (hetv.org, 2012), 4.08e-5 (cia.gov, 2010), 4.33e-5 (WHO, 2012), and 4.27e-5 (un.org, 2012). Combining the estimates of these various value gave a mean death rate of per human/day and range of 4.05e-5 to 5.03e-5 per human/day.

Sudan Similarly from India, the per-capita natural death rate was found to be 4.55e-5 (Coutinho, 2005), $4.38e-5$ (cia.gov, 2012), $4.49e-5$ (unicef.org, 2012), $4.09e-5$ (WHO, 2012) and 4.54e-5 (un.org, 2012). The mean death rate of $4.3e-5$ per human/day and range of $4.e-5$ to $4.54e-5$ per human/day.

ϕ : The per-capita rate of progression of humans from the asymptomatic state to the infectious state here is taken at incubation of VL before becoming symptomatic. The incubating period is known to vary from weeks to years among different individuals.

India The day^{-1} asymptomatic rate has been estimated to be 0.0086 (day^{-1}) (140), 0.0055 (147; 103) and range between $0.0055 - -0.0164$ (day^{-1}) (29) and 0.0167 to 0.0083 (day^{-1}) (105). We consider these estimates and took the asymptomatic rate incubating period, ϕ, to be 0.00975 (day^{-1}) with a range of 0.006–0.0167 (day^{-1}).

Sudan For this region, the day^{-1} asymptomatic rates ranges were estimated to be 0.0083 to 0.01667 (day^{-1}) (62), 0.0055 to 0.0164 (day^{-1}) (22; 29), and specific mean rates are give in 0.0167 (day^{-1}) with a rang of 0.0111 to 0.0042 (day^{-1}) (65). The asymptomatic rate incubating period, taken as an average of all these studies was taken to be $\phi = 0.0098$ (day^{-1}) and range from 0.0042 to 0.0167 (day^{-1}).

θ**:** Treatment rate from VL here is defined as the mean duration of illness before seeking treatment in some treatment fertility.

India Current estimates for treatment were found to be 1.996 (who2007), 4 months (0.5–19 months) (1), 4 months (12), and 3.5 (13). From these study we took the mean estimated treatment rate per day was $\theta = 0.0351$ (day^{-1}) with a range of 0.0067 to 0.0597 (day^{-1}).

Sudan The estimated mean rates per person/day varied from 0.0164 (31; 100), 0.0130, 0.0055 (3), 0.0108 (0.0027–0.0408) (78), (0.0033–0.0235) (95) and a range of 0.0111–0.0056 in (127). We took the mean estimate for θ as 0.014275 (day^{-1}) with a range of 0.0027 to 0.0408 (day^{-1}).

Λ_h**:** The per-capita recruitment rates is defined as the sum per-capita birth rate and per-capita net migration rate of the population.

India To estimate the per-capita recruitment rate, we use demographic data on population size, birth rate, and migration from CIA World Factbook. The average estimated recruitment rate was calculated as the sum of the birth rate and net immigration per day and is given by 8.3e-5 persons per day, ranging from 7.67e-5 to 9.22e-5 persons per day.

Sudan Similar to the estimation for India, the average estimated recruitment was 1.27e-4 persons per day, with a range of 1.1e-4 to 1.35e-4 persons per day.

Λ_v**:** The per-capita daily adult sandfly recruitment rate of female phlebotomus sandfly. Seasonality plays a role in the abundance of the sandfly population in each geographical region. Few studies have established an average recruitment rate for sandflies to $0.02128 \times N_h$ per day (128) and 0.299 per day (79). For our model, we consider the recruitment rate for both species to be $\Lambda_v = 0.1601$ per day and range from 0.0213 to 0.299 per day.

P_{I_h}**:** Prevalence for VL in humans is defined as the proportion of people with the disease at a given point in time.

India To estimate the per day prevalence, a study based on Serodiagnostic Test in Madhepura District of Bihar, India, was considered by Srivastava N, et al., 2014 (136). From this study, we use the annual prevalence per 10000 of 26.92 in 2010 and 23.78 in 2011 together with the total population of Madhepura assumed to be at risk to estimate the per person per day prevalence. The prevalence range was estimated to be between 0.0013 to 0.0015 persons per day.

Sudan A Survey study by Khalil et al. 2000 (81), gave the prevalence of active disease a range from 40 to 80 per 1000. Using these estimates, together with reported estimates of the at risk population in Pigott et al., 2014 (114), a rough estimate of the daily prevalence range of 0.0006 to 0.0013 persons per was generated for Sudan's population.

P_{I_v}**:** Prevalence for VL in sandflies is defined as the proportion of sandflies with VL at a given point in time.

	Point Prevalence of sandflies			
Species	Min	Max	Mean	Reference
P. argentipes	0.0085	0.0284	-	(146)
	0.005	0.05	-	(98)
	0.007	0.02	-	(108; 119; 124; 144)
P. orientalis	0.019	0.05	-	(59)
	0.0054	0.037	0.0157	(70)
	0.035	0.071	-	(57)

Table B.1: Point Prevalence Estimates for VL in India and Sudan for Host and Vector From Various Sample-Based Field Studies.

$\mathcal{R}_C$**:** Estimated ranges for both countries were taken from previous mathematical and modeling studies.

India $\mathcal{R}_{C_I}$ was estimated to 2.0 ± 0.25 (138; 97)

Sudan $\mathcal{R}_{C_S}$ was estimated to be 1.3 ± 0.25 (52)

India						
Year	μ_v	μ_h	N_h	$\Lambda_h = \mu_h N_h$	$N_v = m_{v:h} N_h$	$\Lambda_v = \mu_v N_v$
2000	0.0833	4.41e-5	1042261758	45937	5492719465	392337105
2001	0.0833	4.38e-5	1059500888	46402	5583569680	398826406
2002	0.0833	4.35e-5	1076705723	46861	5674239160	405302797
2003	0.0833	4.33e-5	1093786762	47311	5764256236	411732588
2004	0.0833	4.30e-5	1110626108	47750	5852999589	418071399
2005	0.0833	4.27e-5	1127143548	48178	5940046498	424289036
2006	0.0833	4.25e-5	1143289350	48597	6025134875	430366777
2007	0.0833	4.23e-5	1159095250	49011	6108431968	436316569
2008	0.0833	4.21e-5	1174662334	49425	6190470500	442176464
2009	0.0833	4.19e-5	1190138069	49847	6272027624	448001973
2010	0.0833	4.17e-5	1205624648	50280	6353641895	453831564
2011	0.0833	4.15e-5	1221156319	50723	6435493801	459678129
2012	0.0833	4.14e-5	1236686732	51173	6517339078	465524220
2013	0.0833	4.12e-5	1252139596	51621	6598775671	471341119
	Min	4.42e-5	1042261758	45937	5492719465	392337105
	Mean	4.55e-5	1149486935	48794	6057796146	432699725
	Max	4.73e-5	1252139596	51621	6598775671	471341119

Table B.2: Estimate for Parameters Λ_h and Λ_h Using Mean Estimates for India in Table 2.2 and World Bank's Demographic Estimates in (63)

Sudan						
Year	μ_v	μ_h	N_h	$\Lambda_h = \mu_h N_h$	$N_v = m_{v:h} N_h$	$\Lambda_v = \mu_v N_v$
2000	0.0857	4.73e-5	27729798	1310	146136035	10438288
2001	0.0857	4.70e-5	28434810	1335	149851449	10703675
2002	0.0857	4.67e-5	29186427	1362	153812470	10986605
2003	0.0857	4.63e-5	29973979	1389	157962869	11283062
2004	0.0857	4.60e-5	30778572	1417	162203074	11585934
2005	0.0857	4.57e-5	31585871	1444	166457540	11889824
2006	0.0857	4.54e-5	32397535	1472	170735009	12195358
2007	0.0857	4.52e-5	33218250	1500	175060178	12504298
2008	0.0857	4.49e-5	34040065	1529	179391143	12813653
2009	0.0857	4.47e-5	34853178	1559	183676248	13119732
2010	0.0857	4.46e-5	35652002	1589	187886051	13420432
2011	0.0857	4.44e-5	36430923	1618	191990964	13713640
2012	0.0857	4.43e-5	37195349	1647	196019489	14001392
2013	0.0857	4.42e-5	37964306	1676	200071893	14290849
Min		4.42e-5	27729798	1310	146136035	10438288
Mean		4.55e-5	32817219	1489	172946744	12353339
Max		4.73e-5	37964306	1676	200071893	14290849

Table B.3: Estimate for Parameters Λ_h and Λ_h Using Mean Estimates for Sudan in Table 2.2 and World Bank's Demographic Estimates in (64)